



THE UNIVERSITY OF QUEENSLAND
AUSTRALIA

**Biogeochemical processes in permeable estuarine
sediments following benthic community change:
implications for system dynamics & *Lyngbya majuscula*
blooms in Deception Bay, Queensland**

Peter Hanington

Bachelor of Applied Science
Masters of Environmental Science

*A thesis submitted for the degree of Doctor of Philosophy at
The University of Queensland in 2014*
School of Geography, Planning and Environmental Management

Abstract

Estuaries are productive and dynamic ecosystems that provide a wide range of environmental services to human society, many of which contribute to people's livelihoods and wellbeing. However, many of these coastal ecosystems have become degraded by the impacts of human activity. Such degradation is often manifested in changes to an ecosystem's structure and function. Such changes impact on the resilience of these ecosystems to recover from natural disasters and maintain essential services that human and ecological communities rely upon.

In shallow-water estuarine ecosystems, sediment-based processes often play a significant role in ecosystem function, such as the biogeochemical cycling of carbon and nutrients. This thesis examines the importance of benthic community composition on key biogeochemical processes that underpin local phenomena such as blooms of the toxic cyanobacterium *Lyngbya majuscula* and materials cycling at ecosystem-wide scales.

The research presented here shows that changes in benthic community composition have implications for system-wide functions such as biogeochemical cycling. In Deception Bay, 100 % of the seagrass community dominated by *Syringodium isoetifolium* was lost after a major flood event in January 2011. The loss of *S. isoetifolium* from Deception Bay was shown to fundamentally change the structure and function of the seagrass meadow from a net heterotrophic seagrass dominated benthic community to a net autotrophic seagrass-microphytobenthic community. Such a change in function has implications for system-wide biogeochemical budgets.

This study has quantified a benthic release of Fe(II) from sediments sampled from northern Deception Bay. To our knowledge, this study represents the first documented benthic release of Fe(II) from permeable sandy sediments of a shallow subtropical embayment. The results suggest that sandy sediments that are relatively low in organic carbon are capable of supplying bioavailable Fe at levels significant for the growth of benthic organisms. The results of this research show that the post-flood sediments of northern Deception Bay are capable of supplying >1700 % of the daily Fe demands and up to 10.6 % of daily P requirements for the growth of *L. majuscula* blooms. This result suggests that the growth of *L. majuscula* blooms in Deception Bay is likely to be P limited and that future management actions that are targeted towards reducing *L. majuscula* blooms in Moreton Bay need to include a strategy for reducing P loads to the Bay.

Declaration by author

This thesis is composed of my original work, and contains no material previously published or written by another person except where due reference has been made in the text. I have clearly stated the contribution by others to jointly-authored works that I have included in my thesis.

I have clearly stated the contribution of others to my thesis as a whole, including statistical assistance, survey design, data analysis, significant technical procedures, professional editorial advice, and any other original research work used or reported in my thesis. The content of my thesis is the result of work I have carried out since the commencement of my research higher degree candidature and does not include a substantial part of work that has been submitted to qualify for the award of any other degree or diploma in any university or other tertiary institution. I have clearly stated which parts of my thesis, if any, have been submitted to qualify for another award.

I acknowledge that an electronic copy of my thesis must be lodged with the University Library and, subject to the policy and procedures of The University of Queensland, the thesis be made available for research and study in accordance with the Copyright Act 1968 unless a period of embargo has been approved by the Dean of the Graduate School.

I acknowledge that copyright of all material contained in my thesis resides with the copyright holder(s) of that material. Where appropriate I have obtained copyright permission from the copyright holder to reproduce material in this thesis.

Publications during candidature

Peer-reviewed papers

Hanington, P., Hunnam, K., Johnstone, R., (2015) Widespread loss of the seagrass *Syringodium isoetifolium* after a major flood event in Moreton Bay, Australia: implications for benthic processes. *Aquatic Botany* **120**: 244-250.

Conference abstracts

Hanington, P., Hunnam, K., Johnstone, R., (2012) Widespread loss of the seagrass species *Syringodium isoetifolium* and macroalgae in Deception Bay after a major flood event. Coast to Coast Conference, Brisbane, Australia.

Hanington, P., Chiffings, T., Johnstone, R., Using dynamic systems models to Inform monitoring programs and their design (2010). Coast to Coast Conference, Adelaide, Australia.

Publications included in this thesis

Hanington, P., Hunnam, K., Johnstone, R., (2015) Widespread loss of the seagrass *Syringodium isoetifolium* after a major flood event in Moreton Bay, Australia: implications for benthic processes. *Aquatic Botany* **120**: 244-250. – incorporated into Chapter 4.

Contributor	Statement of contribution
Author Hanington, P. (Candidate)	Experimental design (70 %) Mapping and spatial analysis (20 %) Writing and editing of manuscript (60 %)
Author Hunnam, K.	Experimental design (30 %) Mapping and spatial analysis (80 %) Writing and editing of manuscript (40 %)
Author Johnstone, R.	Overall intellectual guidance

Contributions by others to the thesis

Overall intellectual guidance was provided by Associate Professor Ron Johnstone (primary supervisor) of the University of Queensland and Dr Tony Chiffings (secondary supervisor) then of the Danish Hydraulics Institute. Editorial comments for all chapters of this thesis were provided by Dr Ron Johnstone and Kim Hunnam.

In chapter 2, guidance on the use of generalised additive models for statistical analysis was provided by Dr Milani Chaloupka of the University of Queensland.

Chapter 3 is a result of a collaboration between Associate Professor Andrew Rose of Southern Cross University and myself. Dr Rose performed all sample analyses for Fe(II) and S²⁻ and provided a review of the resulting manuscript submitted for publication.

Chapter 4 is a result of a collaboration between Kim Hunnam (UQ Technical Assistant) and myself. Historical benthic survey data collected by myself and Kim Hunnam was combined with the data collected during this study to produce a manuscript submitted for publication. Kim Hunnam made a significant contribution with regards to the mapping of benthic communities.

Chapter 5 is a result of a collaboration between Jaya Seelam (UQ PhD candidate) and myself. Jaya Seelam made a significant contribution by establishing the basic hydrodynamic model framework which I then developed and applied to my research in Deception Bay.

Statement of parts of the thesis submitted to qualify for the award of another degree

None

Acknowledgements

I would like to thank my primary supervisor Ron Johnstone for his advice, enthusiasm, support and patience during what can be described as an arduous but invaluable experience. I am also thankful for our friendship over the many years that we have worked together and for the many other interesting opportunities that have been afforded to me during my PhD candidature.

I wish to thank my other supervisor Tony Chiffings for his support and valuable contributions. I thank Olga Pantos for her support in the field and laboratory and for our morning chats over coffee.

I thank Milani Chaloupka, Andrew Rose, Kim Hunnam and Jaya Seelam who I have had the pleasure of collaborating with and whose academic inputs have improved the quality of this work.

Finally and most importantly, I wish to thank my partner Kim for her countless contributions in the field, laboratory and help in improving my thesis structure. But most of all, I thank her for her unselfish love and support without which I could not have undertaken such a journey.

This research was funded by the Queensland Government National and International Research Alliances Program.

Keywords

Benthic processes, *Lyngbya majuscula*, biogeochemistry, iron and phosphorus fluxes, seagrass, estuarine sediments, Deception Bay.

Australian and New Zealand Standard Research Classifications (ANZSRC)

ANZSRC code: 039901, Environmental Chemistry, 50 %

ANZSRC code: 050102, Ecosystem Function, 30 %

ANZSRC code: 060701, Phycology (inc. Marine Grasses), 20 %

Fields of Research (FoR) Classification

FoR code: 0399, Other Chemical Sciences, 50 %

FoR code: 0501, Ecological Applications, 30 %

FoR code: 0607, Plant Biology, 20 %

Contents

Chapter 1 Introduction.....	1
1.1. Estuarine ecosystems.....	1
1.2. Benthic processes and community change.....	2
1.3. Study site.....	3
1.4. Thesis Aims.....	5
Chapter 2 Fine-scale horizontal distributions of carbon and nutrients in surface sediments of Deception Bay, a shallow subtropical estuarine bay subjected to annual <i>Lyngbya majuscula</i> blooms.....	8
2.1. Abstract.....	8
2.2. Introduction.....	8
2.3. Study site description.....	10
2.4. Sampling design and methods.....	11
2.5. Sample analyses.....	12
2.6. Data analysis and visualisation.....	12
2.7. Results.....	13
2.8. Discussion.....	19
2.9. Conclusion.....	24
Chapter 3 The significance of benthic iron and phosphorus fluxes for the growth of a bloom forming toxic cyanobacteria <i>Lyngbya majuscula</i> , Moreton Bay, Australia.....	26
3.1. Abstract.....	26
3.2. Introduction.....	27
3.3. Materials and methods.....	28
3.4. Results.....	33
3.5. Discussion.....	39
3.6. Conclusions.....	43
Chapter 4 Changes to seagrass community composition after a major flood event in Moreton Bay, Australia: implications for benthic carbon cycling and <i>Lyngbya majuscula</i> blooms.....	45
4.1. Abstract.....	45
4.2. Introduction.....	46
4.3. Methods.....	47
4.4. Results.....	51
4.5. Discussion.....	61
4.6. Conclusions.....	72
Chapter 5 Hydrodynamic processes and particle transport in a shallow estuarine embayment, northern Deception Bay.....	74
5.1. Abstract.....	74
5.2. Introduction.....	74
5.3. Materials and methods.....	76
5.4. Results and discussion.....	80
5.5. Conclusions.....	89
Chapter 6 Synthesis and conclusions.....	91
6.1. Summary and key findings.....	91
6.2. Implications of the work.....	95
6.3. Future research.....	96
References.....	98

List of Figures

Figure 1	Location of study site, Moreton Bay, Queensland	3
Figure 2	Conceptual diagram showing the main pathways for organic matter and nutrient cycling in Deception Bay sediments (POM: particulate organic matter, DOM: dissolved organic matter).....	6
Figure 3	Location of study site in northern Deception Bay (a), showing the location of sediment sampling sites and study site bathymetry (b).....	10
Figure 4	Shepard ternary diagram (a) and spatial distribution maps of % sand (b), % silt (c), and % clay (d) for surface sediments (0-1 cm) of northern Deception Bay.....	15
Figure 5	Spatial and depth distribution maps of TOC, TN, TP, and Fe (% dry wt) across the study site, northern Deception Bay	18
Figure 6	Spatial and depth distribution maps of C:N, N:P and % clay across the study site, northern Deception Bay.	19
Figure 7	Location of sampling sites in northern Deception Bay.	29
Figure 8	Benthic fluxes of (a) PO_4^{3-} , (b) NH_4^+ , (c) NO_x^- , (d) Fe(II) and (e) DO measured under light and dark conditions on sediment cores sampled from northern Deception Bay on 1 February 2011 and 25 October 2011. Error bars = SE of 4 replicate samples.	35
Figure 9	Diel variations in water-column DO and temperature during neap-tides at site 40 in northern Deception Bay during (a) pre-flood conditions from 14 to 16 December 2010 and (b) post-flood conditions from 12 to 14 February 2011. Shaded areas represent night-time hours.	37
Figure 10	In situ microprofiles of (a) oxygen measured on 18, 22 and 30 November 2010 pre-flood conditions in sediments adjacent to seagrass at sites 40, 75 and 99 in northern Deception Bay, and (b) oxygen and Redox measured on 4 December 2011 post-flood conditions in bare sediments at site 40 in northern Deception Bay.....	38
Figure 11	Mean <i>L. majuscula</i> biomass at sample site T ₂₋₅ , sampled during the 2006-2007 summer bloom. The graph shows the linear growth rate averaged over the development of the bloom used to estimate <i>L. majuscula</i> N and P demands (modified from Johnstone et al., 2007).....	42
Figure 12	Location of study site in northern Deception Bay (a), showing the location of sampling sites (b)	48
Figure 13	Benthic macroflora community distributions in northern Deception Bay based on detailed field surveys undertaken in April-June 2008 (a), August 2011 (c) and July 2012 (e). Note map (a) is reproduced from Hunnam (2008). Benthic macroflora cover derived from aerial imagery (obtained from www.nearmap.com) taken on 19 August 2010 (b) and 28 July 2011 (d)	55
Figure 14	Hourly gauged river flows from (a) Caboolture River (station no. 142001A), (b) Bremer River (station no. 143107A) and (c) Lockyer River (station no. 143203B) during 2010 – 2011. Source: EHMP event monitoring, SEQ Healthy Waterways Partnership.....	58
Figure 15	Light penetration at the benthos expressed as total daily light (a) and daily mean percentage of surface irradiance (b) measured at sites 24, 40, 75 and 99 at northern Deception Bay, between December 2010 and February 2011.....	59

Figure 16 Ambient bottom water salinity data measured at EHMP site 1118 and at the study site, Deception Bay, February 2010 to June 2011. Source: EHMP, SEQ Healthy Waterways Partnership.....	60
Figure 17 Organic carbon mass balance for the Deception Bay study site for pre- and post-flood benthic community distributions. Pre-flood export estimates are based on sediment fluxes reported by Eyre and France (1997); flood inputs are based on average sediment deposition rates measured across the study area during a 28 day period following the major flood peak. All fluxes in $t\ C\ d^{-1}$. Burial estimated from Duarte et al. (2005). (GPP: gross primary production; R: respiration).....	71
Figure 18 Model domain, remotely operated monitoring station (ROMS) and current meter deployment sites in Deception Bay (A); location of model domain within Moreton Bay (B).....	76
Figure 19 Model domain mesh and bathymetry.....	77
Figure 20 Model domain mesh zoomed in at study site.....	78
Figure 21 Measured wind direction and speed at the Deception Bay remotely operated monitoring station (ROMS) during April and November 2006 (source: Healthy Waterways Partnership).....	80
Figure 22 Comparison between measured and modelled water surface elevations in Deception Bay during a period of neap tides, November 2006.....	81
Figure 23 Comparison between measured and modelled current speed and direction in Deception Bay during a period of neap tides, November 2006.....	82
Figure 24 Calculated residual current flow and mean current speed for April 2006 showing the location of Chapter 2 sediment sampling area (red rectangle).....	83
Figure 25 Calculated residual current flow and mean current speed for November 2006 showing the location of Chapter 2 sediment sampling area (red rectangle).....	83
Figure 26 Starting sites for particle tracking at study site.....	85
Figure 27 Clay particle tracking simulation for April 2006 starting at study site.....	86
Figure 28 Clay particle tracking simulation for November 2006 starting at study site.....	86
Figure 29 Starting sites for particle tracking at Pumicestone Passage and the mouth of the Caboolture River.....	87
Figure 30 Clay particle tracking simulation for April 2006 starting at Pumicestone Passage and the mouth of the Caboolture River.....	88
Figure 31 Clay particle tracking simulation for November 2006 starting at Pumicestone Passage and the mouth of the Caboolture River.....	88
Figure 32 Conceptual diagram showing changes in net ecosystem metabolism as a result of flood related changes in benthic community composition. Rates are given in units of $t\ C\ yr^{-1}$ based on Chapter 4 benthic community areas. (GPP: gross primary production; R: respiration; NEM: net ecosystem metabolism.).....	93

List of Tables

Table 1	Summarised results of spatial composition of sediments in northern Deception Bay (n=100), sampled in January 2009	14
Table 2	Partial correlation coefficients and Pearson correlation coefficients (in brackets) for physical and chemical sediment composition (pairwise deletion). (n = 496 for all variables except n = 400 for sand, silt & clay); (* correlation significant at p<0.05).....	21
Table 3	Summary of benthic metabolic rates for community respiration (R), gross primary production (GPP) and net community production (NCP). All rates are expressed in mg C m ⁻² d ⁻¹ . p/r represents the ratio between community productivity and respiration.	36
Table 4	Pre and Post-flood sediment composition for Site 40, northern Deception Bay, January 2009 (see Chapter 2) and 25 October 2011. Figures in brackets are the mean of all sediments (n=100), SD denotes standard deviation.....	39
Table 5	Summary of results from pre-flood and post-flood benthic macroflora community surveys and seagrass cover estimates derived from aerial imagery, northern Deception Bay.	54
Table 6	Sediment trap deposition rates and solid phase composition, northern Deception Bay, January to February 2011 (values are the mean of 3 replicates, SE in brackets).	61
Table 7	Benthic process rates for subtropical / tropical seagrass dominated and unvegetated sediments relevant to the current study site at northern Deception Bay. Rates for community respiration (R), gross primary production (GPP) and net community production (NCP) are expressed in mg C m ⁻² d ⁻¹ . p/r represents the ratio between community productivity and respiration. The data listed here is not the result of an exhaustive review of the literature and is provided as estimates only for the assessment of system wide dynamics.	69
Table 8	Benthic process rates used to derive net ecosystem metabolism (NEM) and post-flood carbon budget for northern Deception Bay. (* denotes rates that are estimates based on measured winter rates).....	70
Table 9	Parameter values used for particle tracking simulation.	78
Table 10	Summary of model inputs and data sources.....	79

Chapter 1

Introduction

1.1. Estuarine ecosystems

Globally, approximately 60 % of the human population is concentrated within 100 km of the coast, with this figure continually rising (Vitousek et al., 1997). Estuaries are among the most productive and dynamic systems on earth (Paerl, 2006) and provide a wide range of services to human society, many of which contribute to people's livelihoods and wellbeing. Fisheries and the manufacture of fish products are estimated to employ 38 million people globally, while coastal tourism is one of the fastest growing sectors of global tourism (UNEP, 2006). Despite their critical importance, the health of these highly productive ecosystems is in decline worldwide (Lotze et al., 2006).

Human activity within the coastal zone has led to widespread degradation of coastal ecosystems and loss of biodiversity. Exploitation of fish stocks, destruction of habitat, and the eutrophication and pollution of coastal waterways have fundamentally changed the structure, function and resilience of estuarine ecosystems (Lotze et al., 2006). This has been demonstrated by the global decline of commercial and recreational fish stocks (UNEP, 2006), and the increased vulnerability of coastal ecosystems to climate-induced changes (Nicholls et al., 2007).

In Australia, over 85 % of the population resides within 50 km of the coast (Australian Bureau of Statistics, 2001). Coastal resources have considerable economic value and contribute significantly to Australia's economy. The gross value of Australian commercial fisheries production in 2006-2007 was \$2.2 billion (Hohnen et al., 2008), while visitors in 2004 spent approximately \$20 billion on recreational and tourist activities directly involving coastal and ocean ecosystems (Ward and Butler, 2006). Australia's coastal environments are also intrinsically linked to Australian culture and lifestyle. Some indigenous Australians have had strong cultural associations with the coast for thousands of years.

Australia's coastal zone includes globally significant ecosystems including coral reefs, mangroves and seagrasses (Voice et al., 2006; Ward and Butler, 2006). However, one quarter of Australia's 1000 estuaries are characterised as being modified or highly

modified by human activity or habitation (NLWRA, 2002). Many of these coastal ecosystems have become degraded by the impacts of human activity.

The impact of human activities in the coastal zone have resulted in fundamental changes to the structure and function of estuarine ecosystems (Lotze et al., 2006). Such change impacts on the resilience of these ecosystems to recover from natural disasters and maintain essential services that human and ecological communities rely upon (Rapport et al., 1998).

1.2. Benthic processes and community change

In shallow-water estuarine ecosystems, sediment-based processes often play a significant role in system-wide nutrient dynamics. Within these systems, the benthos can receive sufficient light to support primary producer communities such as seagrass, macroalgae and benthic microalgae, which in turn influence the cycling of nutrients (McGlathery et al., 2007). Many studies have been undertaken to describe the interactions between individual benthic plant communities and biogeochemical cycling, including seagrasses (Johnson and Johnstone, 1995; McGlathery et al., 2004), macroalgae (Tyler et al., 2001) and benthic microalgae (Eyre and Ferguson, 2002; Sundback and McGlathery, 2005; Tyler et al., 2001). Previous work has also explored the link between eutrophication in shallow estuaries and changes to benthic primary producer communities, such as seagrass dominated systems replaced by benthic algal and/or phytoplankton communities (McGlathery et al., 2007; Valiela et al., 1997). These research efforts also highlight the complexity of sediment-plant interactions and the uncertainty of predicting biogeochemical feedback responses to altered benthic community composition.

The benthos in shallow estuaries, by virtue of their shallow water depths, are greatly influenced by physical processes such as wind and wave currents which tend to resuspend and transport benthic material. This physical reworking of sediment has a profound effect on benthic carbon and nutrient cycling. These phenomena have been well documented in the literature for deltaic continental margin sediments and to a lesser extent, in shallow estuarine environments (see Burdgie (2012) and references therein).

Relationships between physical processes, sediment-plant interactions and biogeochemical processes are challenging to study in estuarine environments since many of these processes change independently and interactively over a range of spatial and temporal scales. However, exploring these relationships is important for elucidating the

linkages between benthic processes and ecosystem responses, such as the growth of nuisance algal blooms (NABs).

1.3. Study site

This study was undertaken in northern Deception Bay (27°05'S, 153°08'E), located in north-west Moreton Bay, Queensland, Australia (Figure 1). The study site is characterised by shallow (<3 m), subtidal and intertidal seagrass meadows, historically comprising the seagrass species *Zostera muelleri*, *Syringodium isoetifolium*, *Halophila ovalis* and *Halodule uninervis*. Since the early 1990s the site has been subject to an increasing occurrence of blooms of the toxic cyanobacterium *Lyngbya majuscula* (Albert et al., 2005; Dennison et al., 1999; Watkinson et al., 2005).

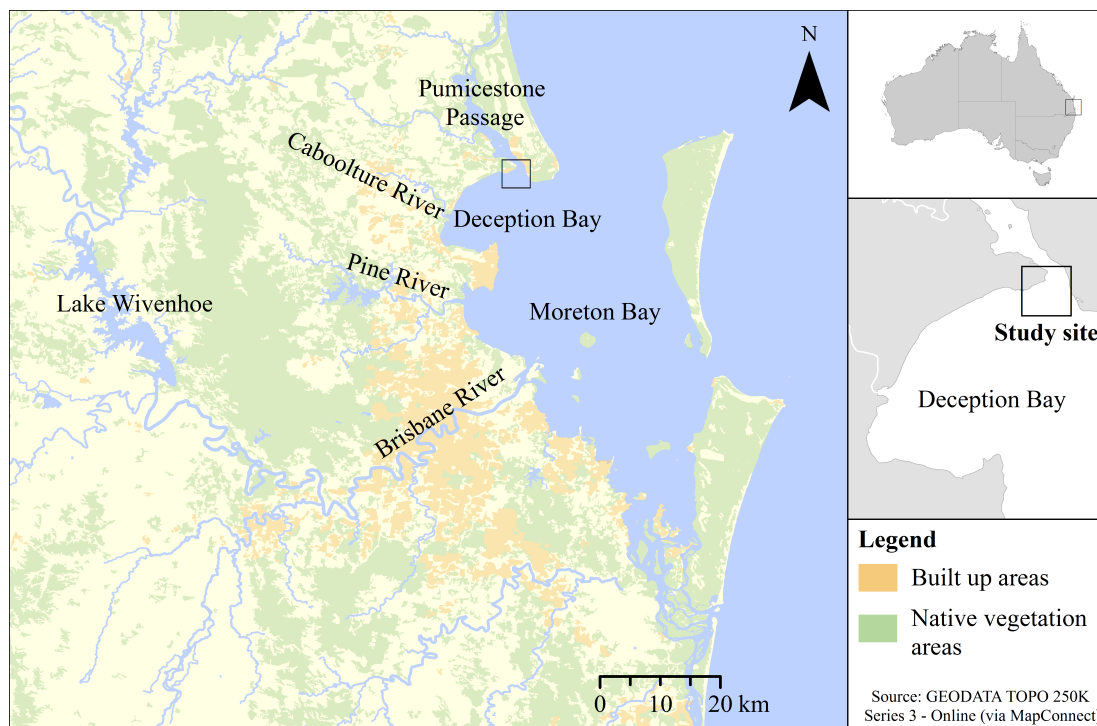


Figure 1 Location of study site, Moreton Bay, Queensland

Moreton Bay, Queensland

Moreton Bay is a semi-enclosed, shallow, coastal embayment located adjacent to Australia's third largest city, Brisbane. The Bay is home to a rich diversity of plant and animal life (Davie, 2011) and is internationally recognised for its ecological significance as

a Ramsar listed wetland. The sheltered waters of the Bay are important to the local economy through recreational and commercial fisheries, tourism and recreational amenity.

The Moreton Bay catchment, occupying an area of 21,220 km², has been extensively modified by human activity and is under increasing pressure from urban development in one of Australia's fastest growing regions (Dennison and Abal, 1999). Increases in human induced nutrient and sediment loads have been identified as the leading cause of declining ecosystem health of the Bay (Dennison and Abal, 1999). Nutrient enrichment (eutrophication) of shallow estuaries often results in blooms of fast-growing macroalgae (also referred to as NABs), which can form visible mats either at the sediment surface or floating at the surface of the water column (Sundback and McGlathery, 2005). NABs are often considered as indicators of ecosystem deterioration and a decline in ecosystem capacity to deal with a range of anthropogenic impacts (Silbergeld et al., 2000).

Over the past 15 years, Moreton Bay has seen an increased occurrence of blooms of the toxic cyanobacterium *L. majuscula* (Albert et al., 2005; Dennison et al., 1999; Watkinson et al., 2005) as well as substantial losses of seagrass meadows (Dennison and Abal, 1999; Kirkman, 1978). These are both signs of a system in stress and declining health, and may represent a change in system dynamics and resilience. Critical to both these phenomena, and central to the aims of this thesis, are the interactions and processes that take place at the benthos, both in terms of the implications of community change and the supply of essential materials for *L. majuscula* growth.

The 2011 Brisbane River flood event

In January 2011, a major flood event occurred in the Moreton Bay catchments, including the Brisbane River, where water levels peaked on 13 January 2011 at a height of 4.46 mAHD at the Brisbane City gauge. This event was the largest flood experienced in the Brisbane River since the construction of the Wivenhoe dam, which was built in response to the January 1974 floods (van den Honert and McAneney, 2011). The average recurrence interval (ARI) of the 2011 flood was estimated at 120 years (Babister and Retallick, 2011). Over a 10 day period, the flood waters were estimated to have supplied a sediment load in excess of 1 million tonnes into the receiving waters of Moreton Bay (DERM, 2011). This sediment load represents three times the annual load normally received by the Bay.

On 25 January 2011, 12 days after the flood peak, dieback of the seagrass species *S. isoetifolium* at the study site was observed. Due to the large amount of sediment in the water column, surveys could not be undertaken immediately to assess the extent of dieback. Surveys were undertaken seven months after the flood peak in August 2011, once conditions had become favourable for visual surveying. Changes in environmental conditions at the study site as a result of the flood were captured by water quality sensors that had been deployed to capture changes in conditions leading up to an anticipated *L. majuscula* bloom. Although an *L. majuscula* bloom never eventuated, the environmental data set that was collected provided a unique opportunity to document conditions during the event that led to the widespread loss of seagrass from northern Deception Bay.

The flood resulted in significant changes to benthic community composition at the study site. These changes necessitated a slight adjustment in research focus and provided an opportunity to assess the consequences of such change on key benthic processes and system function. This was done whilst continuing to explore the significance of benthic processes for the supply essential elements for *L. majuscula* growth.

1.4. Thesis Aims

This study was driven by the need to better understand the linkages between benthic processes and the growth of the bloom forming cyanobacterium *L. majuscula*. Midway through this study, a major flood event occurred in the Brisbane River, causing widespread loss of seagrass and macroalgae communities at the study site. Through a combination of necessity and opportunism, the focus of this study evolved to include a new set of objectives focused around understanding the implications of such community change for sediment biogeochemical processes.

The aims of this study were to 1) quantify the rates and pathways of carbon and nutrient flows within the flood impacted sediments of Deception Bay, 2) determine the potential for these sediments to underpin key local phenomena such as *L. majuscula* blooms and biogeochemical cycling, 3) explore the implications of benthic community change for the cycling of nutrients at an ecosystem scale. Figure 2 summarises the main pathways for organic matter and nutrient cycling in Deception Bay sediments.

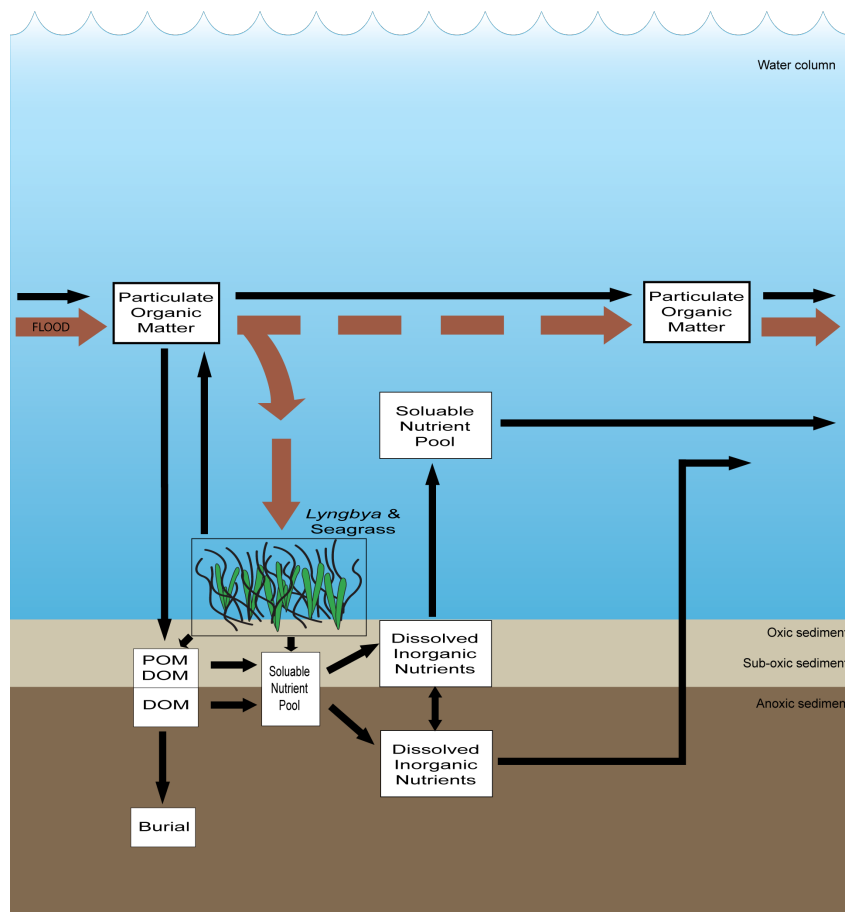


Figure 2 Conceptual diagram showing the main pathways for organic matter and nutrient cycling in Deception Bay sediments (POM: particulate organic matter, DOM: dissolved organic matter).

In addressing the above aims, the thesis has been set out in the following chapters:

Chapter 1

This chapter provides an introduction to benthic processes and the significant role the benthos can play in the cycling of nutrients in shallow estuarine ecosystems. The chapter highlights the important role that benthic primary producer communities play in influencing biogeochemical processes. From this context, the concept of change in benthic community composition is identified as a potential driver for change in ecosystem function. The chapter then concludes by identifying the need to explore the linkages between sediment-plant interactions and biogeochemical processes in order to better understand the consequences of benthic community change and local phenomenon such as the blooms of the toxic cyanobacterium *L. majuscula*.

Chapter 2

This chapter presents the results of chemical and physical characterisation of the sediments of northern Deception Bay prior to the January 2011 Brisbane River flood, and immediately after a summer *L. majuscula* bloom event. This investigation provides a better understanding of local sediment conditions as well as insight into the sequestration of carbon and nutrients to the benthos.

Chapter 3

This chapter quantifies the exchange of nutrients across the sediment water interface with the aim to evaluate the potential for sediment processes to underpin the growth of *L. majuscula* blooms.

Chapter 4

This chapter quantifies a change in benthic macroflora community composition following the January 2011 Brisbane River flood event and assesses the implications of such change for key benthic processes and ecosystem function.

Chapter 5

This chapter explores the interaction between local hydrodynamic processes and sediment distribution and transport in order to gain a better understanding of the dynamics of carbon and nutrient cycling that supports the growth of *L. majuscula* blooms in northern Deception Bay.

Chapter 6

This chapter provides a synthesis of key findings and demonstrates that benthic processes are significant in driving key ecosystem responses such as the growth of the bloom forming cyanobacterium *L. majuscula* and that changes to benthic community composition can have significant implications for ecosystem-wide functions.

Chapter 2

Fine-scale horizontal distributions of carbon and nutrients in surface sediments of Deception Bay, a shallow subtropical estuarine bay subjected to annual *Lyngbya majuscula* blooms

2.1. Abstract

A 120 m horizontal resolution distribution of sediment grain-size, organic carbon, nitrogen, phosphorus and iron has been determined for surface sediments from northern Deception Bay following a summer bloom of the toxic cyanobacterium *Lyngbya majuscula*. Two-dimensional surface smoother plots were derived from generalised additive modelling (GAM) to explore spatial relationships in sediment composition. Correlation analyses identified co-dependencies between sediment parameters, while GAMs identified significant spatial relationships for most of the sediment parameters measured. However, only a portion of the statistical deviance could be explained by spatial relationships alone, suggesting that other processes such as water circulation, biological interactions and benthic processes add deviance that does not correlate with the observed spatial patterns. The relatively low levels of sediment organic carbon (mean surface sediment Total Organic Carbon of 0.31 %) found by this study, suggests either low rates of organic matter deposition and/or high rates of organic matter decomposition. The results also suggest that the bulk of the *L. majuscula* biomass does not accumulate in the local sediments, but instead, is exported from the bloom site. This study highlights the complex nature of sediment / carbon dynamics in shallow coastal waterways and the dominant role physical processes can play in the transport and deposition of material to and from the benthos.

2.2. Introduction

Estuaries are highly dynamic ecosystems that receive and process vast amounts of organic matter derived from a variety of local and remote sources (Bouillon et al., 2004). Within shallow estuaries the benthos often plays a crucial role in key ecosystem functions such as such as primary production, remineralisation and nutrient cycling (Eyre et al., 2011b; Herbert, 1999; Hopkinson et al., 1999). However, many estuaries are now suffering from anthropogenic nutrient over-enrichment (eutrophication), which is having detrimental impacts on their trophic structure and the function of benthic communities. These impacts have been observed in changes to the dominant primary producer groups (Cardoso et al.,

2004), changes in benthic metabolism and nutrient flux (Eyre and Ferguson, 2002), enhanced primary production (Paerl, 2006) and the growth of nuisance algal blooms (Sundback et al., 2003).

Within this context, blooms of the nitrogen (N₂)-fixing cyanobacterium *Lyngbya majuscula* have been observed in recent years in Moreton Bay, Queensland (Albert et al., 2005; Dennison et al., 1999; Watkinson et al., 2005). The occurrence of this toxic cyanobacterium is of growing concern due to its negative impact on human health, tourism, commercial fisheries and the ecology of the bay (Osborne et al., 2008; Osborne et al., 2001; Pittman and Pittman, 2005). Recent laboratory studies have shown the growth of *L. majuscula* to be stimulated by Phosphorus (P) (Elmetri and Bell, 2004), and the combination of Iron (Fe) and chelating organic compounds (Ahern et al., 2006; Bell and Elmetri, 2007). The rapid increase in the occurrence of *L. majuscula* over the last decade has been linked to elevated P loads in Moreton Bay (Elmetri and Bell, 2004; Wulff et al., 2011) and as evidence in support of the notion that Moreton Bay is potentially P limited (Wulff et al., 2011).

Research undertaken in Deception Bay (north-west Moreton Bay) over two summers in 2005-2006 and 2006-2007 suggests a strong link between benthic processes and the supply of essential nutrients for *L. majuscula* bloom initiation and growth (Johnstone et al., 2007). However, little is known with regards to the role of the bulk sediment underlying these bloom sites and the significance of their chemical composition, particularly at a spatial scale relevant to the observed growth of *L. majuscula*. In addition to this, resolving the P versus N limitation debate cannot be fully addressed without key knowledge sets, such as sediment composition and dynamics at scales relevant to system function.

This chapter investigates the spatial distribution of sediment grain-size (sand, silt and clay fractions) and the chemical composition (organic carbon, nitrogen, phosphorus and iron) of surface sediments across the seagrass beds of Deception Bay following a summer *L. majuscula* bloom.

2.3. Study site description

This study was undertaken in northern Deception Bay ($27^{\circ}05'S$, $153^{\circ}08'E$), located in north-west Moreton Bay, Queensland, Australia (Figure 3). Moreton Bay is a semi-enclosed shallow water embayment located adjacent to the city of Brisbane. Moreton Bay has an area of approximately $1,523 \text{ km}^2$, a water depth up to 29 m (average = 6.25 m), and is characterised by a subtropical climate with summer-dominated rainfall.

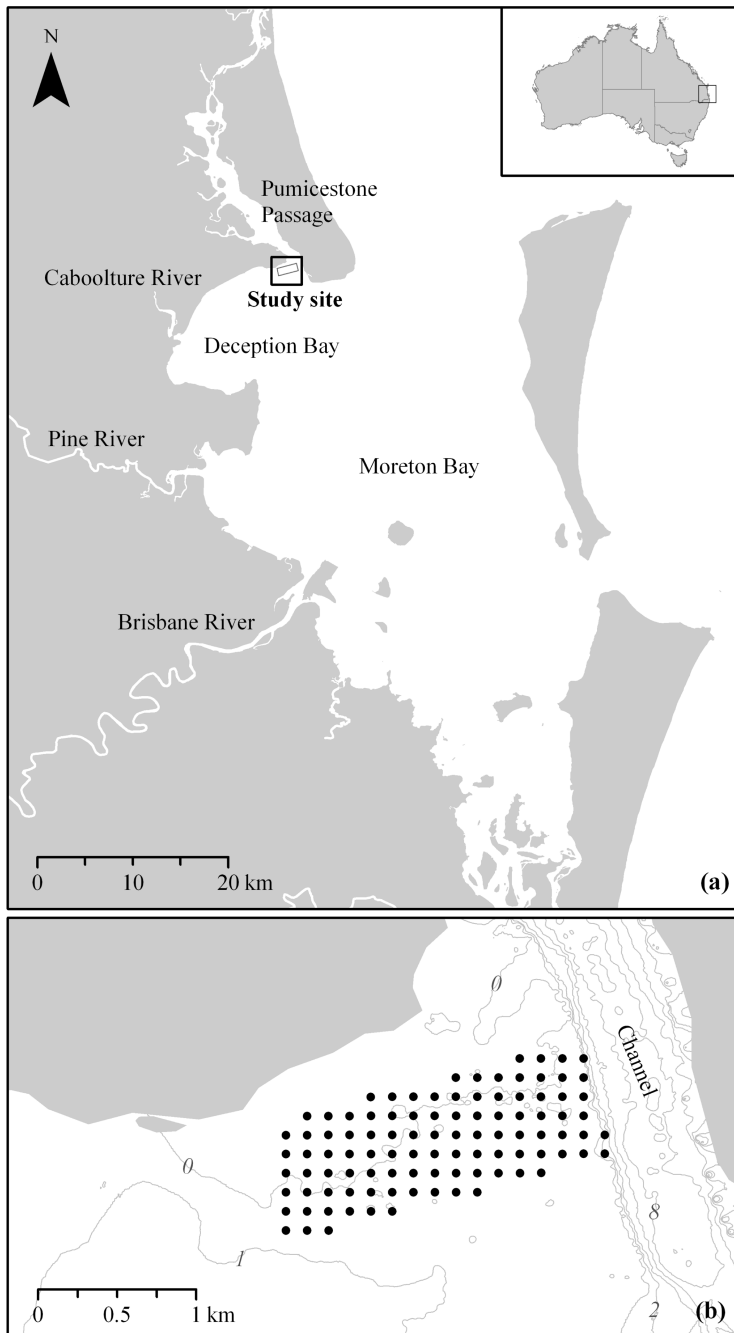


Figure 3 Location of study site in northern Deception Bay (a), showing the location of sediment sampling sites and study site bathymetry (b)

The study site (1.5 km²) is characterised by shallow (< 3 m), subtidal and intertidal sandy sediments comprised of the seagrass species *Zostera muelleri*, *Syringodium isoetifolium*, *Halodule uninervis* and *Halophila ovalis*. These seagrass beds have been subjected to extensive and frequent *L. majuscula* blooms since the early 1990's (Watkinson et al., 2005). The broader area of Deception Bay receives riverine inputs from the Caboolture River and terrestrial runoff from a number of small tidal creeks and urban stormwater drains that are predominantly located along its southern and western shoreline. In the north of the bay and adjacent to the current study site, bay waters exchange with the estuarine waters of Pumicestone Passage (Eyre and France, 1997), and the ocean via a large (16 km wide) opening to the north. Water quality and residence times within northern Deception Bay are thought to be influenced by this oceanic water exchange and hence, has maintained favourable light regimes for existing seagrass beds (Dennison and Abal, 1999). In contrast, significant seagrass loss (15 km²) has occurred in the more turbid waters of southern Deception Bay (Dennison and Abal, 1999).

2.4. Sampling design and methods

To characterise the physico-chemical composition of surficial sediments across the study site, a systematic sampling strategy was employed consisting of 100 sampling locations approximately 120 m apart (Figure 3b). Sampling was undertaken over a four-week period in mid January 2009, immediately after the decline of a summer *L. majuscula* bloom. At each sampling location in-tact sediment cores were collected by hand via SCUBA using 86 mm diameter acrylic cores, retaining approximately 150 mm of sediment and 1 litre of overlying water. Care was taken during sampling to ensure minimal disturbance of the sediment vertical structure. Cores were transported to the laboratory in an ice-water bath and kept at < 4°C until processing.

Each sediment core was sectioned under nitrogen gas within 12 hours of collection at 5 depth intervals: 0-1 cm, 1-2 cm, 2-3 cm, 4.5-5.5 cm and 9.5-10.5 cm. Each section was then homogenised after coarse fragments (> 2 mm) such as shell, gravel and living biota were removed. A subsample for chemical analyses was immediately frozen and stored at -30°C until further processing; the remaining sediment was stored at < 6°C for determination of grainsize distribution.

2.5. Sample analyses

Sediment samples for chemical analyses (500 in total) were dried at 65°C until constant weight, then ground into a fine powder using a ring mill grinder fitted with an agate grinding head. Total Organic Carbon (TOC) and Total Nitrogen (TN) were simultaneously determined on acid digested (HCl) samples on a Shimadzu TOC-5000A Analyser fitted with a solid sample module. The acid digestion was used to remove carbonates from the sediment sample for the determination of organic carbon and nitrogen contents. Total Phosphorus (TP) and Fe were determined after strong acid digestion (nitric and perchloric) at 120°C for 3 hours and analysed using a Varian Liberty inductively-coupled atomic emission spectrometer following procedures outlined in Loring and Rantala (1992). The lower temperature acid digestion procedure employed here was used to selectively extract the more reactive, bio-available forms of iron by excluding the extraction of iron bound to silicates and other refractory minerals. Analytical accuracy and precision have been evaluated through the analyses of certified reference materials supplied by the National Research Council of Canada (standard marine sediment MESS-1), and analysis of 25 randomly selected replicate samples.

Grain size distribution was determined at all 100 sampling locations in sections 0-1 cm, 1-2 cm, 2-3 cm and 4.5-5.5 cm (400 samples in total) by laser diffraction (Malvern Mastersizer 2000) and classified using a modified version of the Wentworth scale for sand (63 μm - 2,000 μm), silt (4 μm - 63 μm) and clay (<4 μm).

2.6. Data analysis and visualisation

Two-dimensional surface smoother plots and summary statistics were derived from a generalised additive modelling (GAM) and a nonparametric regression modelling approach, using the *mgcv* package (Wood, 2006) in R (R Development Core Team, 2011). The surface plots were used to illustrate the spatial distribution of sediment grainsize and chemical composition across the study site and with depth in the sediment.

Partial correlation (pairwise deletion) and Pearson correlation analyses were used to identify relationships between variables and help define the GAMs used for further data exploration.

2.7. Results

Grainsize distributions

The dominant sediment fraction in surface sediments (0-1 cm depth) across the study site was sand (Figure 4a), with mean and maximum sand content of 75.2 % and 91.2 % respectively. The distribution of sand (Figure 4b), silt (Figure 4c) and clay (Figure 4d) in surface sediments were significantly spatially correlated at $p=0.003$ (sand), $p=0.004$ (silt) and $p<0.001$ (clay). Sand, silt and clay contents were also significantly spatially correlated ($p<0.001$) at sediment depths 1-2 cm, 2-3 cm and 4.5-5.5 cm (Table 1).

Table 1 Summarised results of spatial composition of sediments in northern Deception Bay (n=100), sampled in January 2009

Sediment parameter	Sediment depth profile composition					2D surface smoother significance	
	Depth (cm)	Mean	SD	Min	Max	(p-value)	% of deviance explained
TOC (% dry wt)	0 - 1	0.31	0.10	0.13	0.70	<0.001	15.1
	1 - 2	0.30	0.11	0.14	0.64	0.003	17.4
	2 - 3	0.29	0.11	0.10	0.69	0.005	43.4
	4.5 - 5.5	0.25	0.10	0.08	0.66	<0.001	39.7
	9.5 - 10.5	0.19	0.06	0.07	0.40	<0.001	34.9
TN (% dry wt)	0 - 1	0.032	0.009	0.016	0.057	0.002	11.6
	1 - 2	0.030	0.009	0.016	0.062	0.008	15.2
	2 - 3	0.028	0.009	0.010	0.054	<0.001	19.5
	4.5 - 5.5	0.024	0.009	0.009	0.045	<0.001	31.6
	9.5 - 10.5	0.019	0.007	0.007	0.035	<0.001	22.7
TP (% dry wt)	0 - 1	0.0084	0.0023	0.0040	0.0163	<0.001	45.9
	1 - 2	0.0071	0.0021	0.0033	0.0141	<0.001	48.5
	2 - 3	0.0066	0.0021	0.0028	0.0145	<0.001	49.9
	4.5 - 5.5	0.0054	0.0019	0.0024	0.0118	<0.001	48
	9.5 - 10.5	0.0042	0.0014	0.0018	0.0078	<0.001	42.1
Fe (% dry wt)	0 - 1	0.251	0.102	0.071	0.592	<0.001	48.6
	1 - 2	0.226	0.099	0.066	0.605	<0.001	51.1
	2 - 3	0.221	0.099	0.056	0.623	<0.001	58.3
	4.5 - 5.5	0.207	0.100	0.062	0.521	<0.001	43.3
	9.5 - 10.5	0.195	0.085	0.065	0.457	<0.001	41.2
C:N (molar)	0 - 1	11.3	1.8	7.5	16.7	0.003	47.3
	1 - 2	11.7	1.8	8.8	16.8	0.003	35.6
	2 - 3	12.1	2.2	8.6	19.2	0.002	28.8
	4.5 - 5.5	12.1	2.2	8.3	19.7	0.013	44.1
	9.5 - 10.5	12.1	1.5	8.2	17.5	0.252	11.8
N:P (molar)	0 - 1	8.7	1.4	4.8	13.4	0.003	41.9
	1 - 2	9.4	1.4	6.7	12.4	<0.001	40.7
	2 - 3	9.6	1.8	4.4	17.4	0.003	38.1
	4.5 - 5.5	9.9	1.8	4.8	16.2	0.009	19.4
	9.5 - 10.5	9.9	1.8	5.5	16.6	0.072	34
Clay (wt%)	0 - 1	2.7	1.3	0.3	5.6	<0.001	60
	1 - 2	2.4	1.2	0.3	5.8	<0.001	39.1
	2 - 3	2.2	1.3	0.2	5.9	<0.001	46.5
	4.5 - 5.5	1.8	1.2	0.1	5.0	<0.001	35.6
Silt (wt%)	0 - 1	22.1	5.1	18.5	35.3	0.004	22.6
	1 - 2	20.5	5.4	9.8	33.3	<0.001	25.8
	2 - 3	20.3	6.5	7.8	32.3	<0.001	28.8
	4.5 - 5.5	18.1	6.5	5.3	35.5	<0.001	22.8
Sand (wt%)	0 - 1	75.2	6.1	60.3	91.2	0.003	44.7
	1 - 2	77.1	6.4	62.3	89.9	<0.001	27.9
	2 - 3	77.4	7.7	63.5	91.9	<0.001	30.3
	4.5 - 5.5	80.1	7.6	60.2	94.5	<0.001	25.2

2D surface smoother statistics derived from generalised additive models as presented in Figure 5 & Figure 6.

Section 1 = 0-1 cm, section 2 = 1-2 cm, section 3 = 2-3 cm, section 4 = 4.5-5.5 cm, section 5 = 9.5-10.5 cm

The spatial distribution of clay in surface sediments (Figure 4d) was higher in the north-eastern corner of the study site adjacent to the channel, tending to decrease to the south-west with distance away from the channel. Higher silt contents (Figure 4c) were located along the northern study site boundary, tending to decrease with distance to the south. The spatial distribution of silt appears to be consistent and generally uniform at all sediment depths, whereas clay distributions tend to vary spatially at different sediment depths (Figure 6). Mean clay and silt contents tended to decrease with increasing sediment depth, with mean clay contents at 2-3 cm ($p=0.01$) and 4.5-5.5 cm ($p<0.001$) significantly lower than surface (0-1 cm) sediments; and mean silt contents showing a similar significant trend at 2-3 cm ($p=0.05$) and 4.5-5.5 cm ($p<0.001$).

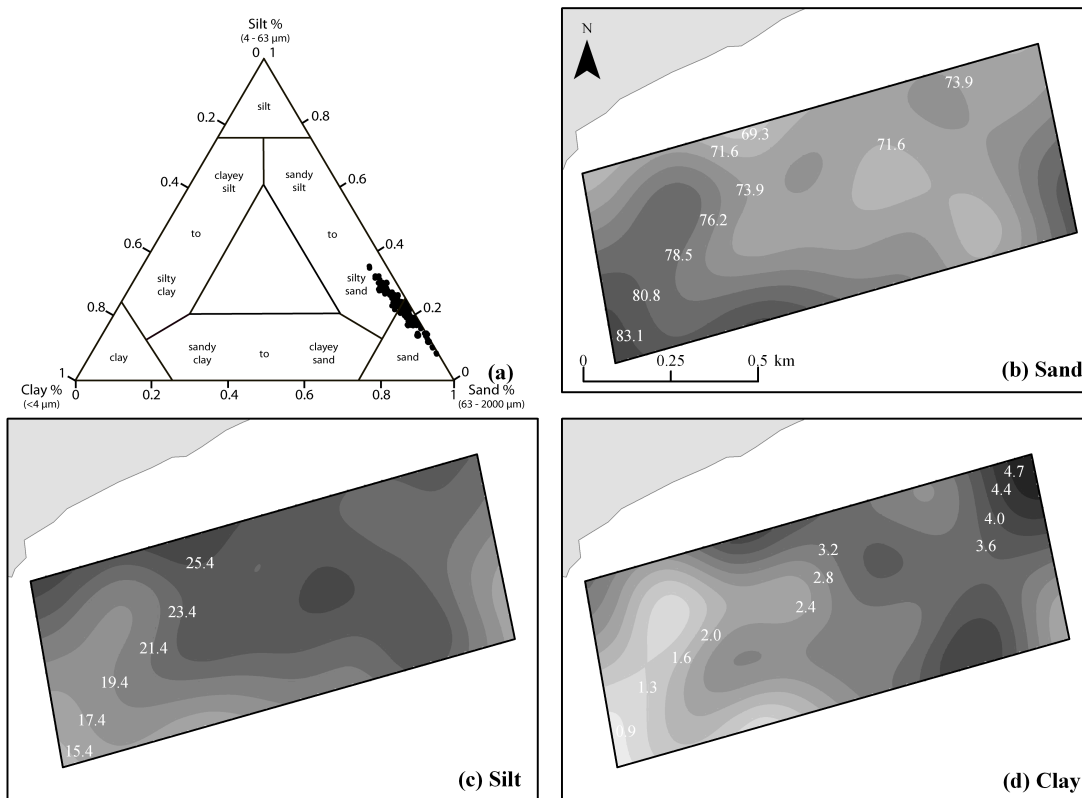


Figure 4 Shepard ternary diagram (a) and spatial distribution maps of % sand (b), % silt (c), and % clay (d) for surface sediments (0-1 cm) of northern Deception Bay.

Sediment chemical composition

Surface sediment (0-1 cm) organic carbon (measured as TOC) ranged from 0.13 % to 0.7 % dry wt., with a mean of 0.31 % (SD 0.1 %). The distribution of TOC in surface sediments was significantly spatially correlated ($p < 0.001$) and highest along the northern site boundary, decreasing with distance to the south (Figure 5). At sediment depths $> 2-3$ cm this spatial trend appeared to change, with TOC levels highest towards the north-east of the study site adjacent to the channel (Figure 5). At all subsurface sediment depths, TOC was significantly spatially correlated (2-3 cm: $p = 0.003$, 3-4 cm: $p = 0.05$, 4.5-5.5 cm and 9.5-10.5 cm: $p < 0.001$). Mean TOC levels tended to decrease with increasing sediment depth, with TOC concentrations at 4.5-5.5 cm and 9.5-10.5 cm significantly less ($p < 0.001$) than surface TOC concentrations.

TN in surface sediments ranged from 0.016 % to 0.057 % dry wt., with a mean of 0.032 % (SD 0.009 %). The distribution of TN in surface sediments was significantly spatially correlated ($p = 0.002$) and appears to be evenly distributed across the study site from higher values in the north-east and gradually decreasing towards the south-west (Figure 5). At all sub-surface sediment depths, TN concentrations were significantly spatially correlated at $p < 0.001$, with the exception of 1-2 cm depth where $p = 0.008$. Mean TN levels decreased with increasing sediment depth, with TN concentrations at sub-surface depths significantly less than surface TOC concentrations (1-2 cm: $p = 0.04$, 2-3 cm, 4.5-5.5 cm, and 9.5-10.5 cm: $p < 0.001$).

TP and Fe in surface sediments ranged from 0.004 % to 0.0163 % and 0.071 % to 0.592 % dry wt., respectively, with mean TP and Fe values of 0.0084 % (SD 0.0023 %) and 0.251 % (SD 0.102 %) dry wt., respectively. The distribution of TP and Fe at all sediment depths were significantly correlated spatially ($p < 0.001$) with higher concentrations in the north-eastern corner of the study site adjacent to the channel and tending to decrease with distance to the south-west away from the channel (Figure 5). TP and Fe show similar spatial distributions (Figure 5) with concentrations of TP and Fe becoming more evenly distributed at lower sediment depths (4.5-5.5 cm and 9.5-10.5 cm), compared with sediments in the top 3 cm. Mean TP and Fe levels tended to decrease with increasing sediment depth. TP concentrations at all sub-surface sediment depths were significantly ($p < 0.001$) less than surface TP concentrations. Fe concentrations were notably more variable compared with TP, but showed a similar and significant trend with

lower concentrations of Fe in sub-surface sediments 1-2 cm ($p=0.07$), 2-3 cm ($p=0.03$), 4.5-5.5 cm ($p=0.002$), and 9.5-10.5 cm ($p<0.001$).

C:N and N:P ratios in surface sediments ranged from 7.5 to 16.7 and 4.8 to 13.4 respectively, with mean C:N and N:P ratios of 11.3 (SD 1.8) and 8.7 (SD 1.4), respectively. Higher C:N ratios tend to dominate the north-western portion of the study site, however, spatial plots of C:N (Figure 6) show variability in surface sediments (0-1 cm) and at sediment depths 4.5-5.5 cm. The distribution of N:P also shows some spatial variation (Figure 6), however the general trend is lower N:P ratios in sediments located towards the east, adjacent to the channel. The distribution of C:N and N:P ratios were significantly spatially correlated at sediment depths 0-1 cm ($p=0.003$), 1-2 cm ($p=0.003$ and $p<0.001$ respectively), 2-3 cm ($p=0.002$ and $p=0.003$ respectively) and 4.5-5.5 cm ($p=0.01$ and $p=0.009$ respectively), but not for sediments at depths 9.5-10.5 cm. Mean C:N and N:P ratios are lowest in surface sediments (0-1 cm) ($p<0.01$ and $p<0.001$, respectively) compared with sub-surface sediments at depths >3 cm.

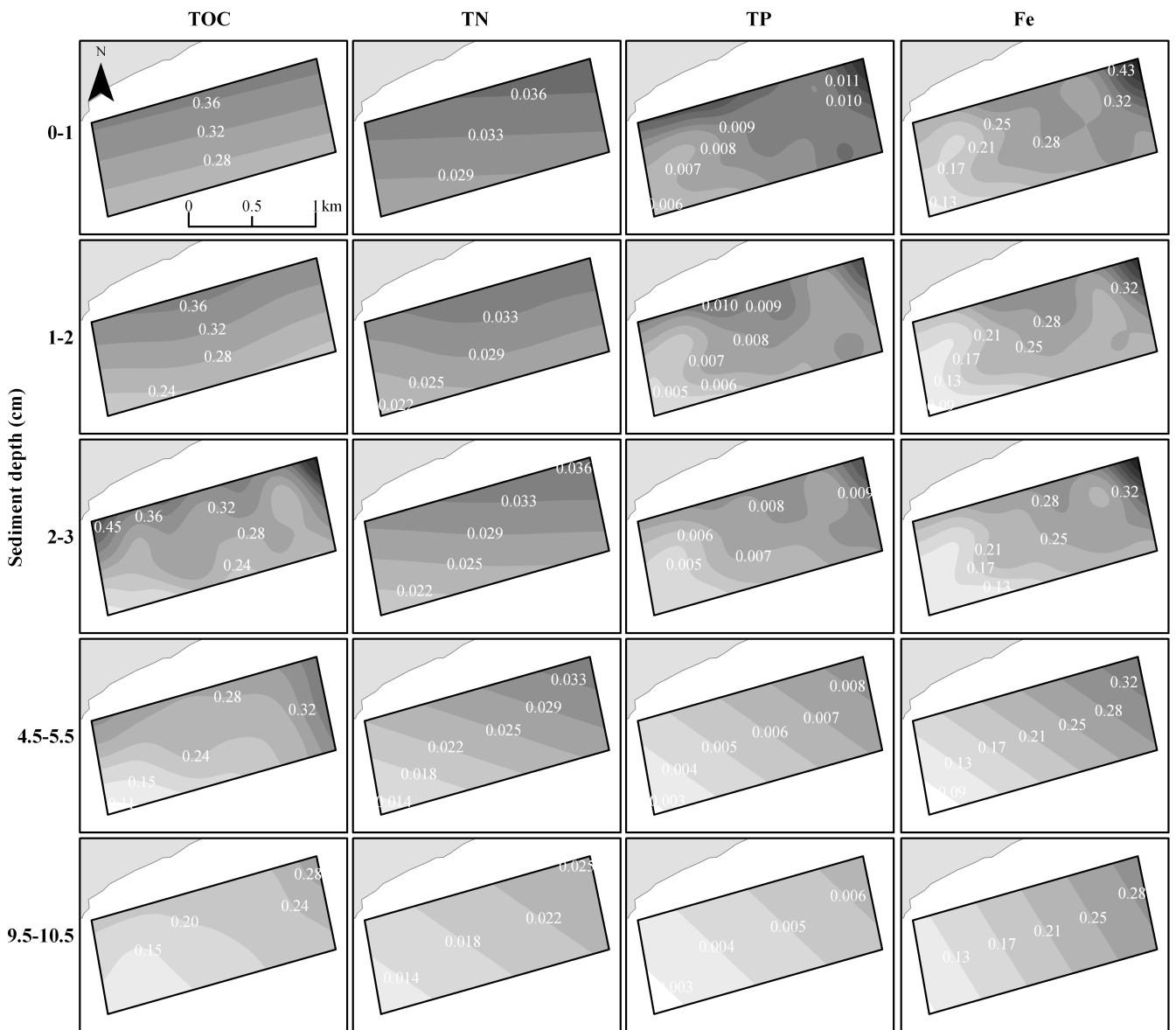


Figure 5 Spatial and depth distribution maps of TOC, TN, TP, and Fe (% dry wt) across the study site, northern Deception Bay

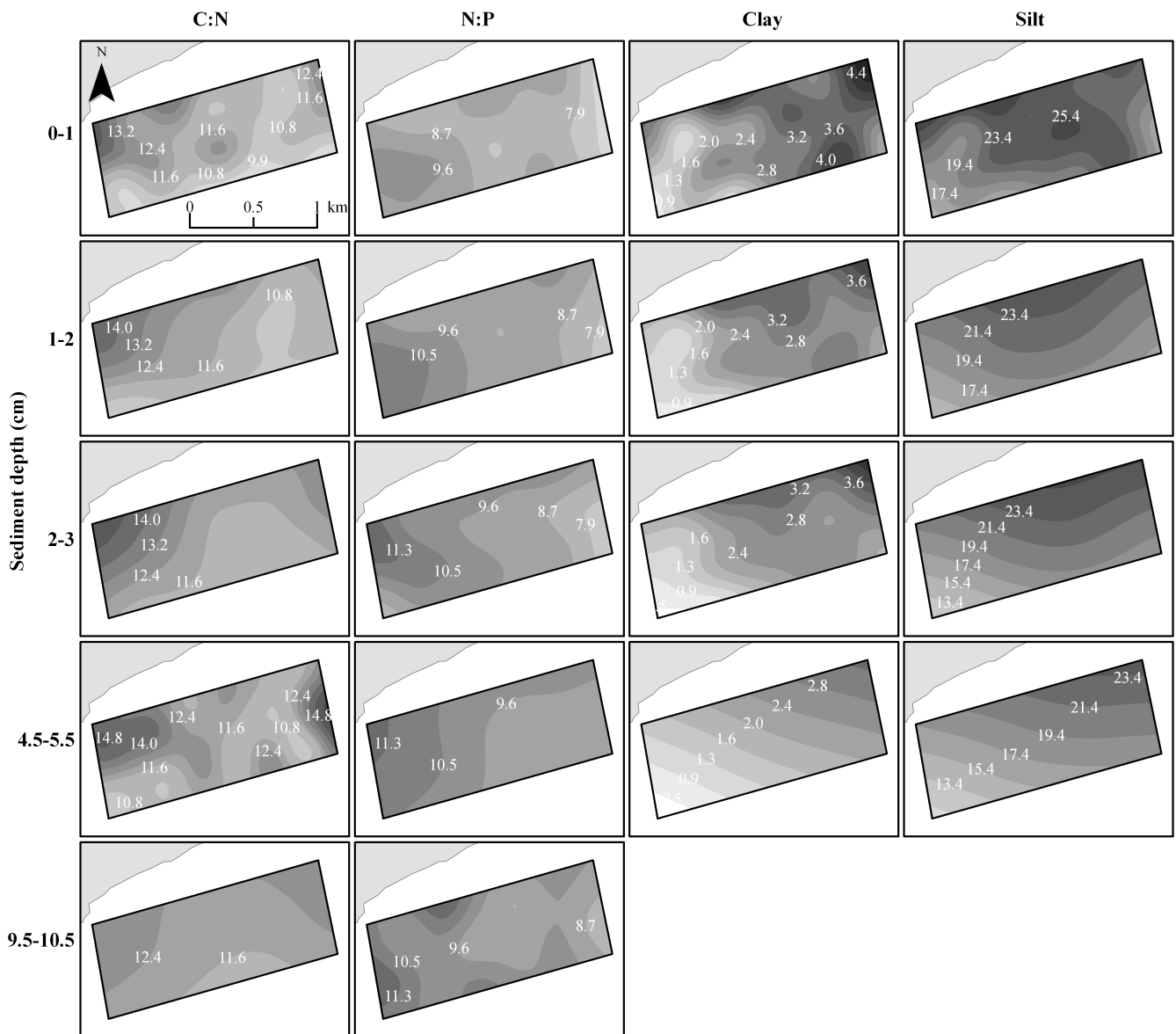


Figure 6 Spatial and depth distribution maps of C:N, N:P and % clay across the study site, northern Deception Bay.

2.8. Discussion

Grainsize distribution and sediment dynamics

Within the study site the spatial and depth distribution of fine-grained sediments (silts and clays) showed a distinctive pattern. There is a clear north to south gradient in the distribution of silts and a north-west to south-east gradient in the distribution of clays. These distributions suggest that the channel located to the north-east may be a conduit for fine-grained sediment transport to and/or from the study site and that the deposition of these sediments are likely to be influenced by benthic substrate (such as seagrass) and

local hydrodynamic processes. The dynamics of sediment transport are explored in further detail in Chapter 5.

Sediment chemical composition

The results of partial correlation and simple correlation (Pearson) analyses identified co-dependencies between sediment parameters. The results of these correlations were used to help define the GAMs, which have identified significant spatial relationships for most of the sediment parameters measured in this study. The modelling also highlights that only a portion of the deviance can be explained by spatial relationships alone, suggesting that other processes such as water circulation, biological interactions and benthic processes add deviance in a manner that does not correlate with spatial relationships. The unexplained portion of the deviance may not just be a missing predictor variable, it may also be the result of non-linear relationships that are not accounted for by the GAM. Further statistical analysis that accounts for non-linear relationships may help to explain more of the variance and capture the complex nature of sediment / carbon dynamics.

The composition of estuarine sediment is known to be influenced by environmental conditions and processes that operate over varying spatial and temporal scales (Berner, 1980). Of greatest influence are factors such as local hydrodynamic processes (Goni et al., 2009), sources and pathways of organic matter delivery and recycling (Bouillon and Boschker, 2006; Dunn et al., 2008), benthic community composition and metabolism (Duarte et al., 2005), and biotic interactions (Kristensen and Kostka, 2005). As a product of these factors, this study provides only a snapshot of the chemical composition of sediments at a given point in time. However, it does offer an insight into sediment conditions immediately following an *L. majuscula* bloom, and through sediment depth profiles, an insight into sediment conditions accumulated over time.

The distributions of sediment TOC, TN, TP and Fe are all spatially correlated, and have significant positive correlations with fine-grained sediment (silt and clay). Strong relationships are known to exist between sediment grainsize and organic matter content, phosphorus and iron, due to the high adsorption capacity of fine-grained sediments (see Berner and Rao, 1994; Dunn et al., 2008 and references therein). However, comparisons between Pearson correlation and partial correlation coefficients (Table 2) and the significance of 2D smoother plots (Table 1) illustrate that grainsize is not the only

influencing factor, with other variables (or processes) interacting to affect the spatial distribution of TOC, TN, TP and Fe. Supporting this notion is the increase in the percentage of deviance that is explained by spatial trends for TOC and N at increasing depths compared with TP and Fe, which remained equal across all depths. This observation may be the result of some benthic processes (C-fixation and/or remineralisation) being N limited and the combination of the coupling of Fe-P bound complexes.

Table 2 Partial correlation coefficients and Pearson correlation coefficients (in brackets) for physical and chemical sediment composition (pairwise deletion). (n = 496 for all variables except n = 400 for sand, silt & clay); (* correlation significant at p<0.05)

	TOC	TN	Fe	TP	C:N	N:P	Sand	Silt	Clay
	(% dry wt)				(molar)			(%)	
Section	0.155	-0.193	0.560*	-0.370*	-0.102	0.016	-0.108	-0.106	-0.099
	(-0.374*)	(-0.469*)	(-0.188)	(-0.570*)	(0.157)	(0.250*)	(0.232)	(-0.221)	(-0.248)
TOC		0.784*	0.192	0.234	0.955*	0.157	0.146	0.144	0.108
		(0.904*)	(0.780*)	(0.826*)	(0.318*)	(0.086)	(-0.746*)	(0.734*)	(0.696*)
TN			-0.080	0.312*	-0.772*	0.424*	-0.137	-0.132	-0.112
			(0.820*)	(0.883*)	(-0.092)	(0.138)	(-0.818)	(0.800*)	(0.781*)
Fe				0.255*	-0.191	-0.048	0.014	0.014	0.051
				(0.852*)	(0.002)	(-0.137)	(-0.808*)	(0.770*)	(0.865*)
TP					-0.182	-0.835*	-0.073	-0.074	-0.053
					(-0.028)	(-0.309*)	(-0.762*)	(0.729*)	(0.809*)
C:N						-0.134	-0.137	-0.134	-0.103
						(-0.098)	(-0.009)	(0.018)	(-0.028)
N:P							-0.079	-0.080	-0.071
							(-0.021)	(0.051)	(-0.129)
Sand								-1.000*	-0.995*
								(-0.995*)	(-0.880*)
Silt									-0.995*
									(0.828*)

The distributions of TP, Fe and clay appear to be tightly coupled as evident by significant and positive correlations (Pearson correlation, Table 2). There are known linkages between the cycling of P and Fe in marine sediments. Fe plays an important role in binding phosphates in oxic conditions (Berner and Rao, 1994; Krom and Berner, 1981; Küster-Heins et al., 2010), and releasing P bound to Fe (Fe-P) upon reduction of Fe (oxyhydroxides) in suboxic and anoxic conditions (Küster-Heins et al., 2010; Slomp et al., 1998). As discussed in later chapters, this relationship between Fe, P and clays may represent a significant factor underpinning the growth dynamics of *L. majuscula* which can reach bloom proportions at the study site. Iron and phosphorus have been shown to be key elements for the growth of *L. majuscula* in Moreton Bay (Elmetri and Bell, 2004; Rose et al., 2005).

The levels of organic carbon in sediments measured by this study are similar to that of previous studies (Johnstone et al., 2007) and to that reported in other parts of Moreton Bay (Dennison and Abal, 1999). The levels are also in the range reported for other sand-dominated, shallow, sub-tropical estuaries (Morse et al., 2007), but are generally at the low end of the range reported for seagrass sediments elsewhere (Bouillon et al., 2004; Duarte et al., 2005; Gacia et al., 2002). These relatively low levels of organic carbon found in the surface and sub-surface sediments immediately after a summer *L. majuscula* bloom event, suggests that the bulk of the *L. majuscula* biomass has been exported from the bloom site rather than accumulating in the sediments. A considerable amount of biomass has been reported to have washed-up on adjacent beaches during bloom events in Deception Bay, however, estimates suggest that these amounts are only a fraction of the total biomass produced during typical bloom events (Chiffings, 2007).

The levels of TP and Fe in Deception Bay sediments appear to vary relative to sediment organic carbon content, which is relatively low. For comparisons with other systems, sediment Fe is lower in Deception Bay compared to the finer-grained sediments of the Gulf of Finland (Baltic) (Pakhornova et al., 2007), but similar to that of sediments with organic carbon contents <1 % as reported by Balzer (1982) in the western Baltic. Although these Baltic systems are very different to that of subtropical Deception Bay, the sediments of these systems show a strong relationship between Fe content, grain size and organic carbon content. Other sand-dominated, shallow, sub-tropical estuaries such as those reported by Morse (2007) in the Central Texas Coast, have similarly low levels of sediment organic carbon and Fe.

TP in Deception Bay sediments are low compared to finer-grained, higher organic carbon content sediments such as those in the Baltic (Lukawska-Matuszewska and Bolalek, 2008; Lukkari et al., 2009), Florida Bay (Koch et al., 2001; Zhang et al., 2004) and California (Vink et al., 1997). Again, these systems are different to that of subtropical Deception Bay so direct comparisons are not possible, however, these systems demonstrate a link between sediment TP, grain size and organic carbon content. Direct comparisons with similar systems are limited as few studies have investigated sedimentary phosphorus pools and P-cycling in shallow sand-dominated sub-tropical coastal estuaries.

Sediment C:N ratios measured by this study were <20 and consistent with values reported in other Australian estuaries, including Moreton Bay (Dunn et al., 2008; Ferguson et al., 2007). C:N ratios in sediment have been widely used as an indicator for identifying organic carbon sources in freshwater and coastal marine systems (Meyers, 1994). In general, low sediment organic matter C:N ratios (C:N <20) suggests input of organic matter from sources such as algae, which typically have a C:N ratio between 4 and 10, compared to vascular plants which have C:N ratios of ≥ 20 (Meyers, 1994). However, this indicator has limited value in isolation as the degradation of sediment organic matter can potentially modify C:N ratios through bacterial decomposition during early diagenesis (Meyers, 1994), and benthic processes such as remineralisation and nitrogen fixation (see Kennedy et al. 2004 and references therein). The low C:N may simply reflect the carbon content of the sediment microbial community, rather than organic matter inputs.

N:P ratios have been used extensively in aquatic biogeochemistry as a predictor of nutrient limitation (see Greider and La Roche (2002)). However, sediment N:P ratios are of limited value as a predictor, as benthic processes such as remineralisation and denitrification, as well as changes in sediment redox conditions, can all potentially modify N and P concentrations in sediments over varying temporal scales.

Potential biogeochemical significance to *L. majuscula* blooms

The results of this study have shown that the sediments of northern Deception Bay are relatively low in organic carbon, phosphorus and iron and appear to be spatially distributed by influences such as local hydrodynamic processes. The results indicate that the sediments contain stocks of iron, phosphorus and carbon that might support benthic *L. majuscula* growth, however, without benthic flux measurements their role or potential remains unclear. Benthic flux estimates reported by Johnstone et al. (2007) suggest that

Deception Bay sediments are capable of providing all of the dissolved inorganic nitrogen needed for *L. majuscula* growth, except for the period of maximum growth, and between five and ten times the P needed for growth at any stage of bloom development. As noted above, both P and Fe have been shown to be key nutrients that stimulate the growth of *L. majuscula* (Ahern et al., 2007b; Elmetri and Bell, 2004), and that the initiation and growth of a bloom is likely to be linked to a benthic release of P and Fe due to changes in sediment oxygen and redox conditions (Johnstone et al., 2007). However, Johnstone et al. (2007) did not quantify benthic Fe fluxes and did not fully explore the linkages between sediment redox conditions and P and Fe release. Therefore, iron and phosphorus fluxes and the oxygen dynamics that drive their release have been quantified and are reported in following chapter (Chapter 3).

Relationships between sediment composition and the spatial distribution of an *L. majuscula* bloom could not be achieved due to the lack of available distribution data at a spatial scale comparable to this study. The only *L. majuscula* bloom distribution maps that have been reported for Deception Bay are those prepared by Ahern et al. (2007a), which are at a very coarse spatial scale relative to the sediment distributions presented by this study. Finer-scale observations made by Johnstone et al. (2007) during the monitoring of *L. majuscula* blooms in 2005 - 2006, describe the bloom distribution as variable both spatially and temporally along three 400 m transects. Data from both these studies are insufficient to test the notion that sediment composition influences *L. majuscula* bloom distribution.

2.9. Conclusion

This study describes the fine-scale horizontal distribution of sediment grain size, carbon and nutrients in surface sediments of northern Deception Bay following a bloom of the toxic cyanobacterium *L. majuscula*. This study has demonstrated that over a relatively small spatial area (1.5 km²), the distribution of sediment physical and chemical composition is variable, and that in shallow estuarine systems such as Deception Bay, sediment composition is likely to be influenced by local hydrodynamic forces operating over varying temporal scales. Similarly, the results of this study may suggest that *L. majuscula* detritus is not a significant source of organic matter to the benthos, with the bulk of *L. majuscula* biomass being removed from the bloom site, potentially as a result of local hydrodynamic conditions. Local hydrodynamic processes are explored further in chapter 5.

The relatively low levels of clay and sediment organic carbon are suggestive of either a low depositional environment or a highly dynamic environment where sediments are quickly mobilised and/or remineralised at the benthos. These notions are explored further in the following chapters. The results of this study demonstrate a need for further statistical analysis of the unexplained variance. This could be done by using other statistical approaches that explore non-linear relationships and testing other important predictor variables.

Chapter 3

The significance of benthic iron and phosphorus fluxes for the growth of a bloom forming toxic cyanobacteria *Lyngbya majuscula*, Moreton Bay, Australia

Publication Status: submitted 9 June 2015

Peter Hanington, Andrew Rose, and Ron Johnstone

The significance of benthic iron and phosphorus fluxes for the growth of a bloom forming toxic cyanobacteria *Lyngbya majuscula*, Moreton Bay, Australia.

Marine and Freshwater Research (under review)

3.1. Abstract

Blooms of the toxic cyanobacterium *Lyngbya majuscula* have been recorded in Deception Bay, Moreton Bay, Australia since the early 1990s. Research on *L. majuscula* growth in Moreton Bay to date has focused on the water column supply of iron and phosphorus with little consideration of benthic sources and supply. This is despite *L. majuscula* occurring at the benthos. This study investigates the potential for benthic sediments to supply iron and phosphorus for *L. majuscula* growth after significant benthic community change following a major flood event in January 2011. Measurements of benthic oxygen, iron and nutrient fluxes were obtained by incubating intact sediment cores sampled from Deception Bay. The sediments were low in organic carbon and were dominated by an active microphytobenthic community. Results suggest that post-flood sediment communities are capable of supplying >1700 % of the daily *L. majuscula* Fe requirements and up to 10.6 % of daily P demands, suggesting that *L. majuscula* growth in Deception Bay is likely to be P limited. The benthic release of PO_4^{3-} and Fe(II) only occurred after water-column dissolved oxygen became depleted below 3 mg/L. This study suggests that the benthic release of PO_4^{3-} and Fe(II) could support the initiation and growth of *L. majuscula* blooms in Deception Bay.

3.2. Introduction

Lyngbya majuscula is a filamentous, non-heterocystous nitrogen-fixing cyanobacterium that naturally occurs in near-shore marine and coastal waters (Diaz et al., 1990). As a benthic species, *L. majuscula* grows from sediments or loosely attached to seagrass, macroalgae, corals and other hard substrates (Albert et al., 2005; Diaz et al., 1990).

Blooms of *L. majuscula* have been observed in Moreton Bay, Australia since the early 1990's (Dennison and Abal, 1999). The frequency and extent of these blooms appear to be increasing (Albert et al., 2005; Dennison et al., 1999; Watkinson et al., 2005), and are a growing concern due to their negative impact on human health, tourism, commercial fisheries and the ecology of the bay (Osborne et al., 2008; Osborne et al., 2001; Pittman and Pittman, 2005). *L. majuscula* blooms have also been reported throughout Australia, including other parts of Queensland, Western Australia and the Northern Territory (O'Neil et al., 2012), and worldwide, in Hawaii, Mozambique, the Philippines, Curacao, Guam and Florida (Dennison and Abal, 1999; O'Neil et al., 2012).

Laboratory studies show that the growth of *L. majuscula* is stimulated by phosphorus (P) (Elmetri and Bell, 2004), and the combination of iron (Fe) and chelating organic compounds (Ahern et al., 2006; Bell and Elmetri, 2007). The rapid increase in the occurrence of *L. majuscula* in Moreton Bay over the last decade has been linked to elevated P loads (Elmetri and Bell, 2004; Wulff et al., 2011) and this has been provided as evidence to support the notion that Moreton Bay is potentially P limited (Wulff et al., 2011).

Most research in Moreton Bay to date has been undertaken on the premise that Fe and P to support biological activity are primarily supplied from the water column (see Dennison and Abal, 1999), despite the low ambient concentrations of their bioavailable forms (PO_4^{3-} and Fe(II)). In oxygenated marine waters, iron generally exists in the form of non-bioavailable insoluble Fe(III) oxyhydroxides. Previous research has demonstrated that *L. majuscula* can use superoxide (a reduced form of oxygen) to facilitate iron uptake in coastal waters through the reduction of Fe(III) to Fe(II) (Rose et al., 2005), consistent with water column supply of Fe. However, surprisingly, few studies have considered the potential role of the benthos, where sediments are known to play a significant role in the cycling of both Fe and P in coastal ecosystems (Rozan et al., 2002). Recent research into the growth dynamics of *L. majuscula* in Deception Bay by Johnstone et al. (2007) suggests

that the initiation and growth of an *L. majuscula* bloom is linked to a benthic release of P and Fe, triggered by a depletion in sediment oxygen concentrations.

In January 2011, a major flood event occurred in the Brisbane River with an average recurrence interval estimated at 120 years (Babister and Retallick, 2011). The flows in the lower reaches of the Brisbane River peaked on 13 January 2011. During this flood, the load of sediments to Moreton Bay over a 10 day period was estimated to be in excess of 1 million tonnes, representing three times the annual load normally received by the Bay (DERM, 2011). The flood resulted in the widespread loss of the seagrass species *Syringodium isoetifolium* and macroalgae from northern Deception Bay, resulting in large areas of unvegetated sediments (Hanington et al., 2015). This study measures benthic fluxes of PO_4^{3-} and Fe(II) from post-flood sediments in northern Deception Bay. These results are used to assess whether benthic sediments, in both post-flood and non-flood conditions, have the potential to supply sufficient P and Fe to support the initiation and growth of *L. majuscula* blooms in northern Deception Bay.

3.3. Materials and methods

Study site description

This study was undertaken in northern Deception Bay (27°05'S, 153°08'E), located in north-west Moreton Bay, Queensland, Australia (Figure 7). Moreton Bay is a semi-enclosed shallow estuarine embayment located adjacent to Australia's third largest city, Brisbane (Figure 7). It has an area of approximately 1,523 km², an average water depth of 6.3 m (max. 29 m), and is characterised by a subtropical climate with summer-dominated rainfall. Moreton Bay contains a diverse range of plant and animal life (Davie, 2011) and is important to the local economy through recreational and commercial fisheries and tourism. The associated catchment (21,220 km²) has been extensively modified by human activity and is under increasing pressure from urban development (Dennison and Abal, 1999).

The study site in northern Deception Bay is characterised by shallow (< 3 m) subtidal and intertidal seagrass meadows that have been subjected to extensive and frequent *L. majuscula* blooms since the early 1990's, including the largest blooms recorded in Moreton Bay (Albert et al., 2005; Watkinson et al., 2005). The broader area of Deception Bay receives riverine inputs from the Caboolture River and terrestrial runoff from a number of small tidal creeks and urban stormwater drains that are predominantly located along its southern and western shoreline. In addition, Deception Bay receives inputs from the

Brisbane River via the net northward movement of water along the western side of Moreton Bay (Dennison and Abal, 1999). In the north of the bay and adjacent to the current study site, bay waters exchange with the estuarine waters of Pumicestone Passage (Eyre and France, 1997), and the ocean via a large (16 km wide) opening to the north. The surrounding geology consists of a Holocene beach ridge system with coastal plain deposits containing iron sulfides (Cox et al., 2007). This geology and its associated groundwaters have been identified as a potential source of Fe, P and N to the study site via groundwater discharge, local watercourses and drainage networks (Ahern et al., 2006; Cox et al., 2007).

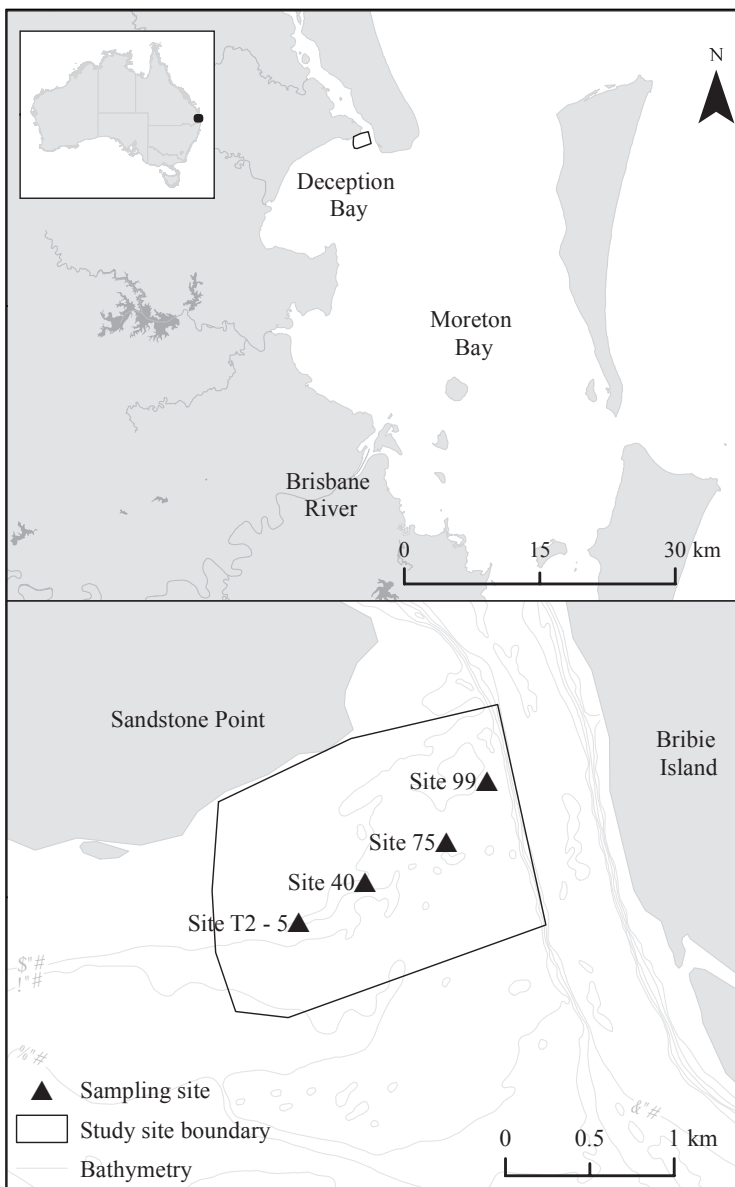


Figure 7 Location of sampling sites in northern Deception Bay.

Benthic flux incubation experiments

Intact sediment core samples were collected from northern Deception Bay at three locations (sites 40, 75 and 99, Figure 7) on 1 February 2011, approximately 3 weeks after the Brisbane River flood peak. A second sampling event was undertaken at site 40 (see Figure 7) on 25 October 2011, approximately 9 months after the flood peak. On each occasion and at each site, four replicate bare-sediment cores were collected by hand on SCUBA using 86 mm diameter acrylic cores, retaining approximately 150 mm of sediment and 1 litre of overlying water. Care was taken during sampling and handling to ensure minimal disturbance of the sediment vertical structure. Cores were transported to the laboratory in an ice-water bath and kept at $< 4\text{ }^{\circ}\text{C}$ until further processing. Site water was collected for use in sediment core incubation experiments via a pump fitted with a $0.5\text{ }\mu\text{m}$ polypropylene filter. Water samples for dissolved nutrient analyses were also collected and filtered using $0.45\text{ }\mu\text{m}$ cellulose-acetate filters, transported to the laboratory on ice, and then frozen at $-30\text{ }^{\circ}\text{C}$ until analysed, usually within 4 weeks of sampling.

In the laboratory, sediment cores were allowed to stabilise for approximately 12 hours in a water bath at *in situ* temperatures. Oxygen levels in the water column overlying each core were maintained by bubbling air and stirring using a Teflon bar-magnet suspended 5 cm above the sediment surface at a rate just below the threshold for sediment resuspension. After the equilibration period, the overlying water in each core was replaced with filtered site water that had been aerated overnight. Incubations commenced 2 hours after the water exchange. Light incubations were undertaken first, with *in situ* light conditions replicated using 4 x 150 W metal-halide lamps; dark incubations were undertaken after another 12 hour equilibration period and water exchange. All incubations were run for approximately 6 hours, with the exception of the October 2011 dark incubations. These incubations were extended beyond 6 hours (total 27 hours) in order to observe fluxes during hypoxic conditions (water column dissolved oxygen $<3\text{ mg L}^{-1}$, as per lowest levels measured *in situ*). Core water was maintained at $30\text{ }^{\circ}\text{C}$ using aquarium heaters to regulate water bath temperature. Teflon stirrers were used to maintain sediment-water boundary conditions at the threshold for sediment resuspension to approximate benthic conditions observed in the field. Water column controls, using filtered site water without sediments, were also incubated to account for fluxes in the water column.

Dissolved oxygen (DO) concentrations were logged at 15 minute intervals throughout the duration of the incubations using a TPS (model WP-61) water quality meter and YSI dissolved oxygen-temperature sensor (Clark membrane). Water samples for nutrient and Fe(II) analyses were withdrawn at regular intervals (approximately every 2 hours) with a plastic syringe and filtered through 0.45 μm cellulose-acetate filters. Extracted water was immediately replaced with an equal amount of filtered site water. Samples for nutrient analyses were immediately frozen at -30°C until analysed, whilst samples for Fe(II) analysis were analysed immediately after sampling.

All water samples were analysed for soluble reactive phosphorus (PO_4^{3-}), ammonium (NH_4^+) and combined nitrate and nitrite (NO_x^-) as per methods described by Parsons et al. (1984). During experiments conducted in February 2011, Fe(II) was determined via the ferrozine method as described by Viollier et al. (2000) using a long optical path length modular spectrophotometry system, consisting of an Ocean Optics USB4000 UV-visible spectrometer coupled to a PX-2 Xe flash lamp and 1 m path length liquid waveguide capillary cell, as previously employed by Rose and Waite (2005). Sulphide (S^{2-}) was determined by the methylene blue method as described by Cline (1969), also using the long optical path length spectrophotometry system. During experiments conducted in October 2011, Fe(II) was determined via the more sensitive luminol method, as described by Rose and Waite (2001), using a Waterville Analytical FeLume chemiluminescence system. Sulphide was not measured during these latter experiments. Quality assurance was maintained during all laboratory analyses with the use of certified reference materials (ENCT Round 14; natural seawater) supplied by Queensland Health Scientific Services.

Fluxes across the sediment-water interface were calculated using linear regression of the concentration data and corrected for water column controls (4 replicates). Reported fluxes were determined from the average of 4 replicate cores from each site and are expressed as a function of incubation time, core water volume and sediment surface area. Positive fluxes indicate an efflux from the sediment to the water column, whereas negative fluxes indicate an uptake by the sediments from the water column.

To determine benthic metabolism, oxygen fluxes were converted to carbon using both a photosynthesis quotient (PQ) and respiratory quotient (RQ) of 1. Benthic respiration (R) was calculated from mean DO fluxes measured in the dark (r_D) over 24 hours ($R = r_D \times 24$). Gross (benthic) primary production (GPP) was calculated by adding light flux rates

(rL) over 12 hours and dark flux rates (rD) over 12 hours ($GPP = (rL \times 12) + (rD \times 12)$). Net (benthic) production was calculated as the difference between GPP and R ($NP = GPP - R$). The ratio of GPP to R was calculated (p/r ratio), with $p/r > 1$ indicating sediments are net autotrophic, and $p/r < 1$ indicates sediments are net heterotrophic (Eyre and Ferguson, 2002).

In situ dissolved oxygen and temperature

Water column DO was measured at the study site using a TPS (model WP-61) water quality meter and YSI dissolved oxygen-temperature sensor (Clark membrane). The DO meter was enclosed in a waterproof casing and deployed on the benthos (at seagrass canopy level) at two locations (sites 40 and 99, Figure 7) during a four month period from 27 October 2010 to 22 February 2011. Sensors were replaced every four to five days to prevent the build up of biofilms across the sensor membrane and recharge logger batteries. The short deployments were sufficient to prevent significant sensor fouling.

Water column temperatures were also logged from 27 October 2010 to 22 February 2011 using a combination of sensors, including TPS water quality meters (as above), Odyssey submersible temperature loggers (Dataflow Systems Pty Ltd, New Zealand) and Hobo (Onset) pendant light / temperature loggers.

Sediment oxygen and redox microprofiles

DO concentrations and redox potentials in sediment porewaters were measured *in situ* using Clark-type oxygen and redox microsensors (100 μm tip diameter, Unisense) attached to an underwater meter and micromanipulator. A total of 57 sediment DO profiles were measured in bare sediments at three locations (sites 40, 75 and 99; see Figure 7) adjacent to seagrass on 18, 22 and 30 November 2010, representing pre-flood conditions.

A total of ten sediment DO and four redox profiles were measured at site 40 on 4 December 2011, approximately 11 months after the Brisbane River flood peak. Oxygen microsensors were calibrated using a two-point calibration at 100 % saturation and zero. Redox microsensors were calibrated using quinhydrone redox buffers and adjusted relative to standard hydrogen electrode (SHE) potentials. Four replicate profiles were measured at each location. Differences in maximum sediment DO concentrations and O_2 penetration depth between pre- and post flood conditions were tested using the unpaired Students' t-test in Microsoft Excel. All fluxes are presented as means of four replicates \pm standard error (SE).

Sediment solid-phase composition

Additional sediment cores (in triplicate) were sampled on 1 February 2011 for bulk density and on 25 October 2011 for solid-phase analyses. Subsamples for chemical analyses were immediately frozen and stored at -30°C until further processing. Four sediment cores were sectioned within 12 hours of collection at five depth intervals: 0-1 cm, 1-2 cm, 2-3 cm, 4.5-5.5 cm and 9.5-10.5 cm. Each section was then homogenised after coarse fragments (> 2 mm) such as shell, gravel and living biota were removed. Sediment samples were analysed for Total Organic Carbon (TOC) and Total Nitrogen (TN) using a LECO CNS2000 Analyser in accordance with methods described by Rayment and Higginson (1992). Total Phosphorus (TP) and Iron (Fe) were determined after acid digestion (nitric and hydrochloric) and analysed using an inductively-coupled plasma mass-spectrometer following procedures outlined in Rayment and Higginson (1992) and method 3125 (APHA, 2005).

3.4. Results

Nutrient fluxes

PO₄³⁻ fluxes were generally directed into the sediments (i.e. uptake) during the six-hour light and dark incubations, and usually greater in light conditions (Figure 8). The extended (27 hour) dark incubation showed an uptake of PO₄³⁻ during the first 6 hours, followed by a release. PO₄³⁻ fluxes in light conditions were consistent between sites and ranged from -1.4 (SE=0.5) μmol m⁻² h⁻¹ at site 75 (February 2011) to -2.1 (SE=0.7) μmol m⁻² h⁻¹ at site 40 (February 2011). PO₄³⁻ fluxes in dark conditions were more variable between sites and also within site replicates, ranging between -0.2 (SE=0.5) μmol m⁻² h⁻¹ at site 75 (February 2011) to 1.2 (SE=0.4) μmol m⁻² h⁻¹ at site 40 during the extended incubations (October 2011).

Benthic NH₄⁺ fluxes were variable between sites and between site replicates (Figure 8). Sediments showed an uptake of NH₄⁺ during light incubations, with mean fluxes ranging from -10.0 (SE=10.1) μmol m⁻² h⁻¹ at site 75 (February 2011) to -54.8 (SE=55.1) μmol m⁻² h⁻¹ at site 40 (February 2011). NH₄⁺ fluxes during dark conditions varied between sites and showed both uptake and release, with mean fluxes ranging from -22.9 (SE=4.3) μmol m⁻² h⁻¹ at site 75 (February 2011) to 16.3 (SE=26.2) μmol m⁻² h⁻¹ at site 40 (February 2011). Benthic NO_x⁻ fluxes showed variability between sites and between site replicates (Figure 8). Sediments generally showed an uptake of NO_x⁻ during light incubations, with

mean fluxes ranging from -6.0 (SE=8.8) $\mu\text{mol m}^{-2} \text{h}^{-1}$ at site 99 (February 2011) to -14.0 (SE=2.1) $\mu\text{mol m}^{-2} \text{h}^{-1}$ at site 40 (October 2011). NO_x^- fluxes during dark conditions varied between sites and showed both uptake and release, with mean fluxes ranging from -2.7 (SE=1.7) $\mu\text{mol m}^{-2} \text{h}^{-1}$ at site 40 (February 2011) to 5.2 (SE=2.0) $\mu\text{mol m}^{-2} \text{h}^{-1}$ at site 99 (February 2011).

Fe(II) and S^{2-} fluxes

Fe(II) fluxes were less than could be calculated from concentration differences using an instrument with a detection limit of $0.01 \mu\text{M}$ during the February 2011 core incubations (Figure 8). However, a small efflux from dark incubated cores taken from site 40 was measured at $0.56 \mu\text{mol m}^{-2} \text{h}^{-1}$ (data not shown). Incubations were repeated from site 40 during October 2011, with an improved detection limit of $0.0005 \mu\text{M}$ due to use of the more sensitive analytical method and extended dark incubation period. No detectable Fe(II) fluxes were observed during light incubations undertaken in October 2011, but during dark incubations an efflux of 0.0125 (SE=0.007) $\mu\text{mol m}^{-2} \text{h}^{-1}$ of Fe(II) was observed between 6 hours and 20 hours incubation time (Figure 8). No Fe(II) fluxes were observed between 0 and 6 hours of incubation or after 20 hours of incubation.

S^{2-} fluxes were less than could be calculated from concentration differences using an instrument with a detection limit of $0.01 \mu\text{M}$ during the February 2011 incubations, and were not determined during the October 2011 incubations.

Dissolved oxygen fluxes and benthic metabolism

Benthic DO fluxes in light conditions showed an efflux from the sediment to the water-column (Figure 8), with mean DO fluxes ranging from 592 (SE=223) $\mu\text{mol m}^{-2} \text{h}^{-1}$ at site 40 (October 2011) to 1269 (SE=237) $\mu\text{mol m}^{-2} \text{h}^{-1}$ at site 75 (February 2011). Oxygen fluxes in dark conditions showed an uptake of DO from the water column into the sediment (Figure 8), with mean fluxes ranging from -185 (SE=36) $\mu\text{mol m}^{-2} \text{h}^{-1}$ at site 40 (October 2011) to -667 (SE=263) $\mu\text{mol m}^{-2} \text{h}^{-1}$ at site 99 (February 2011).

Rates of benthic gross primary production (GPP), benthic respiration (R) and net community production (NCP) were calculated from all sediment core incubations, with rates varying between sites (Table 3). Sites 40 and 75 were strongly net autotrophic with p/r ratios of 1.3 and 1.9 respectively in February 2011 and p/r of 2.1 for site 40 in October 2011. Conversely, site 99 showed net heterotrophic conditions (p/r = 0.8) in February 2011.

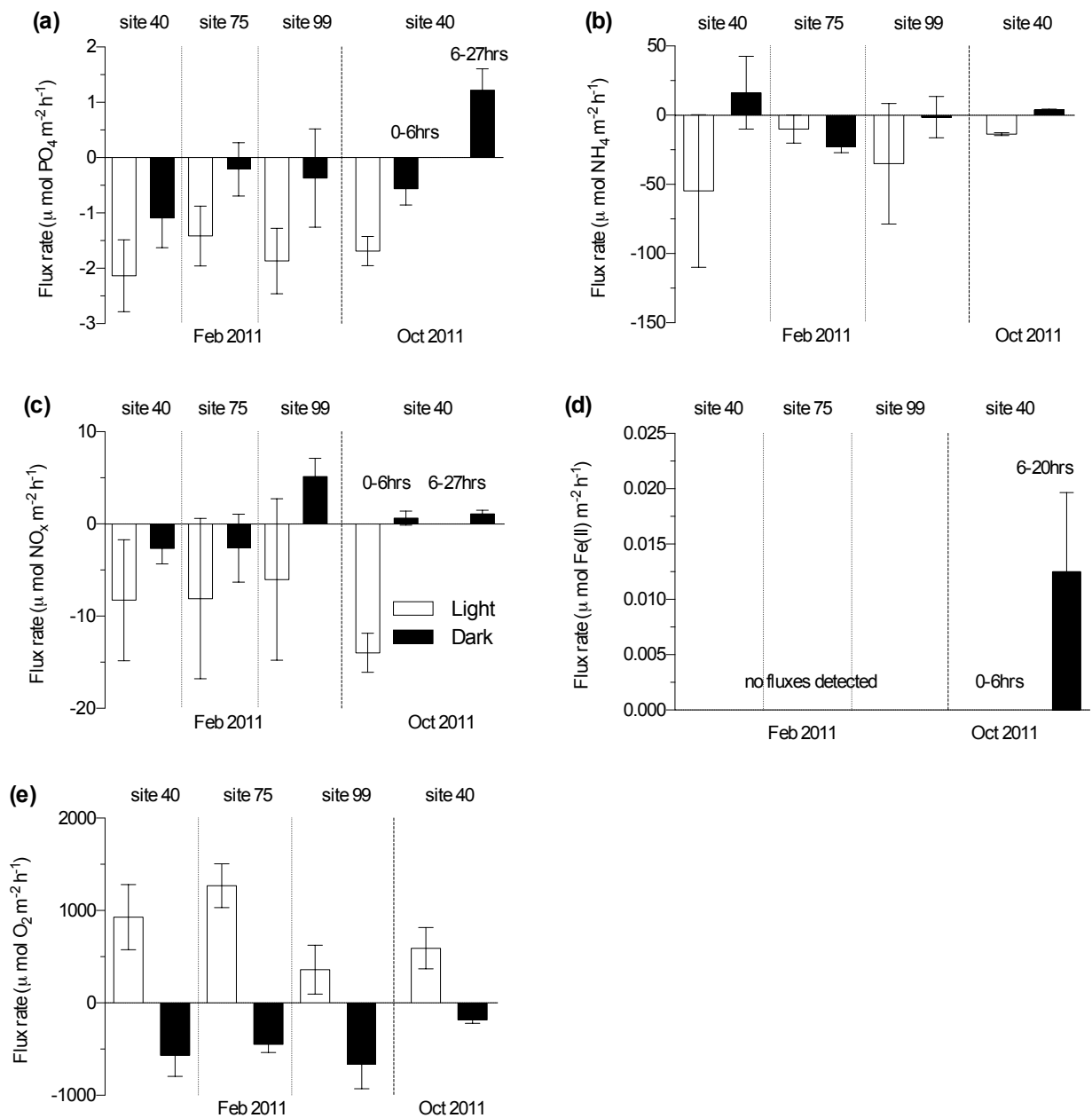


Figure 8 Benthic fluxes of (a) PO_4^{3-} , (b) NH_4^+ , (c) NO_x^- , (d) Fe(II) and (e) DO measured under light and dark conditions on sediment cores sampled from northern Deception Bay on 1 February 2011 and 25 October 2011. Error bars = SE of 4 replicate samples.

Table 3 Summary of benthic metabolic rates for community respiration (R), gross primary production (GPP) and net community production (NCP). All rates are expressed in $\text{mg C m}^{-2} \text{d}^{-1}$. p/r represents the ratio between community productivity and respiration.

Location	R	GPP	NCP	p/r
1 February 2011 sampling				
Site 40	-163	215	52	1.3
Site 75	-129	247	118	1.9
Site 99	-192	148	-44	0.8
25 October 2011 sampling				
Site 40	-53	112	59	2.1

In situ dissolved oxygen and temperature

From November 2010 to February 2011, water column DO ranged from 2.37 mg/L (at site 40 at 01:21 on 16 December 2010), to 7.42 mg/L (at site 40 at 17:37 on 22 November 2010), while temperatures ranged from 22 °C to 30.1 °C. A subset of the logged water column DO is shown in Figure 9. Diel patterns in water column DO and temperature were evident during both pre- and post-flood neap-tide conditions. The lowest DO concentration occurred during pre-flood conditions on an out-going neap tide, while the highest concentration occurred late afternoon on an in-coming spring tide.

Sediment oxygen and redox microprofiles

All pre-flood (November 2010) sediment DO profiles showed DO penetration depths ranging from 1 mm to 7 mm into the sediment (Figure 10). The majority of profiles showed highest DO concentrations just below the sediment-water interface, at depths ranging between 0 mm and 3 mm; the maximum DO concentration was 275 $\mu\text{mol L}^{-1}$.

All post-flood (December 2011) sediment DO profiles showed DO penetration depths ranged from 5 mm to >15 mm into the sediment (Figure 10). All post-flood profiles showed DO production below the sediment-water interface, with a maximum DO concentration of 815 $\mu\text{mol L}^{-1}$ measured at depths ranging between 1 mm and 4 mm below the sediment surface. Maximum DO concentrations and DO penetration depth were significantly higher ($p < 0.001$) in post-flood sediments compared with pre-flood sediments from the same site (site 40).

Four redox profiles were also measured in post-flood sediments (Figure 10). From this limited data set, the lowest sediment oxidation-reduction potential (ORP) was recorded as -468 mV at 15mm depth. ORP tended to become more reducing with increasing sediment depth and decreasing DO concentrations.

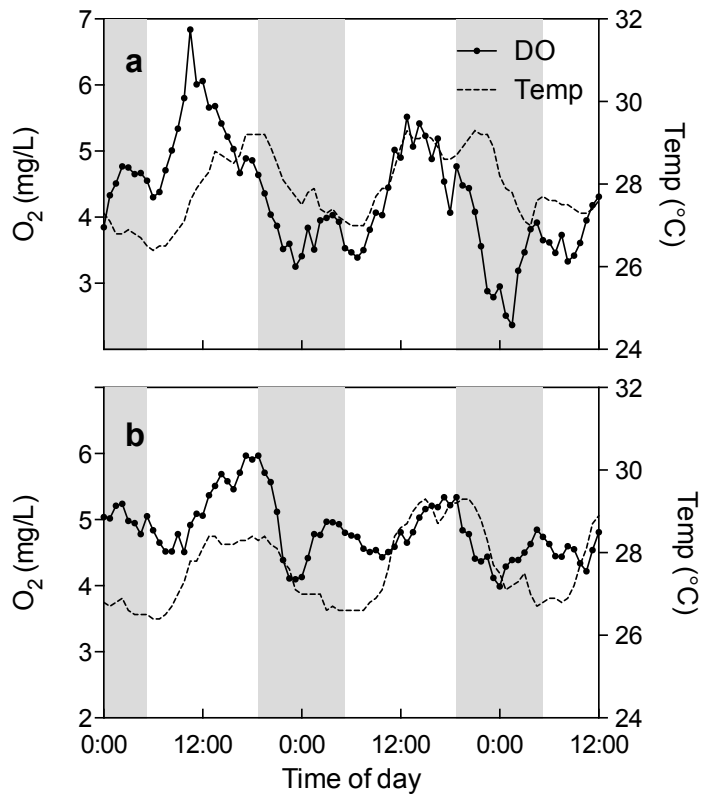


Figure 9 Diel variations in water-column DO and temperature during neap-tides at site 40 in northern Deception Bay during (a) pre-flood conditions from 14 to 16 December 2010 and (b) post-flood conditions from 12 to 14 February 2011. Shaded areas represent night-time hours.

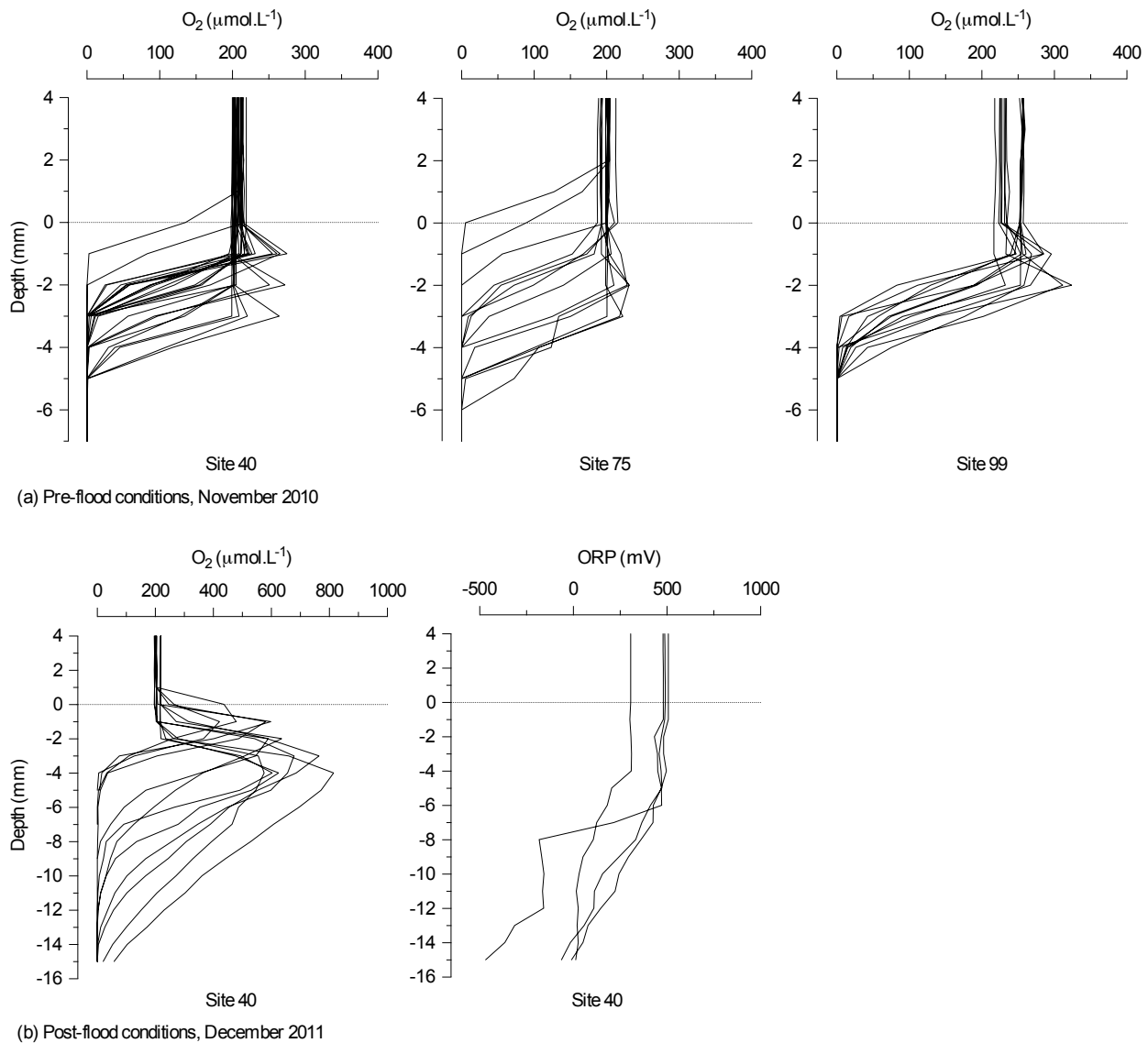


Figure 10 In situ microprofiles of (a) oxygen measured on 18, 22 and 30 November 2010 pre-flood conditions in sediments adjacent to seagrass at sites 40, 75 and 99 in northern Deception Bay, and (b) oxygen and Redox measured on 4 December 2011 post-flood conditions in bare sediments at site 40 in northern Deception Bay.

Sediment solid phase composition

The post-flood mean concentration of organic carbon (measured as TOC) in surface sediment (0-1 cm) sampled from site 40 (25 October 2011) was 0.04 (SD=0.01) % dry wt (Table 4), an order of magnitude less than that recorded during pre-flood conditions (0.31 (SD=0.10) % dry wt study site mean; see Chapter 2). Concentrations of TOC in post-flood sediments remained low at all sediment depths, with the highest mean concentration of 0.07 (SD=0.04) % dry wt at sediment depth 4.5 – 5.5 cm. Post-flood sediment TOC

appeared to vary with depth, whereas pre-flood sediments showed a trend of decreasing TOC with depth. Post-flood concentrations of TN, TP and Fe were also considerably less than mean pre-flood concentrations (Table 4) and tended to remain consistent with depth. Conversely, concentrations of TN, TP and Fe in pre-flood sediments tended to decrease with depth (see Chapter 2). The low sample replication at site 40 and the limited spatial extent of the post-flood sampling prevents any robust statistical-based comparisons between sampling events.

Table 4 Pre and Post-flood sediment composition for Site 40, northern Deception Bay, January 2009 (see Chapter 2) and 25 October 2011. Figures in brackets are the mean of all sediments (n=100), SD denotes standard deviation.

Depth	Pre-flood mean sediment composition (n=1) (% dry wt)				Post-flood mean sediment composition (n=3) (% dry wt)			
	TOC	TN	TP	Fe	TOC	TN	TP	Fe
0-1 cm	0.70 (0.31)	0.052 (0.032)	0.015 (0.0084)	0.54 (0.251)	0.04 SD=0.01	0.02 SD=0.007	0.004 SD=0.0004	0.10 SD=0.01
1-2 cm	0.64 (0.30)	0.046 (0.030)	0.012 (0.0071)	0.45 (0.226)	0.06 SD=0.04	0.01 SD=0.005	0.003 SD=0.0006	0.11 SD=0.06
2-3 cm	0.49 (0.29)	0.047 (0.028)	0.010 (0.0066)	0.40 (0.221)	0.04 SD=0.04	0.01 SD=0.007	0.003 SD=0.0004	0.10 SD=0.03
4.5 – 5.5 cm	0.39 (0.25)	0.033 (0.024)	0.008 (0.0054)	0.39 (0.207)	0.07 SD=0.04	0.02 SD=0.005	0.004 SD=0.0002	0.15 SD=0.05

3.5. Discussion

Phosphorus-iron-oxygen interactions

Benthic PO_4^{3-} fluxes measured in this study were similar to those reported by Eyre et al. (2011a) for non-vegetated sandy sediments in southern Moreton Bay, and within, but at the lower end of, the range reported for estuaries elsewhere (see Cowan et al., 1996). Dissolved inorganic nitrogen (DIN) fluxes ($\text{NH}_4^+ + \text{NO}_x^-$) were also within, but at the lower end of, the range reported for estuaries elsewhere (see Cowan et al., 1996). We are not aware of any studies that have investigated the flux of Fe from similar sub-tropical coastal systems.

Our results show that the benthic cycling of P and Fe are clearly influenced by changes in water column DO concentrations and associated sediment conditions. *In situ* sediment DO microprofile measurements indicate an oxidised surface layer maintained by

an active microphytobenthic (MPB) community. Within this oxidised sediment layer, Fe is likely to exist in the form of insoluble Fe(III) oxyhydroxides (Rose et al., 2005). The more bioavailable and soluble form of Fe occurs as Fe(II) which is unstable and quickly oxidised in the presence of oxygen. Any Fe(II) diffusing from deeper anaerobic sediments tends to accumulate, and is effectively trapped, in the oxidised surface layer as Fe(III) oxyhydroxides.

This oxidised sediment layer also regulates dissolved PO_4^{3-} diffusing into the surface sediment from the water column, as well as from deeper sediments where the anaerobic decomposition of organic matter acts to remineralise PO_4^{3-} . A known mechanism for the uptake of P into marine sediments occurs via the sorption of PO_4^{3-} to oxyhydroxides in oxidised surface layers (Hopkinson et al., 1999). Our results show that the incubated sediments tend to take up PO_4^{3-} when water column DO concentrations are above 3 to 4 mg L^{-1} . This supports the notion of a DO regulated PO_4^{3-} uptake and release from surface sediments.

The results of sediment core incubations presented here demonstrate that during dark conditions, when oxygen concentrations within the water column become depleted ($< 3 \text{ mg L}^{-1}$), an efflux of both Fe(II) and PO_4^{3-} occurs from the sediment. Numerous studies (e.g. Cook et al., 2010; Ingall and Jahnke, 1997; McManus et al., 1997; Sundby et al., 1992) show that the benthic cycling of P and Fe is influenced by DO and associated sediment redox conditions, with the benthic release of PO_4^{3-} resulting from the reduction of Fe-bound P driven by low water column DO concentrations. The interactions between Fe, P and DO play an important role in the benthic cycling and release of PO_4^{3-} and Fe(II) in systems such as northern Deception Bay, where sediments are sandy and relatively low in organic carbon.

Oxygen dynamics

Rates of GPP and R in non-seagrass sediments measured during this study were at the lower end of the range reported for sediments in southern Deception Bay (Ferguson and Eyre, 2010) and for other parts of Moreton Bay and elsewhere (Eyre et al., 2011b, and references therein). These relatively low rates of benthic metabolism are likely to reflect post flood conditions (see Hanington et al., 2015) and site-specific conditions, such as the sandy, low organic carbon content of the sediments.

In situ monitoring of DO shows that during early summer, water-column DO concentrations can decrease substantially over a diurnal cycle, to as low as 2.37 mg L⁻¹ at night. This lowest recorded water column DO occurred during a period of neap-tides, when tidal influences on water movement are lowest. Short-term hypoxic events are often common in deeper stratified systems but are less common in shallow estuaries (Paerl, 2006; Testa and Kemp, 2012). However, this study demonstrates that short-term hypoxic conditions can occur within a shallow, well-mixed estuary when conditions are suitable, i.e. at night during summer when water temperatures are warm, in combination with low water movement (neap tides and calm conditions). The occurrence of these conditions is central to our hypothesis that the initiation and growth of an *L. majuscula* bloom is linked to a benthic release of P and Fe triggered by a depletion in sediment DO driven by short-term water column hypoxia.

Contribution of benthic phosphorus and iron fluxes to L. majuscula growth

To assess the capacity of benthic sediments to supply P and Fe for *L. majuscula* growth, *L. majuscula* P demands were estimated from studies undertaken by Johnstone et al. (2007) documenting the development of two consecutive *L. majuscula* blooms in Deception Bay from 2005 to 2007. Daily P demands (0.06 g P m⁻² d⁻¹) were derived from changes in *L. majuscula* biomass averaged across the growth phase of the 2006-07 Deception Bay bloom (Figure 11) and measured changes in *L. majuscula* tissue carbon and nutrient content during this growth phase. Based on these demand estimates and the rates of benthic flux measured in this study, the post-flood sediments in Deception Bay are capable of supplying <1 % of the daily *L. majuscula* P requirements. This estimate is based on a net sediment-water flux (including uptake by MPB). However, tufts of *L. majuscula* at the benthos are likely to see higher P effluxes as MPB communities are displaced by an expanding *L. majuscula* bloom. By subtracting MPB P demands, derived from benthic community metabolism rates (Table 3), the sediments at the study site are capable of providing between 5.2 % to 10.6 % of P requirements for *L. majuscula* growth.

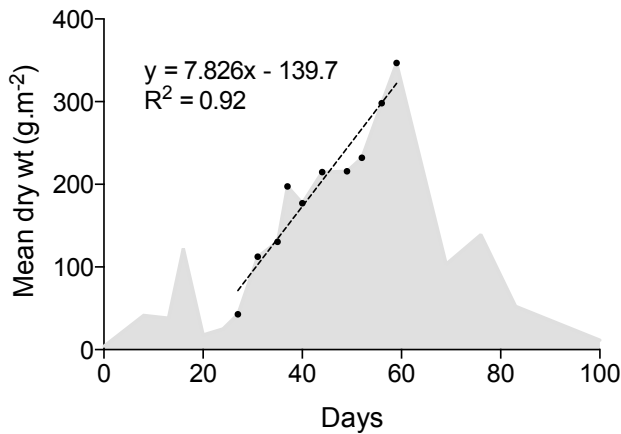


Figure 11 Mean *L. majuscula* biomass at sample site T₂₋₅, sampled during the 2006-2007 summer bloom. The graph shows the linear growth rate averaged over the development of the bloom used to estimate *L. majuscula* N and P demands (modified from Johnstone et al., 2007).

Our results show that the availability of P in post-flood benthic sediments is likely to limit the growth of *L. majuscula* in Deception Bay, a notion supported by other studies such as Elmetri and Bell (2004) and Ahern et al. (2007a). Note that given *L. majuscula* is diazotrophic, N demands can be met by atmospheric sources, and therefore N supply is not a limiting factor for its growth.

However, the contribution of P from benthic sediments in Deception Bay is likely to be higher in more typical conditions. Estimates here are based on fluxes from unvegetated sediments after a major flood event, which caused widespread loss of seagrass and macroalga at the study site (Hanington et al., 2015). These post-flood sediments were low in TOC and P compared with pre-flood sediments at the study site (Table 4). Numerous studies show that seagrasses enhance sediment microbial activity, which drives benthic remineralisation processes and the flux of nutrients from the benthos (e.g. Holmer et al., 2001; Kaldy et al., 2006; Marbà et al., 2006; Mateo et al., 2006). Seagrasses achieve this by increasing the sedimentary organic matter pool by trapping particulate organic matter from the water column and releasing dissolved organic matter (DOM) via root exudates (Marbà et al., 2006). This release of DOM often accounts for a significant proportion of the overall dissolved organic carbon pool in shallow oligotrophic estuarine sediments (Marbà et al., 2006), like that of Deception Bay. In Deception Bay, seagrasses may promote the efflux of PO_4^{3-} from the benthos by enhancing sediment microbial activity and heterotrophic processes. Clearly more research is needed to confirm this and elucidate the interactions between individual seagrass species and the biogeochemical cycling of P.

The presence of *L. majuscula* at the benthos has also been shown to induce anaerobic conditions in its underlying sediments (Johnstone et al., 2007), likely further promoting benthic release of PO_4^{3-} . As *L. majuscula* biomass increases, it smothers larger areas of the benthos, halting photosynthetic DO production, thereby turning sediments anaerobic and increasing the likelihood of further benthic releases of PO_4^{3-} . Benthic flux measurements undertaken at the study site by Johnstone et al. (2007) indicated that a benthic community comprised of seagrass and *L. majuscula* was capable of supplying between 5 and 10 times the P needed for the growth of an *L. majuscula* bloom.

In the case of Fe, Rose et al. (2005) reported *L. majuscula* uptake demands of 10-100 pmol of $\text{Fe g}^{-1} \text{ h}^{-1}$ *L. majuscula* dry mass. Based on these demands and the growth dynamics of an *L. majuscula* bloom (Figure 11), the Fe(II) sediment effluxes measured in this study represent >1700 % of the daily *L. majuscula* Fe requirements (based on night time fluxes over a 6 hour period). Although these Fe(II) fluxes were induced experimentally by maintaining highly hypoxic conditions, they were within the range of water column DO concentrations that have been measured at the study site. In addition, the magnitude of the Fe(II) fluxes are so much greater than *L. majuscula*'s Fe demand that lower fluxes (i.e. fluxes that were below the detection limit of our experiments) may be sufficient to sustain its growth.

3.6. Conclusions

Iron is a key element that has been linked to the growth of *L. majuscula* blooms in Moreton Bay. Our results demonstrate that post-flood sediment communities in northern Deception Bay are more than capable of supplying all *L. majuscula* growth requirements for bioavailable Fe. However, the benthic supply of P from these sediments is likely to limit the growth of *L. majuscula* blooms without supplementary water column supplies.

This study provides insights into how benthic sediment communities may act to initiate and support the growth of *L. majuscula* blooms. In particular, it suggests that the initiation and growth of a bloom is likely to be linked to a benthic release of PO_4^{3-} and Fe(II) triggered by a depletion in sediment oxygen concentrations. To our knowledge, this study also represents the first documented benthic release of Fe(II) from permeable sandy sediments in a shallow subtropical embayment. Our results have implications for other coastal systems by demonstrating that benthic sediments are capable of supplying biologically significant amounts of bioavailable Fe at the sediment - water interface.

Further studies are needed to assess the capacity of other benthic community types within Moreton Bay, such as seagrass-dominated communities, for their capacity to support the growth requirements of an *L. majuscula* bloom. Our results support the notion that *L. majuscula* growth in Deception Bay may be P limited and that any future management actions targeted towards reducing *L. majuscula* blooms in Moreton Bay need to include a strategy for reducing P loads to the Bay.

Chapter 4

Changes to seagrass community composition after a major flood event in Moreton Bay, Australia: implications for benthic carbon cycling and *Lyngbya majuscula* blooms

Chapter 4 is an expanded version of a paper that has been published in the international journal *Aquatic Botany*. It has been modified here for clarity and greater relevance to the overall aims of this thesis.

Hanington, P.[†], Hunnam, K.[†] and Johnstone, R. (2015). Widespread loss of the seagrass *Syringodium isoetifolium* after a major flood event in Moreton Bay, Australia: Implications for benthic processes. *Aquatic Botany*, Vol. 120, pp. 244-250.

[†] Joint first authors

4.1. Abstract

The distribution of a seagrass community dominated by *Syringodium isoetifolium* declined by 100 % in northern Deception Bay (Moreton Bay, Australia) after a major flood event in January 2011. Seagrass surveys conducted immediately post-flood showed dieback of *S. isoetifolium*, while the co-dominant species *Z. muelleri* appeared unaffected. Follow-up visual transect surveys undertaken seven months post-flood showed nearly complete loss of *S. isoetifolium* and two macroalgal species *Caulerpa taxifolia* and *Udotea argentea*. Relatively little loss of *Zostera muelleri* and an intertidal mixed species community had occurred. Monitoring data collected during the flood period and comparison with previous studies suggests that difference in species tolerance to low salinity levels in combination with light deprivation is the most likely cause of the observed loss. Additional surveys undertaken eighteen months post-flood indicated patchy seagrass re-colonisation dominated by the early colonising species *Halophila ovalis*. Benthic metabolism data suggests these changes in benthic community composition have resulted in a switch from net benthic heterotrophy to net benthic autotrophy within the study site. Such a change in benthic metabolism has implications for the cycling of carbon and nutrients through seagrass ecosystems and the ecological services they underpin.

4.2. Introduction

Seagrass meadows are a key component of shallow coastal marine ecosystems, providing a range of important ecological functions. They often play a significant role in coastal biogeochemical cycling through a range of processes and feedbacks that influence the dynamics of carbon, nutrients, trace elements and oxygen within an ecosystem (see review by Marbà et al., 2006). These biogeochemical processes are often significant at an ecosystem level, where seagrass benthic communities act to sequester carbon and regenerate nutrients that support benthic and pelagic productivity. The loss of seagrass and the concomitant change to benthic community composition therefore has the potential to significantly alter key processes and hence the ecosystem services they underpin.

Seagrass ecosystems are typically dynamic, and natural and anthropogenic influences can result in total or partial seagrass mortality (e.g. Kirkman, 1978; Moore and Short, 2006; Preen, 1995; Valiela et al., 1997), a shift to an algal-dominated system (Duarte, 1995), and/or change in seagrass community composition (e.g. Campbell and McKenzie, 2004; Preen, 1995; Terrados et al., 1998). However, large-scale losses of seagrass have been reported in recent years in Australia (Campbell and McKenzie, 2004; Preen et al., 1995) and worldwide (Short and Wyllie-Echeverria, 1996; Waycott et al., 2009). The global decline of seagrass-dominated ecosystems has occurred through a multitude of human induced impacts, both direct and indirect, as well as from natural events such as severe weather and floods (Duarte, 2002). Changes in landuse within the coastal zone leading to increased nutrient and sediment runoff are thought to have exacerbated the effects of natural events on seagrass ecosystems (Orth et al., 2006), leading to changes in community structure (Douglass et al., 2010), and a decline in their resilience, or ability to recover from such large-scale disturbance (Lotze et al., 2006).

Moreton Bay (south-east Queensland, Australia) has extensive seagrass meadows (19000 ha; Roelfsema et al., 2009) that support economically important commercial and recreational fisheries. They are also a direct food source for dugong and sea turtle populations that reside in the Bay. The seagrass meadows of Moreton Bay are under threat from a host of human activities brought about by changes in catchment landuse that have resulted in increasing loads of sediment and nutrients entering the Bay (Dennison and Abal, 1999). Permanent loss of seagrass from Moreton Bay has occurred along the western shores of the Bay including in southern Deception Bay, located north of the Brisbane River mouth (Dennison and Abal, 1999). The loss of seagrass (1500 ha) within

this area is thought to be due to high levels of turbidity sustained by increasing inputs of sediment from the catchment and continued resuspension of benthic sediments (Dennison and Abal, 1999). While recent investigations undertaken in 2011 detected seagrass in southern Deception Bay for the first time since 1987, the majority of seagrass in Deception Bay is now restricted to the north (Roelfsema et al., 2013).

The marine cyanobacterium *Lyngbya majuscula* was first reported in the Deception Bay / Pumicestone Passage area in the early 1990s (Watkinson et al., 2005). Over the last 15 years, the northern Deception Bay seagrass meadow has been subjected to extensive and frequent blooms of *L. majuscula* (Dennison et al, 1999, Watkinson et al, 2005), which have been observed to smother benthic communities causing localised seagrass mortality during bloom events (Johnstone et al., 2007). The long-term impact of recurrent *L. majuscula* blooms and declining water quality on the northern Deception Bay seagrass meadow is unknown, as is how these pressures have affected the resilience of the seagrass meadow and its ability to recover from large-scale disturbance events.

In January 2011, a major flood event with an average recurrence interval (ARI) estimated at 120 years (Babister and Retallick, 2011) occurred in Moreton Bay catchments, including the Brisbane River. Over a 10 day period, an estimated sediment load in excess of 1 million tonnes was deposited into the receiving waters of Moreton Bay (DERM, 2011). This sediment load represents three times the annual load normally received by the Bay. A flood event of similar proportions last occurred in Brisbane in January 1974 (van den Honert and McAneney, 2011). This chapter investigates the change in benthic macroflora community composition in northern Deception Bay after the January 2011 Brisbane River flood. It considers the possible causes of this change and the potential implications for benthic processes, such as the biogeochemical cycling of carbon and nutrients through seagrass ecosystems. In addition, this chapter also examines the effectiveness of various techniques used to generate seagrass community distribution maps for detecting change.

4.3. Methods

Study site description

This study was undertaken in northern Deception Bay (27°05'S, 153°08'E), located in north-west Moreton Bay, Queensland, Australia (Figure 12). Moreton Bay is a semi-enclosed estuarine embayment located adjacent to Australia's third largest city, Brisbane.

The region is one of Australia's fastest growing urban areas, with rapid development having caused significant landuse change, creating pressure on the region's rich biodiversity. Moreton Bay is located between temperate and tropical bioregions and thus supports a unique blend of flora and fauna within a diverse range of habitat types (Davie, 2011). Moreton Bay is recognised for its ecological significance as a Ramsar listed wetland. The study site (259 ha) is characterised by shallow (<3 m) subtidal and intertidal sandy sediments, historically comprising of the seagrass species *Zostera muelleri*, *Syringodium isoetifolium*, *Halophila ovalis* and *Halodule uninervis*. The study site was positioned to capture the ecotone between the two dominant seagrass communities, *Z. muelleri*- and *S. isoetifolium*- dominated, and the areal extent of historical *L. majuscula* blooms. It was restricted in extent by water depth limitations for visual surveys. Based on seagrass mapping undertaken in 2004 (Roelfsema et al., 2009), the study site represents approximately 81 % of the northern Deception Bay seagrass meadow where the mapped seagrass cover was ≥ 25 % (18 % of the total meadow area).

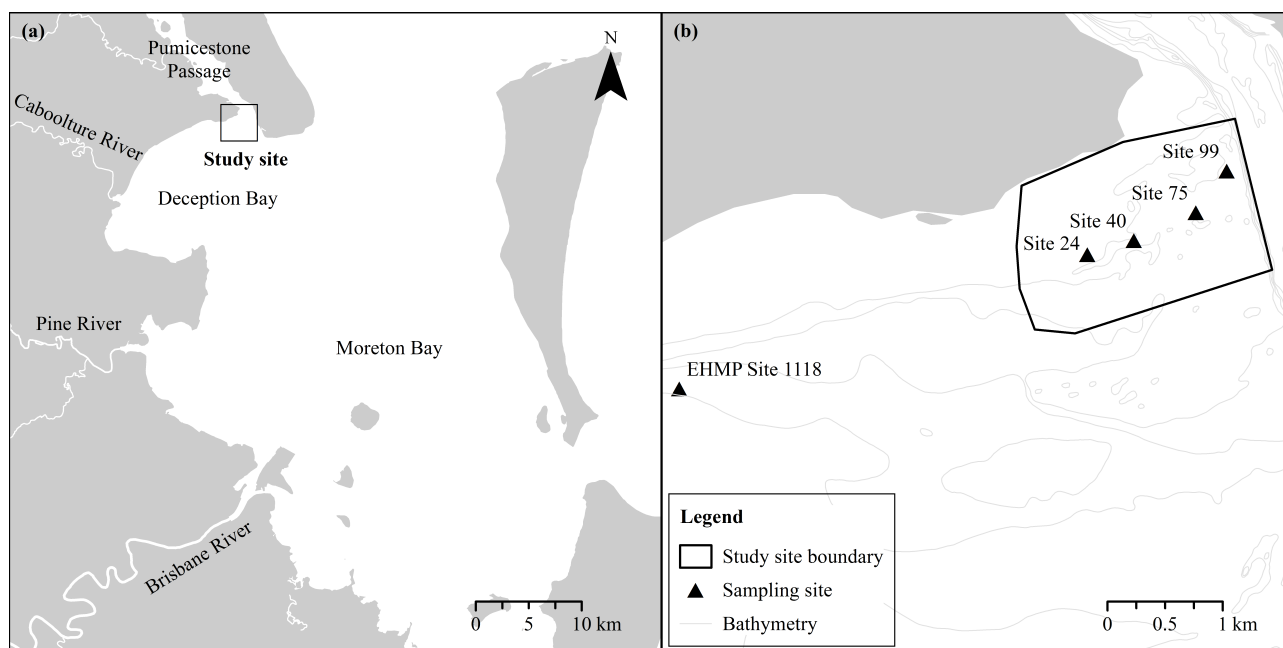


Figure 12 Location of study site in northern Deception Bay (a), showing the location of sampling sites (b)

Benthic macroflora community mapping – field-data interpolation

Detailed surveys of the benthic macroflora were undertaken in April – June 2008 (Hunnam, 2008), seven months post-flood in August 2011 and 18 months post-flood in July 2012. A rapid visual assessment was also undertaken on 25 January 2011, 12 days after the Brisbane River flood peak, using SCUBA at four locations (sites 24, 40, 75 and

99, Figure 12). Operational conditions and high water-column turbidity prevented a repeat of the detailed 2008 survey until August 2011. The field survey and mapping methodology employed in this study replicated that of Hunnam (2008), who conducted the visual benthic survey of the study site in 2008. In brief, detailed surveys were carried out using an underwater viewer attached to a boat, which allowed for clear visual assessment of the benthos up to 3 m deep during calm conditions. Community composition data (based on dominant macroflora) were recorded every 10 m along transects to identify and map the main benthic community types present. All observations were made by the same observer. Benthic community data were recorded at 2049 locations in 2008 (Hunnam, 2008), 1534 locations in 2011 and 1934 locations in 2012.

Community distribution maps for each detailed survey were created by interpolation of field data using indicator kriging, as used in previous studies (Holmes et al., 2007). Modelling and interpolation were performed using Geostatistical Analyst (ArcMap extension, v9.2 2004, ESRI Inc.). Continuous probability maps (10 m x 10 m grid) were generated from interpolated presence/absence data for each community type. Binary maps at the 50 % probability threshold were compiled in a geographic information system (GIS) to create a map showing all communities. Cross-validation of measured values against predicted values showed interpolation models correctly mapped 88–90 % of sites for the 2008 and 2011 maps; and 75 % for the 2012 map (likely due to higher spatial variability of patchy seagrass recovery). Fieldwork undertaken for Chapter Two of this thesis allowed for opportunistic validation of the 2008 map based on 100 sites surveyed in a systematic grid pattern in January 2009. These observations suggested the 2008 map had an accuracy of 81 % (allowing ± 10 m for positional error). Further detail of the survey technique and mapping methodology employed is given in Hunnam (2008).

Benthic macroflora cover mapping—airial imagery

High-resolution aerial images for 19 August 2010 and 28 July 2011 were obtained from www.nearmap.com to assess benthic macroflora cover four months pre-flood and six months post-flood. These were the latest and earliest images in time available, before and after the flood (respectively), which were of sufficient clarity (in terms of cloud cover, water depth and water turbidity) to undertake a benthic macroflora cover assessment. Maps of benthic macroflora cover were created by manual digitising at a scale of 1:5000.

Environmental variables

Light

Photosynthetic photon flux density (PPFD) was measured using Odyssey submersible 2π photosynthetic active radiation (PAR) loggers (Dataflow Systems Pty Ltd, New Zealand). PAR loggers were deployed in the water column and on the benthos at seagrass canopy level at two locations (Sites 75 and 99, Figure 12) and on the benthos only at two locations (Sites 24 and 40, Figure 12) during a three month period between 18th November 2010 to 25th February 2011. Gaps in the data set exist for some sites during the study period due to logger malfunction and / or lost loggers. However, logged light data at site 75 provides a continuous data set over the entire study period.

An additional PAR logger was deployed above water to measure the incident radiation at the study site. All loggers were inspected and manually cleaned every 4 to 5 days to prevent the build up of sediment and biofilms across the sensor. During inspection and cleaning, an independent PAR logger was used as a quality check to assess the degree of sensor fouling. The regular interval of 4 to 5 days between cleaning was sufficient to prevent the accumulation of biofilms across the sensor.

The PAR loggers were calibrated in air under varying light intensities using a LiCor PAR light meter. After calibration, all light intensity data collected from submerged PAR loggers were then multiplied by 1.33 (as per Kirk, 2011) to allow for differences in light absorption properties between air and water. Available light at the benthos is expressed as total daily light and daily mean % of surface irradiance. Both these measures are commonly used to quantify light penetration to the benthos and therefore the amount of light available to seagrass. The daily mean % of surface irradiance was determined from periods where the above-water PPFD was greater than $150 \mu\text{mol photons m}^{-2}\text{s}^{-1}$. This was done to minimise errors associated with differences between above and below water irradiance measures at low light intensities, where localised changes in incident light levels due to clouds (for example) can produce erroneous results. The value of $150 \mu\text{mol photons m}^{-2}\text{s}^{-1}$ was chosen as it has been considered as a minimum for photosynthetic light saturation for some seagrass species in Moreton Bay (Longstaff, 2003).

Salinity

Salinity data were obtained from the South East Queensland (SEQ) Healthy Waterways Partnership, collected as part of the Partnership's Ecosystem Health

Monitoring Program (EHMP). Salinity was measured throughout the water column using an electrical conductivity sensor incorporated into a multiprobe water quality meter. For the purposes of this study, monthly bottom water salinity measurements are presented for EHMP site 1118, which is the nearest EHMP site to the study area. Additional salinity measurements were also taken at the study site using a WP-84 conductivity meter (TPS) between February 2010 and June 2011.

Sediment deposition and composition

Sediment traps were deployed at three locations (sites 40, 75 and 99, Figure 12) during the period between 20 January to 11 February 2011. Sediment traps were deployed in triplicate at each site, fixed to the benthos via a stake and set at a distance of 0.5 m above the sediment surface to minimise inputs from sediment resuspension. The traps consisted of cylindrical PVC pipe with an internal diameter of 50 mm, capped at the bottom and with a height / diameter ratio of 3. A height / diameter ratio of ≥ 3 is considered to be optimal for cylindrical traps with a diameter of 50 mm (Blomqvist and Hakanson, 1981). Sediment traps were deployed for a maximum period of 5 to 6 days before sampling.

Upon return to the laboratory, subsamples of the trapped sediment were homogenised after living biota were removed, then oven dried at 60°C and ground to a fine powder using a mortar and pestle. Samples were analysed for Total Organic Carbon (TOC) and Total Nitrogen (TN) using a LECO CNS2000 Analyser in accordance with methods described by Rayment and Higginson (1992). Total Phosphorus (TP) and Iron (Fe) were determined after acid digestion (nitric and hydrochloric) and analysed using an inductively-coupled plasma mass-spectrometer following procedures outlined in Rayment and Higginson (1992) and method 3125 (APHA, 2005).

4.4. Results

Benthic community mapping

Pre-flood survey (April-June 2008) and aerial imagery (19 August 2010)

A summary of the results of the 2008 survey undertaken by Hunnam (2008) is provided as follows and presented in Figure 13a and Table 5. Seagrass and attached macroalgae was mapped across 90 % (234.6 ha) of the study area. Four seagrass species were recorded: *S. isoetifolium* was the most common, followed by *Z. muelleri*, *Halophila ovalis* and *Halodule uninervis* / *Z. muelleri* (small). *Halophila spinulosa* and *Cymodocea*

serrulata have also been observed within northern Deception Bay, but due to their relatively rare occurrence within the study area, were not recorded at any survey sites. *Z. muelleri* morphology was variable, with medium-sized plants (leaf width 4 mm; length 100-150 mm) in near-shore areas and large plants (length > 150 mm) in deeper water. Small *Z. muelleri* (width < 2 mm; length < 60 mm) and *Halodule uninervis* were recorded as a combined seagrass type due to their similar external appearance. *Z. muelleri* / *Halodule uninervis* and *Halophila ovalis* were less common and tended to be co-distributed.

Five broad community types were identified based on dominant species, species composition and morphology. *S. isoetifolium* and *Z. muelleri* (medium-tall) existed as primarily monospecific seagrass communities, which were present across 55 % (143.2 ha) and 22 % (57.5 ha) of the study area. The *S. isoetifolium* community tended to be distributed furthest from shore, while *Z. muelleri* was predominantly near-shore in shallower subtidal areas. The third community, comprised *Z. muelleri* / *Halodule uninervis* and *Halophila ovalis* typically colonised intertidal patches and was mapped across 7 % (17.1 ha) of the study area. A small area of the study area (3 %, 8.8 ha) was dominated by the algal species *Caulerpa taxifolia*, while a further 3 % (8.0 ha) was mapped as co-dominated by *C. taxifolia* and a seagrass species (usually either *S. isoetifolium* or *Z. muelleri*). *C. taxifolia* was also present as a minor benthic component across an additional 33.7 ha within the study area. Finally, un-colonised, bare sediment occurred in small, isolated patches, which could not be mapped using spatial interpolation methods (0.7 % of survey locations).

The attached macroalga *Udotea argentea* also formed a key component of the benthic communities surveyed. The alga was mapped across 72 % (187.3 ha) of the study area and present in all identified seagrass and algal-dominated communities types. Free-floating macroalgae, such as *Hydroclathrus clathratus*, and patches of *L. majuscula* were also observed. However, given the dynamic nature of the distribution of these species, only attached macrophytes were mapped. Note that Figure 13a does not illustrate the presence of *U. argentea* given its widespread distribution across the study site and its presence as a component of the community rather than the dominant species.

Approximately 10 % (24.8 ha) of the study area could not be identified from the interpolated maps. While a small proportion of this area may be attributed to bare sediment, the majority is likely to be vegetated substrate, which could not be distinguished

using the mapping methodology due to the high spatial variability (patchiness) of community types in these locations.

Aerial imagery taken on 19 August 2010 (4 months pre-flood) shows 247.1 ha (95 %) of benthic macroflora cover within the study area (Figure 13b, Table 5). This area and spatial distribution are consistent with the 2008 field interpolated map (Figure 13a and b, Table 5), and justify the use of the 2008 map as a baseline for comparison with post-flood mapping.

Post-flood rapid assessment (25 January 2011), survey (August 2011) and aerial imagery (28 July 2011)

The results of the rapid visual assessment survey undertaken on 25 January 2011, 12 days after the major flood peak showed dieback of *S. isoetifolium*, while *Z. muelleri* appeared unaffected.

The detailed survey undertaken seven months later (August 2011) showed seagrass was present across 47 % (123.1 ha) of the study area (Figure 13c, Table 5). Again, four seagrass species were recorded; however *Z. muelleri* was the most common, followed by *Halophila ovalis* and *Halodule uninervis* / *Z. muelleri* (small). *S. isoetifolium* was the least common, with small isolated individual plants observed at only 1.3 % of survey locations within the study area. Attached macroalgal species, *C. taxifolia* and *U. argentea*, were not observed at any survey locations within the study area. Using the same community classification as the 2008 survey, in August 2011 the previously widespread *S. isoetifolium*-dominated community had disappeared. Occurrences of individual *S. isoetifolium* plants were too sparse and isolated for spatial interpolation. The *Z. muelleri*-dominated community was mapped across the largest area (38 %, 99.2 ha), followed by the mixed intertidal seagrass community comprising *Halophila ovalis* and *Halodule uninervis* / *Z. muelleri* (9 %, 23.9 ha). The remaining study area (53 %, 136.3 ha) was not mapped as containing vegetated benthic communities. Bare sediment was recorded at 48.8 % of survey locations and predominantly distributed offshore in the subtidal areas where the *S. isoetifolium* community had previously been widespread.

Mapping derived from aerial imagery taken on 28 July 2011 confirms the presence of benthic macroflora cover across 37 % (95.1 ha) of the study area (Figure 13d, Table 5). It shows a similar distribution to the detailed survey map, with macroflora predominantly restricted to near-shore areas, but with finer patch detail (Figure 13c and d).

Table 5 Summary of results from pre-flood and post-flood benthic macroflora community surveys and seagrass cover estimates derived from aerial imagery, northern Deception Bay.

Community	Pre-flood area (ha)		Post-flood area (ha)		
	Survey Apr-Jun 2008	Aerial imagery Aug 2010	Aerial imagery July 2011	Survey Aug 2011	Survey July 2012
<i>Z. muelleri</i>	57.5 (22 %)	-	-	99.2 (38 %)	92.4 (36 %)
<i>S. isoetifolium</i>	143.2 (55 %)	-	-	0.0 (0 %)	0.0 (0 %)
Mixed community (<i>H. ovalis</i> , <i>Z. muelleri</i> & <i>H. uninervis</i>)	17.1 (7 %)	-	-	23.9 (9 %)	22.1 (9 %)
Macroalgae (<i>C. taxifolia</i>)	8.8 (3 %)	-	-	0.0 (0 %)	0.0 (0 %)
<i>Z. muelleri</i> & <i>C. taxifolia</i>	5.4 (2 %)	-	-	0.0 (0 %)	0.0 (0 %)
<i>S. isoetifolium</i> & <i>C. taxifolia</i>	2.6 (1 %)	-	-	0.0 (0 %)	0.0 (0 %)
Seagrass recovery	-	-	-	-	73.2 (28 %)
Total benthic macroflora	234.6 (90 %)	247.1 (95 %)	95.1 (37 %)	123.1 (47 %)	187.7 (72 %)
Bare sediment	24.8 (10 %)	12.3 (5 %)	164.3 (63 %)	136.3 (53 %)	71.7 (28 %)

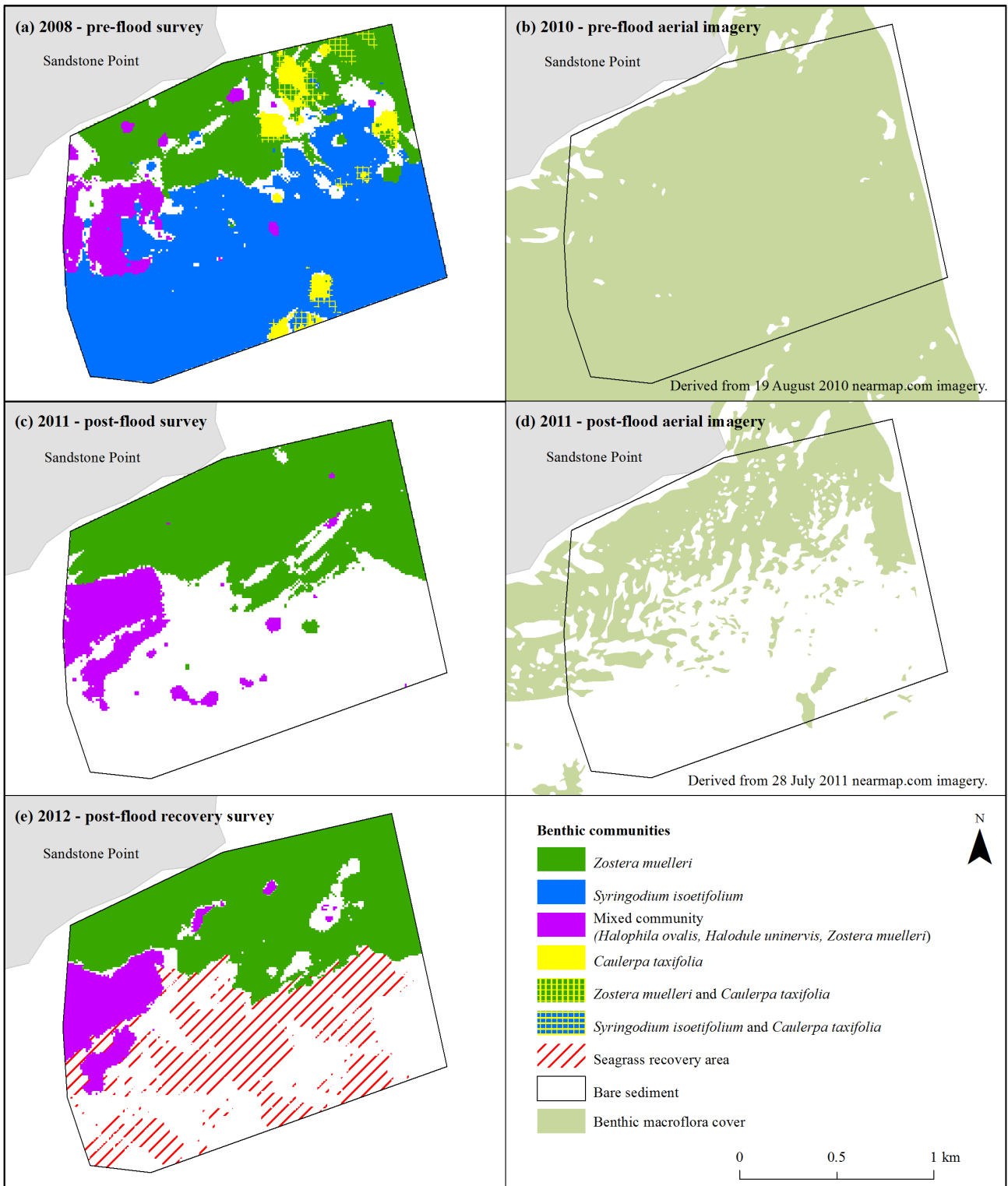


Figure 13 Benthic macroflora community distributions in northern Deception Bay based on detailed field surveys undertaken in April-June 2008 (a), August 2011 (c) and July 2012 (e). Note map (a) is reproduced from Hunnam (2008). Benthic macroflora cover derived from aerial imagery (obtained from www.nearmap.com) taken on 19 August 2010 (b) and 28 July 2011 (d)

Changes in benthic community distribution

In August 2011, 47.5 % (111.5 ha) of seagrass and attached macroalgae mapped in 2008 had disappeared from the study area. Loss of seagrass was restricted to the community dominated by *S. isoetifolium*, which declined in distribution by 100 % (143.2 ha) since 2008. Only small, isolated individuals of *S. isoetifolium* were observed in 2011, compared with dense mono-specific meadows in 2008. The 2008 and 2011 distributions of the other two seagrass communities, *Z. muelleri*-dominated and the mixed species intertidal community, were comparable. Both communities showed an increase in area (by 41.7 ha and 6.8 ha respectively), however this may be due, at least in part, to less spatial variability observed in 2011 resulting in less conservative interpolation models.

Comparison of the 2008 and 2011 benthic macroflora distribution maps also suggests a complete loss of the two benthic macroalgal species. Neither *C. taxifolia* nor *U. argentea* were observed within the study area in 2011, suggesting a 100 % decline in the distribution of these species (50.6 ha and 187.3 ha respectively) since 2008.

Comparison of August 2010 and July 2011 aerial imagery indicates the loss of 152 ha (61.5 %) of benthic macroflora cover, and confirms that it occurred at some point between these imagery dates (Figure 13b and d, Table 5).

Recovery survey (July 2012)

The July 2012 survey indicated seagrass re-colonisation across a 73 ha area that was bare sediment in August 2011 and predominantly *S. isoetifolium* community pre-flood (recovery area, Figure 13e, Table 5). Species identification was difficult from above water visual surveys as seagrass regrowth in these areas was small, very sparse and often obscured by the macroalgae *Hydroclathrus clathratus*. The early colonising species *Halophila ovalis* was observed at 52 % of survey sites within the 'recovery area', followed by *Z. muelleri* and/or *Halodule uninervis* (43 % of sites) and *S. isoetifolium* (15 % of sites). *Halophila spinulosa* was also observed at one site. The July 2012 distributions of the established *Z. muelleri* and mixed intertidal communities were similar to August 2011 (Figure 13c and e, Table 5).

Environmental variables

Environmental data have been compiled from various sources and presented here to assess the possible reasons for the observed loss of *S. isoetifolium* from Deception Bay.

River flow

Hydrographs showing measured river discharge (flow) of the Caboolture River and Brisbane River (Locker Creek and Bremer River) indicate major flow events in late December 2010 and early January 2011, with the highest flows occurring on 11 and 12 January 2011 (Figure 14). The flows in the lower reaches of the Brisbane River peaked on 13th January 2011.

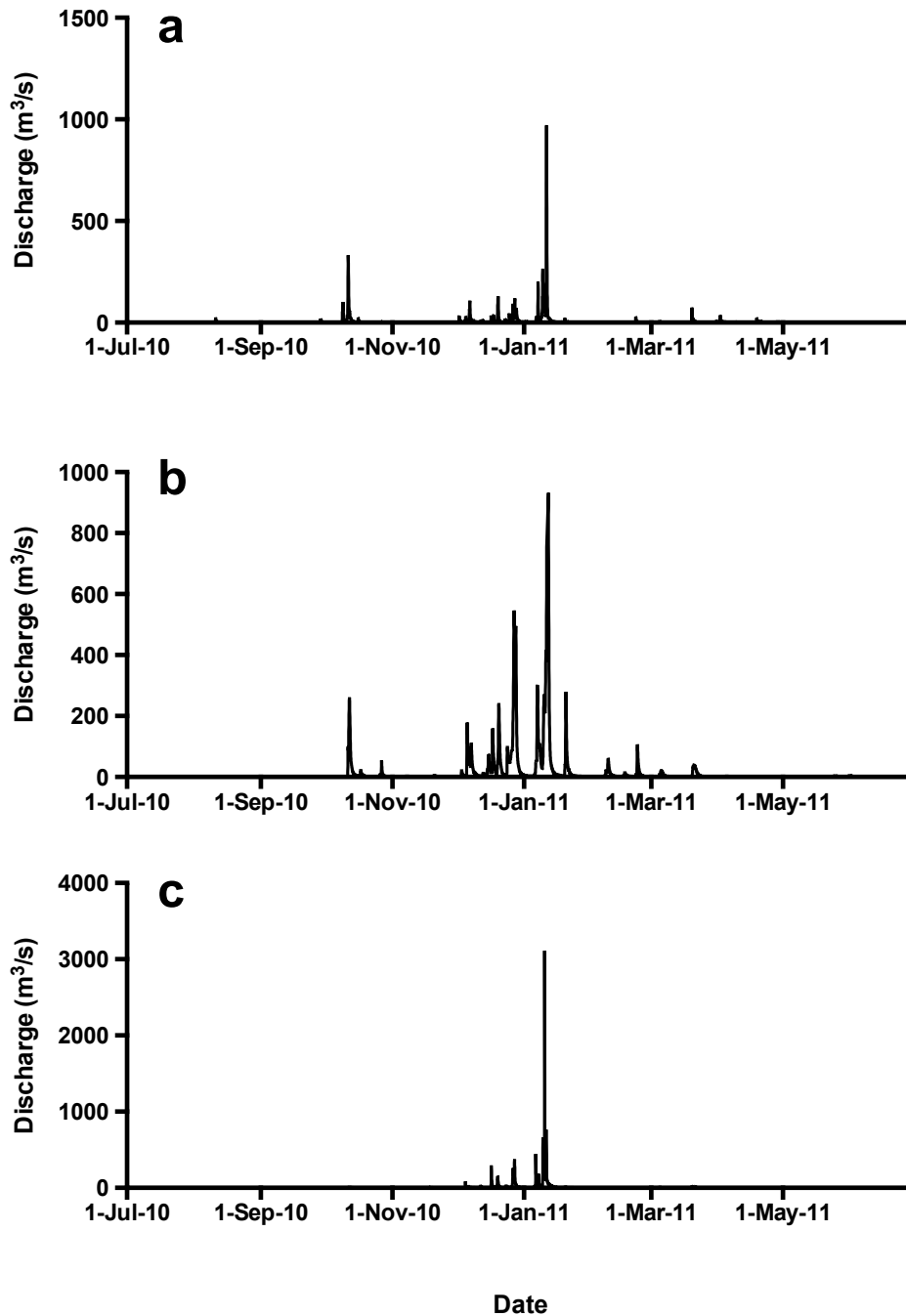


Figure 14 Hourly gauged river flows from (a) Caboolture River (station no. 142001A), (b) Bremer River (station no. 143107A) and (c) Lockyer River (station no. 143203B) during 2010 – 2011. Source: EHMP event monitoring, SEQ Healthy Waterways Partnership.

Light

Available light at the benthos is shown in Figure 15, expressed as total daily light and daily mean percentage of surface irradiance. Light conditions in the water column and at the benthos varied daily and spatially during the study period. Differences in light

conditions between sites were apparent and most pronounced during the first two weeks of December 2010 prior to major flow events measured in the Caboolture and Brisbane Rivers (Figure 14). Decreases in available light within the water column and at the benthos occurred in mid to late December 2010 and in early January 2011 coinciding with major flow events.

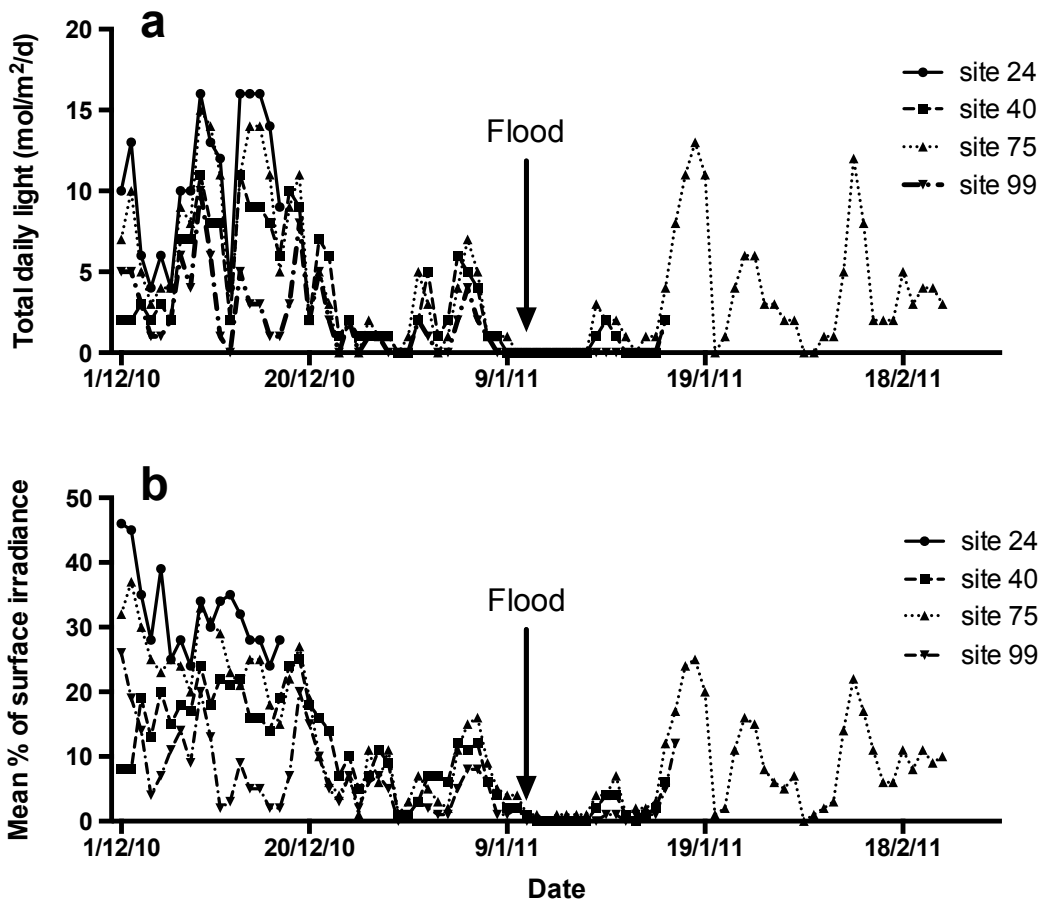


Figure 15 Light penetration at the benthos expresses at total daily light (a) and daily mean percentage of surface irradiance (b) measured at sites 24, 40, 75 and 99 at northern Deception Bay, between December 2010 and February 2011.

Salinity

Ambient water column salinity profiles are measured monthly at EHMP site 1118 in northern Deception Bay. Figure 16 shows sixteen months of monthly bottom water salinity measurements for EHMP site 1118 and additional salinity measurements taken at the study site between February 2010 to June 2011. On 20th January 2011, approximately seven days after the Brisbane River flood peak, a substantial drop in bottom water salinity (to 9.6) was observed, with the entire water column profile at EHMP site 1118 having a

salinity of <10. Five days later, salinity at the study site was measured at 19, with pre-flood salinity (~30) returning at approximately 25 days after the major flood peak (Figure 16).

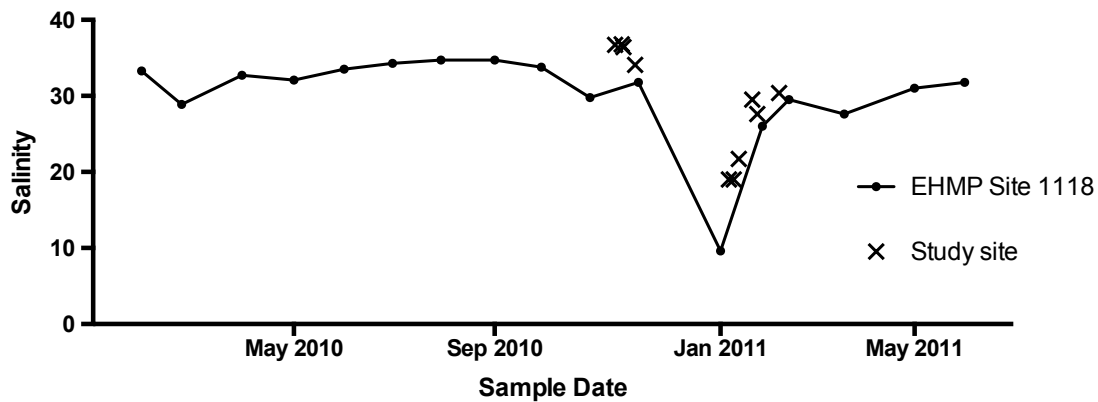


Figure 16 Ambient bottom water salinity data measured at EHMP site 1118 and at the study site, Deception Bay, February 2010 to June 2011. Source: EHMP, SEQ Healthy Waterways Partnership.

Sediment deposition

Rates of sediment deposition varied across the study site and ranged from 246 (SE=85) g m⁻²d⁻¹ at site 40 to 788 (SE=102) g m⁻²d⁻¹ at site 75, sampled over a six day period between 25th January to the 31st January 2011 (Table 6). The chemical composition of sediment from traps located at site 99 was determined for two sampling events for TOC, TN, TP and Fe. Missing sediment trap data as shown in Table 6 is a result of lost sediment traps. The sediment trap method used here to estimate sediment deposition rates is likely to have resulted in an over estimate of the true rate of sediment deposition due to the inherent difficulties in accounting for sediment resuspension within such shallow, dynamic coastal environments. Nonetheless, these deposition rates reported here are the only known measurements undertaken during the flood period and reflect the extreme magnitude of the event, which has been estimated to have delivered a sediment load equivalent to three times the annual load normally received by the Bay (DERM, 2011).

Table 6 Sediment trap deposition rates and solid phase composition, northern Deception Bay, January to February 2011 (values are the mean of 3 replicates, SE in brackets).

Deployment date	Sediment trap deposition rates (g/m ² /d)			Composition of Site 99 sediment traps (% dry weight)			
	Site 99	Site 75	Site 40	TOC	TN	TP	Fe
20 Jan - 25 Jan 2011	612 (149)	-	-	2.12 (0.22)	0.26 (0.03)	0.062 (0.005)	2.25 (0.19)
25 Jan – 31 Jan 2011	641 (110)	788 (102)	246 (85)	1.77 (0.19)	0.22 (0.02)	0.050 (0.004)	2.00 (0.15)
11 Feb – 17 Feb 2011	-	601 (73)	377 (54)	-	-	-	-

4.5. Discussion

Benthic community mapping

This study documents the complete loss of a *S. isoetifolium* dominated seagrass community in northern Deception Bay. The complete loss of macroalgal species *U. argentea* and *C. taxifolia* was also observed. Notably, seagrass species such as *Z. muelleri* appeared to be relatively unaffected.

From comparisons of historical distribution maps and anecdotal reports, it appears that the diversity of seagrass species in northern Deception Bay has remained fairly consistent over time, while seagrass species/community distributions have fluctuated (Hunnam, 2008). Seagrass surveys were conducted across Moreton Bay in the early 1970s (Young and Kirkman, 1975), in 1987 (Hyland et al., 1989), in 1998 (Dennison and Abal, 1999) and in 2004 (EHMP, 2006), using a variety of methods including aerial photography, satellite imagery, field-based surveys, or a combination of one or more methods. Importantly, in all previous surveys, *Z. muelleri* (*capricorni*), *Halophila ovalis* and *S. isoetifolium* were identified in northern Deception Bay. Also, *Halodule uninervis* was mapped only in the 1970s and 1998 survey, possibly due to its similar appearance to *Z. muelleri* (small morphology); while *H. spinulosa* was mapped only in 2004. No reference was made to the alga *C. taxifolia* in the detailed 1970s community descriptions, suggesting recent expansion into the area, as supported by other studies (Burfeind and Udy, 2009; Thomas, 2003).

The inconsistency of previous survey and mapping methods, as well as a lack of detail around the accuracy of the resulting distribution maps, limits the extent to which conclusions can be drawn regarding historical changes in benthic community distributions

(Hunnam, 2008). However, previous loss of a sub-littoral stand of *S. isoetifolium* in mid-1973 has been reported; followed by a mixed intertidal community in the late 1970s determined to be due to sand movement and seagrass burial initiated by an unknown cause (Kirkman, 1978).

The inconsistency of survey and mapping methods partially reflects the disparate origins of the respective surveys, but is also indicative of the challenges of mapping subtidal environments. A variety of approaches have been used globally to map seagrass distributions including field surveys using quadrats (e.g. de longh et al., 1995), aerial photography (e.g. Kendrick et al., 2002; Larkum and West, 1990; Zharikov et al., 2005), satellite imagery (e.g. Phinn et al., 2008), and underwater video transects (e.g. Holmes et al., 2007). Remote sensing approaches are advantageous in that they have complete coverage over large areas. However, while aerial photography and satellite imagery have been effectively used to map seagrass extent and percent cover over large spatial areas, they have generally been less successful in distinguishing and mapping at a species level. In addition, these techniques are often ineffectual in coastal waters where riverine inputs create turbid water column conditions. In comparison, field-based approaches can accurately identify to a species level but are problematic in that they interpolate information from sparse samples covering a relatively small area, leading to large mapping errors and spatially variable mapping confidence. These approaches are also often resource intensive and therefore can be impractical over large areas.

As an attempt to overcome the inconsistency issues mentioned earlier, this study used a consistent methodology to collect benthic macroflora field data and interpolate this data to create probability-based maps. By mapping to a species level, these maps illustrate species-specific responses to the flood event in 2011. Continuous probability maps produced this way can also indicate recovery hot spots, and low probability maps can identify areas to target for finding less common species (Holmes et al., 2007).

However, this approach is likely to underestimate less common species / communities due to the averaging effect of kriging on predicted values (Webster and Oliver, 2001). Also, as with other field-derived mapping techniques, greatest uncertainty and error were associated with areas between transects. Further modelling and/or integration with other techniques may improve results. For example, the mixed community was observed to be associated with intertidal areas, and therefore may be more accurately mapped using co-kriging or generalised linear spatial models which allow

for incorporation of additional data such as bathymetry (Goovaerts, 1997; Guisan and Zimmermann, 2000). Also, integration of satellite or aerial imagery assessment with this approach (where clear imagery is available) would achieve greater coverage and may be an effective means of mapping large areas to a species/community level.

Impacts of the January 2011 Brisbane River flood

This study documents species-specific changes in the composition of a shallow, estuarine seagrass meadow following a major flood event. Dieback of seagrass species *S. isoetifolium* in northern Deception Bay was first observed and photo-documented approximately twelve days after the major flood peak in January 2011, although dieback may have commenced prior to this time due to the increasing level of freshwater and sediment reaching the site prior to flood peak. Complete loss of the *S. isoetifolium* community and widespread disappearance of macroalgal species *U. argentea* and *C. taxifolia* was documented seven months post-flood, when water turbidity had sufficiently cleared to allow detailed visual surveys.

Although the baseline (2008) map was surveyed several years prior to the flood, high-resolution aerial imagery taken 4 months pre-flood shows widespread benthic cover consistent with the 2008 distribution. Regular field observations over the 2010–2011 summer, including less than 4 weeks prior to the flood peak, confirmed the presence of *S. isoetifolium* and noted only minor occurrence of *L. majuscula* with no bloom formation. This suggests that the 2011 flood event was the most probable cause of the observed loss of *S. isoetifolium*, *C. taxifolia* and *U. argentea*.

The January 2011 Brisbane River flood resulted in the discharge of freshwater and sediment into Moreton Bay, including northern Deception Bay. Monitoring of environmental variables indicated that the flood resulted in a number of temporary changes in Deception Bay including a reduction in benthic light availability and a reduction in bottom water salinity. In addition, the altered riverine flows into the area may have also influenced biogeochemical and biological processes, leading to increased sediment mobility, insufficient light for photosynthesis resulting in energy deficiencies and potential sediment anoxia, and exceedance of species tolerance thresholds.

Flood impacts appeared to be restricted to *S. isoetifolium*, *C. taxifolia* and *U. argentea*. The scale of the flood event, relative to the size of the study area suggest it is unlikely that impacts in Deception Bay were spatially restricted. Therefore

community / species responses to the flood were likely determined by differences in species tolerance to these temporary changes based on either inherent traits or regular exposure and acclimation (or not) to similar conditions in their specific habitats.

Z. muelleri and *Halophila ovalis* occur in both subtidal and intertidal habitats, including estuarine environments, which would expose these species to a range of salinities (Long et al., 1993; Young and Kirkman, 1975). Manipulative experiments suggest *Z. muelleri* can maintain photosynthesis at salinities as low as 5.25 (Kerr and Strother, 1985), while *Halophila ovalis* has been shown to tolerate rapid transfer from normal seawater (35) to salinities as low as 8.75 for a period of 5 days without signs of significant photosynthetic stress (Ralph et al., 2007). In contrast, in Moreton Bay, *S. isoetifolium* is restricted to a few subtidal areas which tend to maintain oceanic salinity (Young and Kirkman, 1975); and surveys along the eastern Queensland coast show it occurs in parts where there are few streams with freshwater runoff (Long et al., 1993). These distributions suggest the species may be susceptible to low salinity and/or light levels.

The flood-induced change in the salinity regime for northern Deception Bay cannot be described in detail due to the absence of continuous salinity measurements. However, based on discrete measurements, a period of low salinity (<10) persisted for less than ten days. There are no known studies on the salinity tolerance threshold of *S. isoetifolium*. However, manipulative experiments undertaken by Lirman and Cropper (2003) demonstrate that the morphologically similar species *Syringodium filiforme* is susceptible to sudden changes in salinity and becomes stressed after 14 days at a salinity of ≤ 10 . While the *S. isoetifolium* in northern Deception Bay may only have been exposed to flood-induced low salinity (<10) for less than ten days, it is possible that low salinity combined with stress from other factors such as light deprivation resulted in the observed *S. isoetifolium* mortality. Low salinity levels alone are likely to be the cause of the observed disappearance of macroalga *C. taxifolia* from the study area. This species has been shown to become highly stressed at reduced salinities, with mortality occurring at a salinity of <10 after just 180 minutes (Theil et al., 2007).

Light deprivation is a known cause of seagrass decline (Longstaff et al., 1999) and has been the subject of much previous research (see review by Ralph et al., 2007). The amount of light available to seagrass for photosynthesis has been shown to limit their distribution (Abal and Dennison, 1996) and affect their capacity for long-term survival (Dennison et al., 1993). The ability of seagrasses to survive in extreme and/or extended

periods of light deprivation is likely to be influenced by its ability to store and access stored carbohydrates (Longstaff et al., 1999). Minimum light requirements (MLR) for seagrasses have been shown to be both species and site specific. However, few studies have quantified MLR for specific species (Ralph et al., 2007), with those reported in the literature ranging from 4.4 to 29.4 % of surface irradiance (Dennison et al., 1993).

The MLR for *Z. muelleri* in Deception Bay was measured by Longstaff (2003) to be 15 % of surface irradiance and total daily light (annual mean) of 4.6 mol photons m⁻² d⁻¹. Shading experiments suggested that light deprivation events (at <MLR) lasting longer than 55 days led to *Z. muelleri* mortality (Longstaff, 2003). Using these determinations, data presented here shows the flood resulted in a period of 35 days light deprivation below the MLR for *Z. muelleri* in northern Deception Bay (Figure 15). This duration is within the period for *Z. muelleri* survival at MLR reported by Longstaff (2003), and is consistent with survey results showing minimal change in *Z. muelleri* distribution in the study area after the flood. There are no known similar studies investigating MLR of *S. isoetifolium* in Deception Bay or elsewhere. The only documented MLR for a *Syringodium* species is for *S. filiforme* from sites in Florida USA and north-west Cuba, which range from 17.2 % to 19.2 % of surface irradiance (Dennison et al., 1993). The period of time for which *S. filiforme* can survive at MLR was not investigated.

Previous seagrass loss in northern Deception Bay has been attributed to sand movement and seagrass burial (Kirkman, 1978). Measurements taken immediately after the flood event recorded sediment trap deposition rates up to 788 g m⁻² d⁻¹ (Table 6). However, field observations during the August 2011 and 2012 survey do not support widespread sediment accumulation or seagrass burial, but instead, scouring at the boundary between bare sediments and remaining seagrass was evident. The boundary between the *Z. muelleri* and *S. isoetifolium* communities in the 2008 survey was still apparent in the post-flood survey, suggesting sedimentation and/or burial was unlikely to have been the cause of *S. isoetifolium* mortality (Figure 13). Given the shallow nature of the study area, local hydrodynamic processes, such as waves and currents, are likely to have resuspended and transported the 2011 flood material and deposited it elsewhere.

Review of previous studies suggests that the most likely cause of the observed post-flood community composition is a difference in species ability to tolerate low salinity levels, coupled with light deprivation. There are no known studies which have investigated the combined effects of light deprivation and low salinity on any *Syringodium* species.

However, Ridler et al. (2006) reported a decline in *S. filiforme* following two hurricane events that resulted in reduced light conditions and abnormally high freshwater discharges to the Loxachatchee River estuary. Low salinity levels of <10 reportedly persisted for eleven continuous days, and light measurements undertaken intermittently post-hurricane for an unknown period (Ridler et al., 2006) were below the minimum light requirements for *S. filiforme* based on limits reported by Dennison et al. (1993). Further research into the salinity threshold and MLR of *S. isoetifolium*, and the combined effect of these variables, is required to substantiate this hypothesis.

Implications for benthic carbon cycling and L. majuscula blooms

The loss of approximately half the seagrass from northern Deception Bay is likely to impact on benthic carbon cycling and remineralisation processes. Seagrasses are known to trap particles and increase sedimentary inputs of particulate organic matter (POM), enhancing sediment microbial activity which drives benthic remineralisation processes (Marbà et al., 2006). Seagrasses also release dissolved organic carbon (DOC) via root exudates and in shallow oligotrophic estuarine sediments such as Deception Bay, this source of DOC can represent a significant component of the overall sediment DOC pool in these systems (Marbà et al., 2006). In addition, seagrasses influence sediment dissolved oxygen concentrations in the rhizosphere via photosynthesis-mediated oxygen transport to the roots. This has a controlling influence on sediment oxygen levels and the extent to which aerobic versus anaerobic organic matter remineralisation occurs.

As noted by Pedersen et al. (2004) the extent and intensity of biogeochemical processes in coastal sediments is influenced by the composition and configuration of the particular community's subcomponents (Pedersen et al., 2004). Species differ in terms of productivity (Duarte and Chiscano, 1999; Mateo et al., 2006), buoyancy and structural brittleness (Alongi, 1998; Waycott et al., 2004), rate of decomposition (Duarte, 2000) and oxygen release from roots (de Boer, 2007; Dennison and Abal, 1999; Marbà et al., 2006; Terrados et al., 1999). Accordingly, seagrass communities comprised of different species at different abundances may differ in the way in which they contribute to the broader ecosystem. In this study, a natural flood event has resulted in species-specific seagrass mortality and thus a change in seagrass community composition within the study area. Several studies have previously investigated the ecological significance of altered seagrass community composition. Ruesink et al. (2006) measured process rates following the introduction of an exotic seagrass to a community previously dominated by one native

seagrass and reported increases in primary production and detritus production, and altered benthic faunal composition due to increased habitat availability. Similarly, work by Micheli et al. (2008) recorded a decline of *Zostera marina* and colonisation by *Halodule wrightii* over a 19-year period, with consequent reductions in abundance and diversity of associated fauna.

Benthic communities can play a significant role in the biogeochemical cycling of materials between benthic and pelagic compartments, especially in shallow water ecosystems. To assess the potential significance of the flood-induced changes in benthic community composition at northern Deception Bay, benthic process rates relevant to the study site have been compiled (Table 7) and used to estimate rates of community metabolism based on pre- and post-flood benthic community compositions (Table 8). Data has been derived using benthic chambers (Hunnam, 2008), in-tact sediment core incubations (Ferguson and Eyre, 2010; Johnstone, 2001; Chapter 3 this study), open-water diel changes in O_2 (*S. isoetifolium* community; see Chapter 3) and a combination of benthic chamber and sediment core incubations (Eyre et al., 2011b). Diel changes in water column dissolved oxygen were measured by sensors deployed *in situ* at seagrass canopy level. The calculation of system metabolism followed the methods of D'Avanzo et al. (1996), and was undertaken during an out-going neap-tide to minimise the influence of tide and adjacent benthic communities (see Chapter 3). Benthic metabolism rates were determined by subtracting estimated summer pelagic production and respiration rates for Deception Bay reported by Ferguson and Eyre (2010). The accuracy of this method is untested within this system, however, it has been used successfully in other small shallow estuarine bays elsewhere (Waquoit Bay, (D'Avanzo et al., 1996); Sunset Cove, Florida Bay, (Nagel, 2007). It is recognised that the data used are limited in temporal and spatial extent. However, the integration of benthic community maps with preliminary knowledge of community biogeochemical processes increases understanding of the potential ecosystem-wide implications of a change in seagrass community composition. It also enables prediction and possible amelioration of the effects of future disturbance events, which may be exacerbated through climate change and/or further human modification of the coastal zone.

Rates of gross primary production (GPP) and benthic respiration (R) vary between benthic communities and between winter and summer months (Table 8). Rates are consistently higher in summer than in winter for all benthic communities. This is likely to be

the result of increased metabolic activity driven by higher ambient temperatures and increased organic matter inputs associated with summer rainfall / runoff events. The rates of GPP and R measured in Deception Bay are within the range of rates reported in other seagrass systems (Hemminga and Duarte, 2000). The benthic productivity / respiration ratios (p/r) for each benthic community also vary between community types and seasons (Table 8). The p/r ratio is a measure of the balance between autotrophic production and heterotrophic respiration, with $p/r > 1$ indicating that the community is net autotrophic.

Table 7 Benthic process rates for subtropical / tropical seagrass dominated and unvegetated sediments relevant to the current study site at northern Deception Bay. Rates for community respiration (R), gross primary production (GPP) and net community production (NCP) are expressed in mg C m⁻² d⁻¹. p/r represents the ratio between community productivity and respiration. The data listed here is not the result of an exhaustive review of the literature and is provided as estimates only for the assessment of system wide dynamics.

Community	Location	R	GPP	NCP	p/r	Reference
<i>Halophila</i> spp.	Sth Moreton Bay (winter)	-346	554	208	1.6	Eyre et al. (2011b) (estimate)
	Sth Moreton Bay (summer)	-922	2582	1660	2.8	Eyre et al. (2011b) (estimate)
Mixed community (<i>H. ovalis</i> , <i>Z. muelleri</i> & <i>H. uninervis</i>)	Nth Deception Bay study site (winter)	-1329	1570	242	1.2	Hunnam (2008)
<i>Zostera muelleri</i>	Nth Deception Bay study site (winter)	-1251	543	-708	0.4	Hunnam (2008)
	Nth Deception Bay study site (summer)	-6629	7398	769	1.1	Johnstone (2001)
	Sth Moreton Bay (winter)	-726	871	145	1.2	Eyre et al. (2011b) (estimate)
	Sth Moreton Bay (summer)	-3197	2877	-320	0.9	Eyre et al. (2011b) (estimate)
<i>Syringodium isoetifolium</i>	Nth Deception Bay study site (winter)	-1235	1062	-173	0.9	Hunnam (2008)
	Nth Deception Bay study site (summer)	-9158	5390	-3768	0.59	This study (Chapter 3)
Unvegetated sediments	Nth Deception Bay study site (winter)	-53	112	59	2.1	This study (Chapter 3)
	Nth Deception Bay study site (summer)	-129 to -192	148 to 247	-44 to 119	0.8 to 1.9	This study (Chapter 3)
	Deception Bay (winter)	-264	253	-12	0.96	Ferguson and Eyre (2010)
	Deception Bay (summer)	-350	399	61	1.14	Ferguson and Eyre (2010)

Based on this compiled data, the annual metabolism of the vegetated communities in northern Deception Bay appears to vary between communities from net autotrophic (*Halophila ovalis*, *Z. muelleri* & *Halodule uninervis* community), to near net balance (*Z. muelleri* and *C. taxifolia*), to net heterotrophic (*S. isoetifolium*). Sediments devoid of macroflora appear to be autotrophic (Table 8). These results are in contrast to most other reported seagrass systems, which appear to be net autotrophic (Hemminga and Duarte, 2000). However, other previous studies have measured systems that switch from net autotrophic to net heterotrophic between seasons (Hemminga and Duarte, 2000), and shown that some seagrass habitats within a system are net heterotrophic (Eyre et al., 2011b) or in near net balance (Santos et al., 2004).

Table 8 Benthic process rates used to derive net ecosystem metabolism (NEM) and post-flood carbon budget for northern Deception Bay. (* denotes rates that are estimates based on measured winter rates)

Community	R (mg C m ⁻² d ⁻¹)		GPP (mg C m ⁻² d ⁻¹)		p/r Annual
	Winter	Summer	Winter	Summer	
Mixed community (<i>H. ovalis</i> , <i>Z. muelleri</i> & <i>H. uninervis</i>)	1329	5316*	1570	6280*	1.18
<i>Zostera muelleri</i>	1251	6629	543	7398	1.01
<i>Syringodium isoetifolium</i>	1235	9158	1062	5390	0.59
Macroalgae (<i>Caulerpa taxifolia</i>)	1376	5504*	1425	5700*	1.04
Unvegetated sediments	53	161	112	203	1.47

Based on the above benthic process rates and the 2008 benthic community distribution map, the pre-flood seagrass meadow within the study area appears to have been net heterotrophic, with an estimated net ecosystem metabolism (NEM) of -977 t C yr⁻¹. This implies that the pre-flood seagrass meadow within the study area as a whole needed to receive allochthonous carbon inputs to support respiratory demands. In contrast, the post-flood (2011) study site, consisting of seagrass and bare-sediment communities, appears to be net autotrophic (NEM, 648 t C yr⁻¹). This represents a shift in ecosystem function within the study area from a net heterotrophic seagrass meadow to an autotrophic seagrass and bare-sediment (microphytobenthic) community. Such a shift towards net benthic autotrophy is likely to result in lower sediment organic carbon levels, reduced sediment microbial activity, a reduction in sediment aerobic-anaerobic sites, and lower benthic nutrient fluxes.

A similar (although inverse) shift in community metabolism was reported by Barron et al. (2004) who documented the effect of seagrass colonisation from a strongly autotrophic unvegetated sandy sediment to a strongly heterotrophic *Cymodocea nodosa* seagrass community.

Changes to organic carbon cycling

To investigate the possible fate of flood deposited organic carbon (OC) and the potential changes to the cycling of OC through the Deception Bay seagrass ecosystem, OC budgets have been made for pre- and post-flood conditions. The budgets (Figure 17) have been constructed using a simple mass-balance approach, assuming that the sum of

all inputs, outputs and storage within the system equals zero. The budget rates for GPP and R are based on benthic community distributions and process rates (Table 8); rate of burial is estimated from Duarte et al. (2005). Pre-flood export estimates are based on sediment fluxes reported by Eyre and France (1997); flood inputs are based on average sediment deposition rates measured across the study area during a 28 day period following the major flood peak in the Brisbane River.

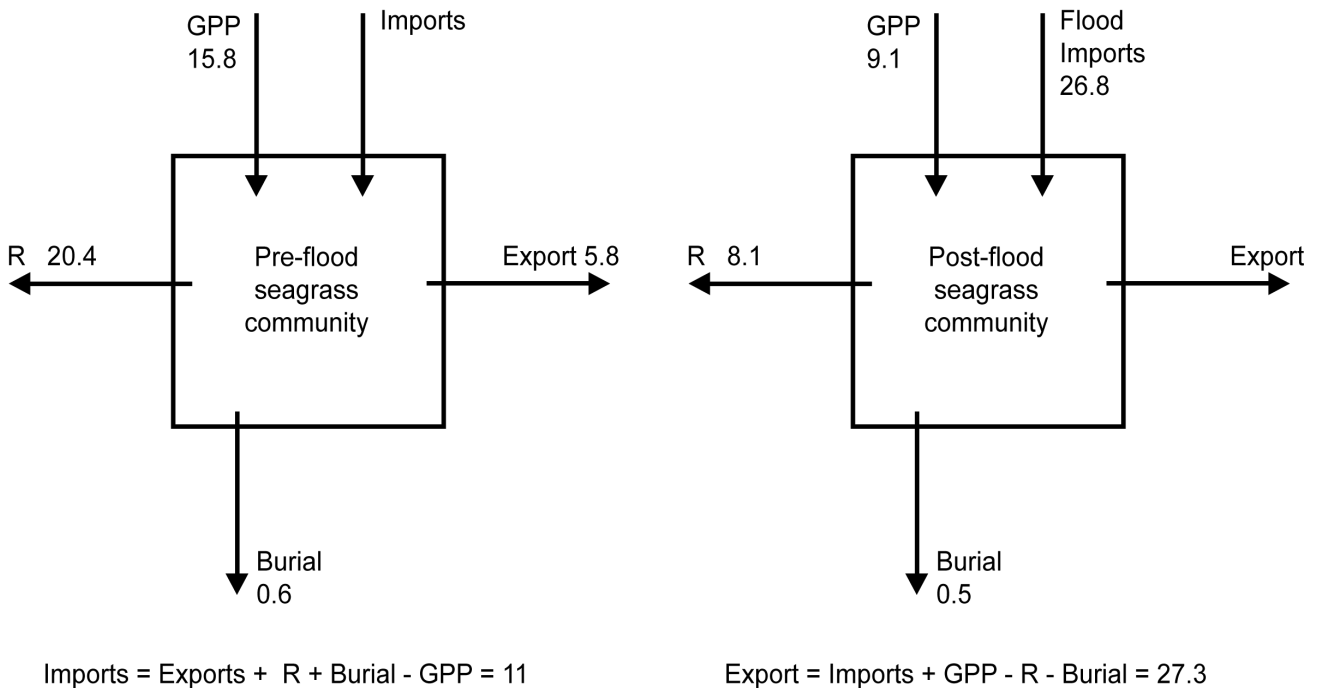


Figure 17 Organic carbon mass balance for the Deception Bay study site for pre- and post-flood benthic community distributions. Pre-flood export estimates are based on sediment fluxes reported by Eyre and France (1997); flood inputs are based on average sediment deposition rates measured across the study area during a 28 day period following the major flood peak. All fluxes in t C d^{-1} . Burial estimated from Duarte et al. (2005). (GPP: gross primary production; R: respiration)

The OC budgets provide an insight into the magnitude of the January 2011 Brisbane River flood event and the potential changes to the cycling of materials through the ecosystem as a result of changes in benthic community composition. The estimated export of OC from the study site as a result of the 2011 flood was 27.3 t C d^{-1} , based on inputs of 26.8 t C d^{-1} . In comparison, the pre-flood budget estimated allochthonous OC imports of 11 t C d^{-1} , based on measured benthic respiratory demands and estimated exports. The OC budgets show that the 2011 flood has delivered approximately 2.4 times the daily OC input to the Deception Bay seagrass ecosystem and that the changed benthic

community would result in the entire flood OC input being exported from the system. This notion is supported by sediment core sampling and analyses that was undertaken 9 months after the flood (October 2011) at site 40 (Chapter 3), with results suggesting that there had been no net accumulation of organic carbon in the sediments as a result of the flood. The pre-flood OC budget shows that the *S. isoetifolium* seagrass community more than doubles the rate of benthic respiration compared with post-flood conditions.

Although these OC budgets could be considered rudimentary and subject to uncertainties derived from the use of estimated import/export rates, the overall direction of the changes in benthic metabolism and therefore cycling of OC through the ecosystem are considered robust. From these budget estimates it is clear that changes in seagrass community composition can impact on the cycling of carbon through the ecosystem and hence affect the ecosystem processes they underpin.

4.6. Conclusions

This study has documented the widespread loss of the seagrass species *S. isoetifolium* and macroalgae *C. taxifolia* and *U. argentea* from northern Deception Bay, most likely due to a major flood event in January 2011. The observed change is likely to be due to low water column salinity combined with reduced light conditions, and differing tolerance thresholds among different species. However, further research is required on light and salinity tolerances of individual seagrass species, and their combined effect on growth and survivorship, particularly for *S. isoetifolium* for which there is a paucity of data in general.

This study has also demonstrated that changes in benthic community composition can have implications for system-wide functions. In northern Deception Bay, the loss of one seagrass species may have resulted in a shift from a net heterotrophic seagrass-dominated community to a net autotrophic bare-sediment and seagrass community. Such a shift in metabolism has flow-on effects for a range of biogeochemical cycles within a system. This demonstrates the importance of different benthic community types and their relative contribution to whole-of-system function. In light of this, it is clear that further work is required to define the species-specific interactions between seagrass, sediment and the water column, as well as at a site specific basis where such interactions and processes are further complicated by various physical forcings. While it is recognised that the benthic metabolism data compiled here are limited in temporal and spatial extent, this study

demonstrates that benthic mapping to the community/dominant species level is important for detecting change and can be integrated with biogeochemical process measurements to improve understanding of the ecosystem-wide implications of disturbance events.

Given the increasing pressures on seagrass systems within Moreton Bay and the historical permanent loss of seagrass from the Bay, there is an urgent need to document the recovery of the Deception Bay seagrass meadow following such a significant loss. Detecting and understanding the ecological implications of change requires spatial information at an adequate resolution collected over time using replicable methods. Field-based surveys such as described in this study, with the inclusion of permanent benthic quadrats and integration with remote sensing approaches (where possible) would allow for the accurate determination of community composition across various spatial scales. Recovery monitoring is important to understand species response to disturbance and enable prediction and potential amelioration of impacts from future disturbance events. Such events may be exacerbated in frequency and/or duration due to climate change and/or further catchment modification, and depending on the ability of *S. isoetifolium* to recover, may result in localised species extinction and loss in seagrass diversity in northern Deception Bay.

Chapter 5

Hydrodynamic processes and particle transport in a shallow estuarine embayment, northern Deception Bay

5.1. Abstract

Simulations of a 2D hydrodynamic model has demonstrated that the combination of wind and tide, rather than either individual force, is the major influence on the movement of water and particulates within northern Deception Bay. Seasonal variation in wind direction and speed results in temporal differences in residual currents and particulate transport across the study area. The results of model outputs and field-based data suggests that the processes of sediment resuspension and deposition in northern Deception Bay tend to vary at fine spatial and temporal scales, and are influenced by water movement and potentially benthic substrate characteristics. The model also supports the notion that autochthonous material, such as *L. majuscula* bloom detritus is readily exported from the study site to other parts of Moreton Bay.

The model was calibrated and validated using water level and current velocity measurements. Comparisons between modelled and measured parameters generally show good agreement and therefore demonstrate a satisfactory calibration of the model has been achieved. Further improvements to the model could be achieved by the collection of finer-scaled bathymetry and current measurements. Further development of the model should be undertaken to include sediment resuspension and deposition processes.

5.2. Introduction

The movement of sediment and particulate organic matter within an estuary is influenced by hydrodynamic forces such as tidal currents, wind, and waves. The dynamics of these materials are fundamentally important to many estuarine ecosystem processes such as biogeochemical cycling, primary production, and trophic interactions (Alongi, 1998). Knowledge of these hydrological processes and the bio-physical interactions that occur is central to understanding how estuarine and coastal ecosystems function. As discussed in previous chapters, the remineralisation of organic matter at the benthos can be significant at an ecosystem level. Understanding the dynamics of these materials is

therefore important when investigating ecosystem-wide processes and interactions that occur at various spatial and temporal scales.

The dynamics of sediment transport and movement in shallow estuaries is complex and quantifying key processes such as sediment resuspension and deposition is inherently difficult (Corbett, 2010; Liu and Huang, 2009). However, insights into the transport and movement of sediment within an estuary can be gained with the use of hydrodynamic models that simulate water movement and therefore sediment dynamics (Davies et al., 2009; Liu and Huang, 2009).

In the case of Deception Bay, hydrodynamic processes are likely to play a significant role in the resuspension and transport of material at the study site. This is evident from the results of sediment characterisation (see Chapter 2) which shows a clear spatial distribution of sediment grainsize and composition across the study site. The transport of material from the study site is also likely to be significant, with relatively low levels of residual sedimentary organic carbon (see Chapter 2) suggesting that burial of detrital *L. majuscula* is low and that the bulk of *L. majuscula* biomass from annual blooms may be remineralised locally or exported to other parts of Moreton Bay.

Hydrodynamic modelling in Deception Bay has been limited to date. One study used a 3D hydrodynamic and advection dispersion model of Deception Bay to model the transport of nutrients (Total Nitrogen, Total Phosphorous and Iron) from diffuse catchment sources to the Lyngbya beds of northern Deception Bay (McAlister, 2007). McAlister's (2007) model showed a southern residual movement of ebbing waters from Pumicestone Passage to the seagrass beds of northern Deception Bay suggesting that Pumicestone Passage was a source of nutrients for *L. majuscula* growth. In contrast to this, direct measurements of sediment and nutrient exchange between Deception Bay and Pumicestone Passage by Eyre and France (1997) suggest that Deception Bay contributes significant quantities of sediment and phosphorus annually to Pumicestone Passage. Although the study by Eyre and France (1997) was based on a very limited number of measurements undertaken over just three 25 hour tidal cycles, these contrasting results highlight the potential variability in sediment transport processes and, thus, the need for further detailed studies on the movement of materials in and out of Deception Bay.

The aim of this chapter was to construct a 2D hydrodynamic model of Deception Bay, use the model to gain a better understanding of the key forces that influence hydrodynamic processes and sediment transport, and explore how these processes might

influence the growth dynamics of *L. majuscula* blooms through materials delivery or removal.

5.3. Materials and methods

Study area

This study was undertaken in northern Deception Bay (27°05'S, 153°08'E), located in north-west Moreton Bay, Queensland, Australia (Figure 18). Moreton Bay is a semi-enclosed shallow water embayment located adjacent to the city of Brisbane. Moreton Bay has an area of approximately 1,523 km², a water depth up to 29 m (average = 6.25 m), and is characterised by a subtropical climate with summer-dominated rainfall.

Deception Bay receives riverine inputs from the Caboolture River and terrestrial runoff from a number of small tidal creeks and urban stormwater drains that are predominantly located along its southern and western shoreline. In the north of the bay and adjacent to the current study site, bay waters exchange with the estuarine waters of Pumicestone Passage (Eyre and France, 1997), and the ocean via a large (16 km wide) opening to the north.

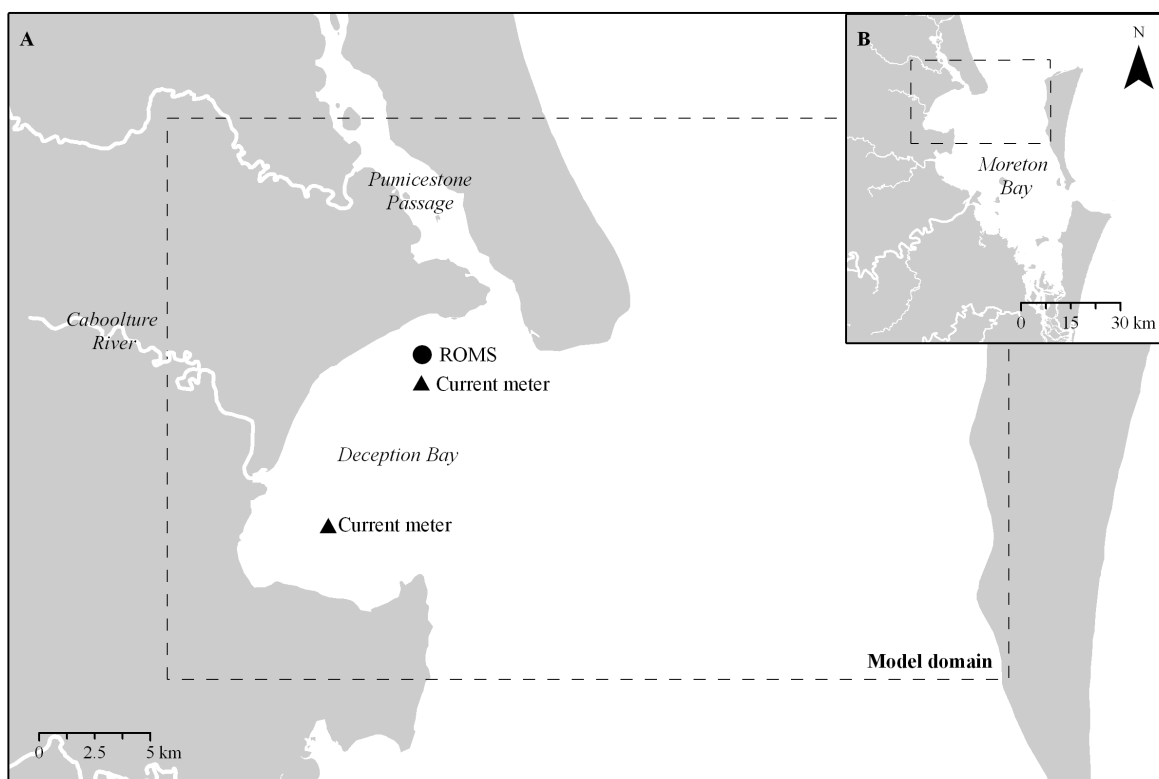


Figure 18 Model domain, remotely operated monitoring station (ROMS) and current meter deployment sites in Deception Bay (A); location of model domain within Moreton Bay (B).

Modelling approach

A two-dimensional flexible mesh hydrodynamic model for Deception Bay was developed using the modelling package MIKE 21 FM (DHI, 2011). The MIKE 21 FM is based on the numerical solution of fluid momentum, continuity, temperature, salinity and density equations in order to predict water level changes, circulation and transport driven by winds, waves, tides and density forcing (DHI, 2011). For this study, wind and tidal elevations were used as external forcing with boundary conditions forced from a regional Moreton Bay hydrodynamic model developed by Davies et al. (2009).

The Deception Bay model domain and bathymetry is shown in Figure 19. A higher resolution mesh was developed for the area of greatest interest around the study site at northern Deception Bay (Figure 20).

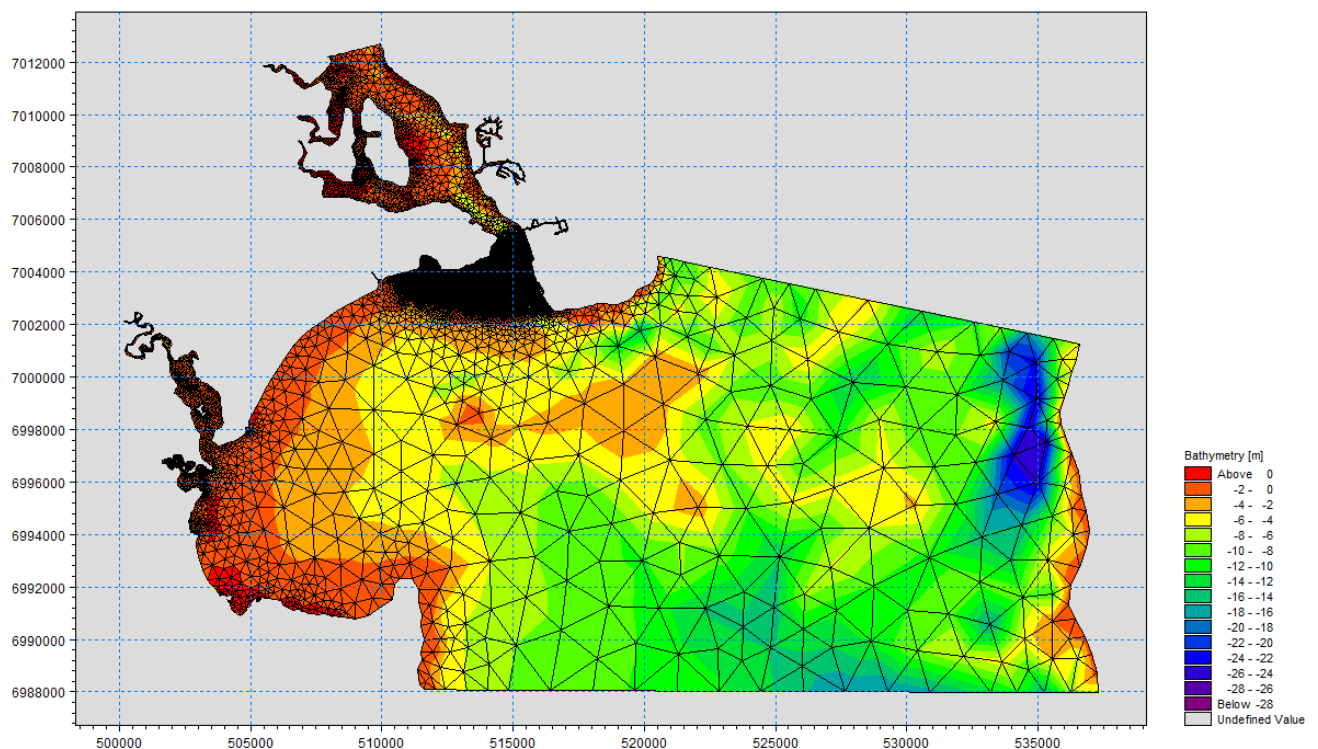


Figure 19 Model domain mesh and bathymetry

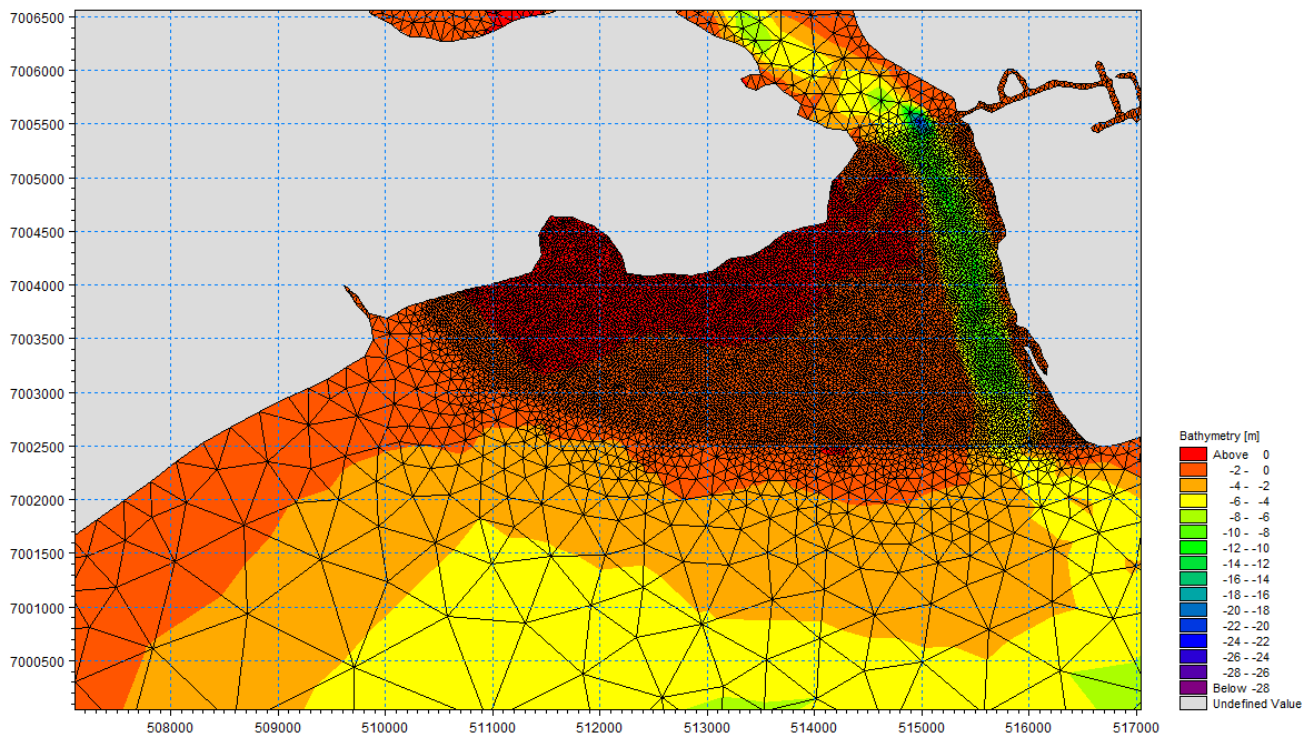


Figure 20 Model domain mesh zoomed in at study site

The particle tracking module included in the MIKE 21 modelling package was used to predict particle movements to and from the study site using the outputs from the hydrodynamic model. Particles with a diameter of 100 μm , 50 μm and 1 μm were used to represent sand, silt and clay respectively. Parameter values used for the particle tracking simulation are detailed in Table 9.

Table 9 Parameter values used for particle tracking simulation.

Parameter	Value	Unit	Notes
<i>Particle density</i> (sand, silt & clay)	2.7	g.cm^{-3}	
<i>Particle diameter</i>			
Sand	100	μm	
Silt	50	μm	
Clay	1	μm	
<i>Settling rate (constant)</i>			Calculated based on Stokes law
Sand	0.00869	m.s^{-1}	
Silt	0.00217	m.s^{-1}	
Clay	8.69×10^{-7}	m.s^{-1}	
<i>Particle flux</i>	1	$\mu\text{g.s}^{-1}$	Constant at source
<i>Erosion</i>	-		Not included
<i>Decay</i>	-		Not included
<i>Dispersion</i>	-		Not included
<i>Drift</i>	From HD model output		
Kinematic viscosity of seawater	1.05×10^{-6}	m^2s^{-1}	at 20 °C

For the purpose of this thesis, two simulation periods were chosen to represent the period where *L. majuscula* blooms have historically initiated (November), and after the end of a typical summer bloom (April). The two simulation periods also have differing wind climates so that the influence of wind on the transport of material could be tested. The year 2006 was chosen for simulations due to the availability of accurate data sets such as current and tidal data for Deception Bay which coincided with a detailed quantitative characterisation of the growth of the 2006-07 *L. majuscula* bloom in Deception Bay (see Johnstone et al., 2007).

The model simulations for April were run across a period between 1/4/2006 to 30/4/2006 and during November between 1/11/2006 to 1/12/2006.

Data sources

The following sources were used as data inputs for the model (Table 10). Wind and tidal data was collected from a remotely operated monitoring station (ROMS) in Deception Bay (see Figure 18) as part of the Healthy Waterways Lyngbya Management Strategy 2005-2007 (see South East Queensland Healthy Waterways Partnership, 2007). Current meters were deployed for four one-month periods at two locations (see Figure 18) with the data used to validate the model. Boundary conditions were set from the Gold Coast Estuarine Modelling Study model developed by Davies et al. (2009).

Table 10 Summary of model inputs and data sources.

Data input	Description	Source
Shoreline	Taken from GEMS MIKE3 FM model	(Davies et al., 2009)
Boundary conditions	Set from GEMS MIKE3 FM model	(Davies et al., 2009)
Wind	ROMS data collected for 2006	(Maxwell et al., 2007)
Tides	Global tidal constituents ROMS data collected for 2006	DHI (Maxwell et al., 2007)
Current data (model validation)	S4 current meter deployment in Deception Bay collected at 2 locations for the entire months of April 2006 and November 2006	(McAlister, 2007)
Bathymetry	CMAP / ETPO 2 global bathymetry	DHI

5.4. Results and discussion

Wind

Wind speed and direction varied between the two model simulation periods (Figure 21). During both periods, winds from the north and south-east tended to dominate the wind climate. During April, winds from the south-east were more dominate, whereas in November winds from the north were more prevalent. Wind speeds during November were generally much greater than that of April, with the strong northerly winds in November being the greatest point of difference between the two months.

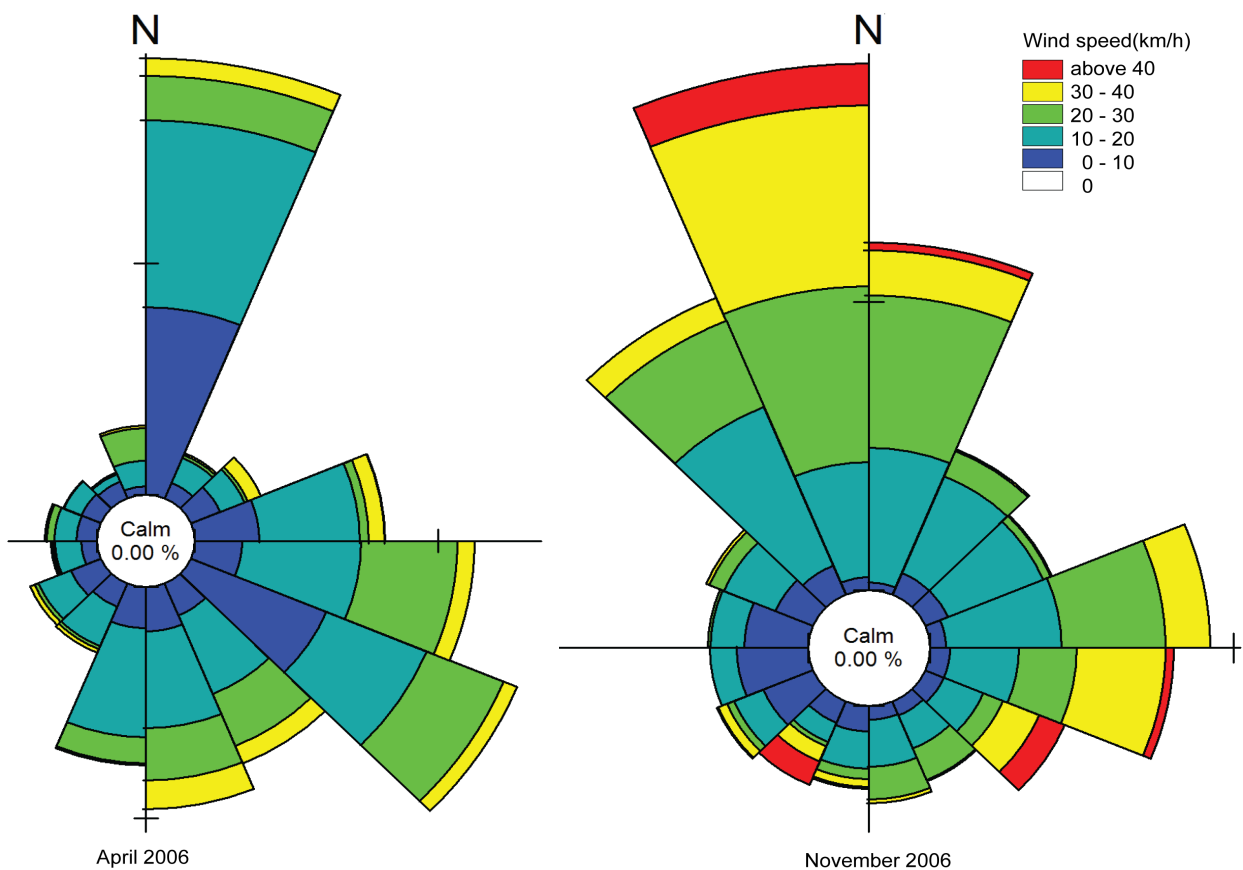


Figure 21 Measured wind direction and speed at the Deception Bay remotely operated monitoring station (ROMS) during April and November 2006 (source: Healthy Waterways Partnership)

Model calibration and validation

The model was calibrated using data collected over the course of 2006 and validated using water level and current velocity measurements recorded in Deception Bay over the model simulation period of April and November 2007 (see Table 10).

Comparisons between measured tidal data and modelled surface elevation data is shown

in Figure 22. Comparisons between measured and modelled current speed and direction are shown in Figure 23. Water level and current direction are generally well reproduced by the model, however current speeds are not as well reproduced by the model (Figure 23). The differences between measured and modelled current speeds could be attributed to potential inaccuracies in the bathymetry and from the fact that current speeds are calculated as an average value over the whole depth of the water column. Improvements in calibration could be achieved with more accurate and finer-scale bathymetry data and additional current measurements at finer spatial scales. Nevertheless, the calibration of the hydrodynamic model is considered satisfactory.

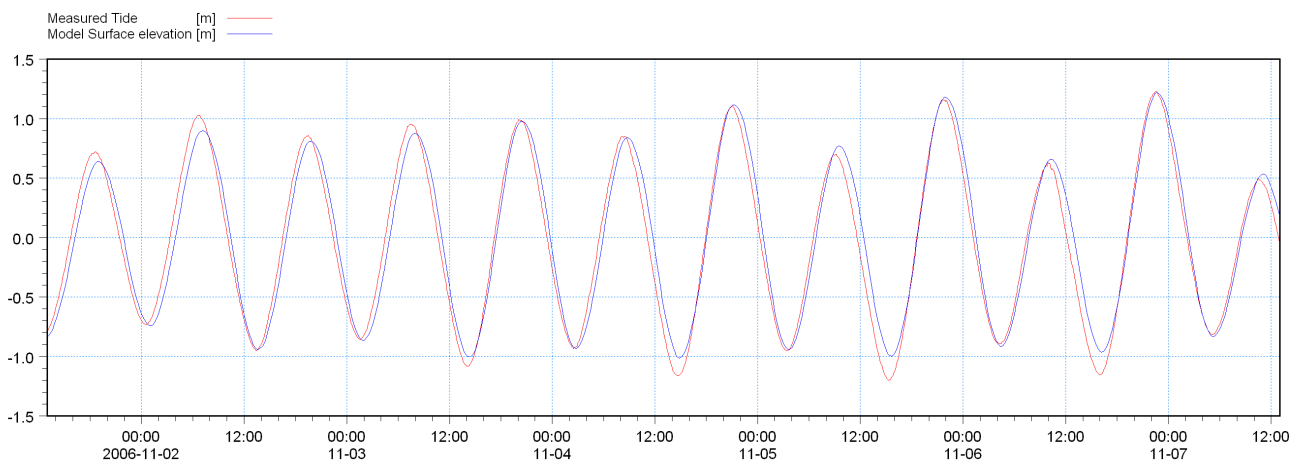


Figure 22 Comparison between measured and modelled water surface elevations in Deception Bay during a period of neap tides, November 2006

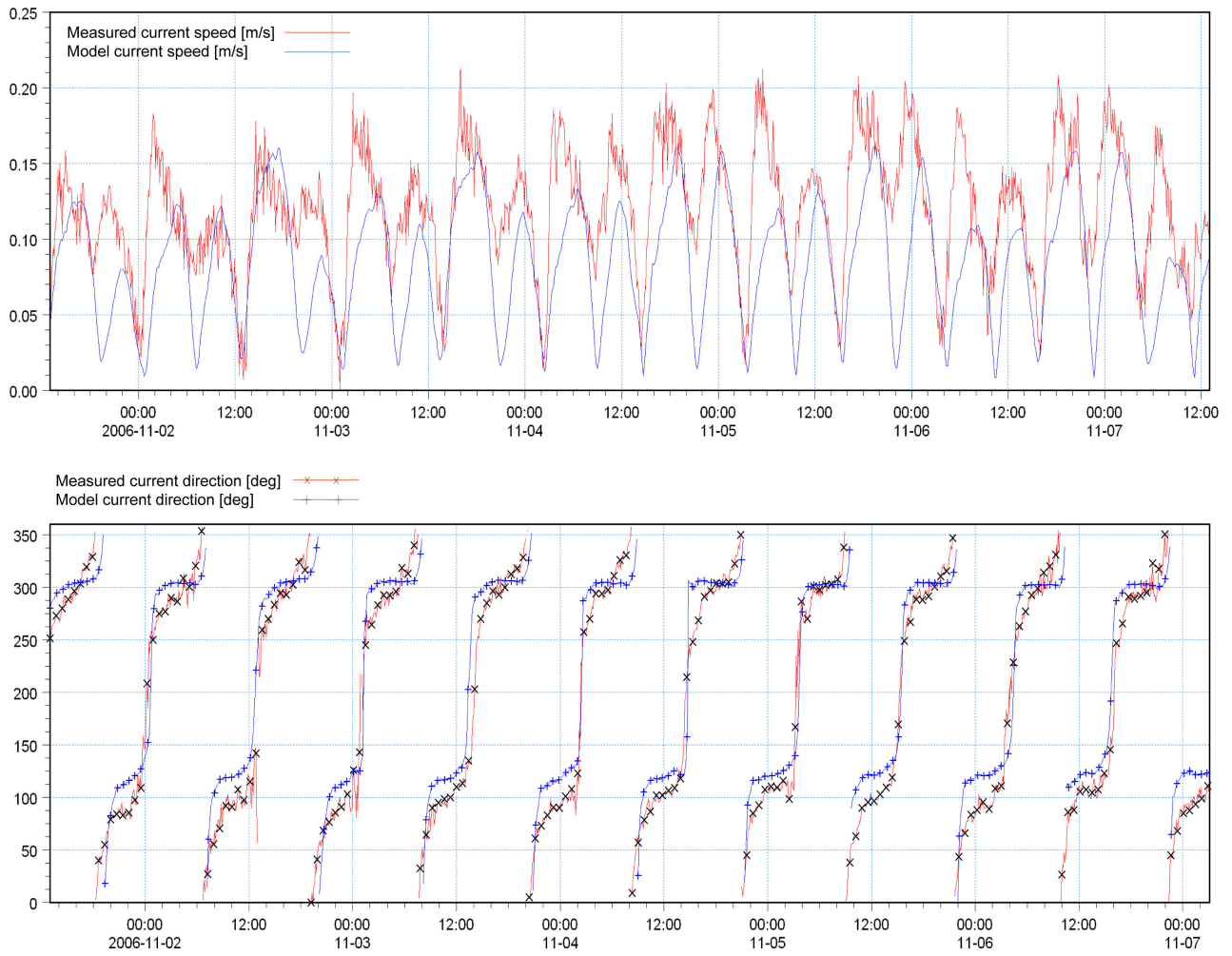


Figure 23 Comparison between measured and modelled current speed and direction in Deception Bay during a period of neap tides, November 2006

Simulation results

The residual flow has been calculated for the two simulation periods of April and November 2006 and plotted in Figure 24 and Figure 25 respectively. These residual flows are the combined result of wind-driven and tide-induced currents averaged over the depth of the water column.

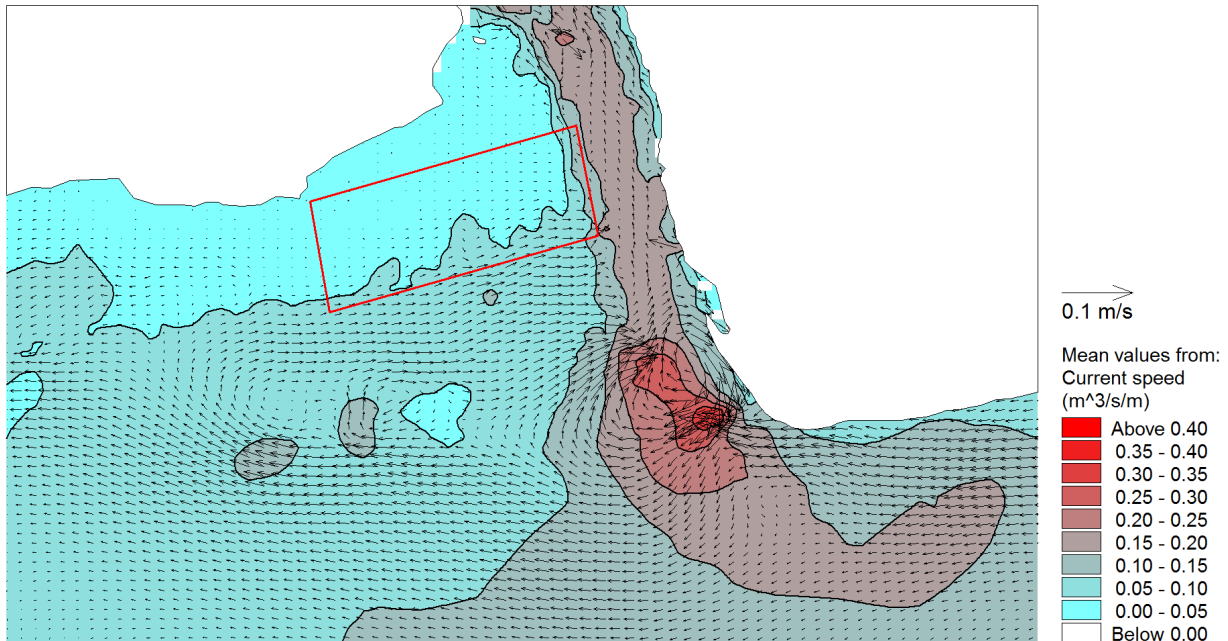


Figure 24 Calculated residual current flow and mean current speed for April 2006 showing the location of Chapter 2 sediment sampling area (red rectangle)

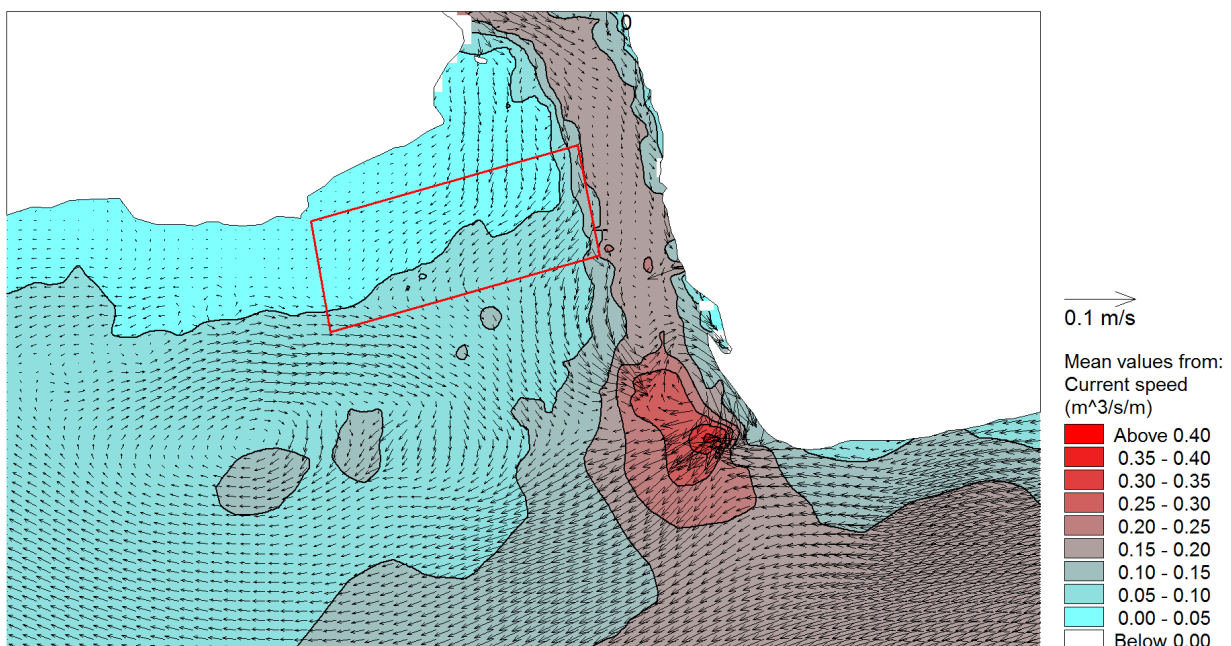


Figure 25 Calculated residual current flow and mean current speed for November 2006 showing the location of Chapter 2 sediment sampling area (red rectangle)

The residual current plots for both simulation periods show a strong clockwise eddy adjacent to the south-western corner of Bribie Island. This eddy formation is likely to be the result of the interaction between waters flowing from Pumicestone Passage meeting waters flowing from the northern passage. In addition, two weaker eddies are also apparent in the more shallow waters west of the channel. The formation of eddies result in areas of turbulent flow where sediments are likely to be mobilised at the outer edges of the eddy, but within the eye of the eddy, sediment deposition can occur.

Comparisons between the residual flows for April and November (Figure 24 and Figure 25) show that during April the residual flows are directed from the Chapter 2 sediment sampling site to the channel (see Figure 24), whereas in November, the residual flow direction is from the channel to the sampling site (see Figure 25). These differences in residual flow directions may be as a result of differences in the prevailing wind climates between the two months, where stronger northerly winds persist during November compared with that of April.

Figure 24 and Figure 25 also show the mean current speeds across the model domain. The spatial pattern of mean current speeds are similar for April and November with the highest mean current speeds occurring within the channel running adjacent to Bribie Island. However, the mean current speeds appear to be higher in November compared with that of April, potentially driven by the stronger northerly winds that persist in November.

Of note is the abrupt change in mean current speeds moving from the channel to the adjacent shallow waters to the west including the northern Deception Bay seagrass meadow. This abrupt change in current flow is likely to encourage the deposition of sediment and other particulate matter that is being transported via the channel. This notion is supported by the results of sediment sampling reported in Chapter 2, which shows significantly higher amounts of finer-grained sediments and sediment carbon located adjacent to the channel.

In addition to residual current plots, particle tracking simulations were carried out to simulate the transport of sediment to and from the study site and help describe in general terms sediment movement across the model domain. Figure 26 shows the starting locations for particle tracking simulations at the study site. Each of the starting locations corresponds to previous sampling sites 24, 40, 75 and 99 (see Figure 12).

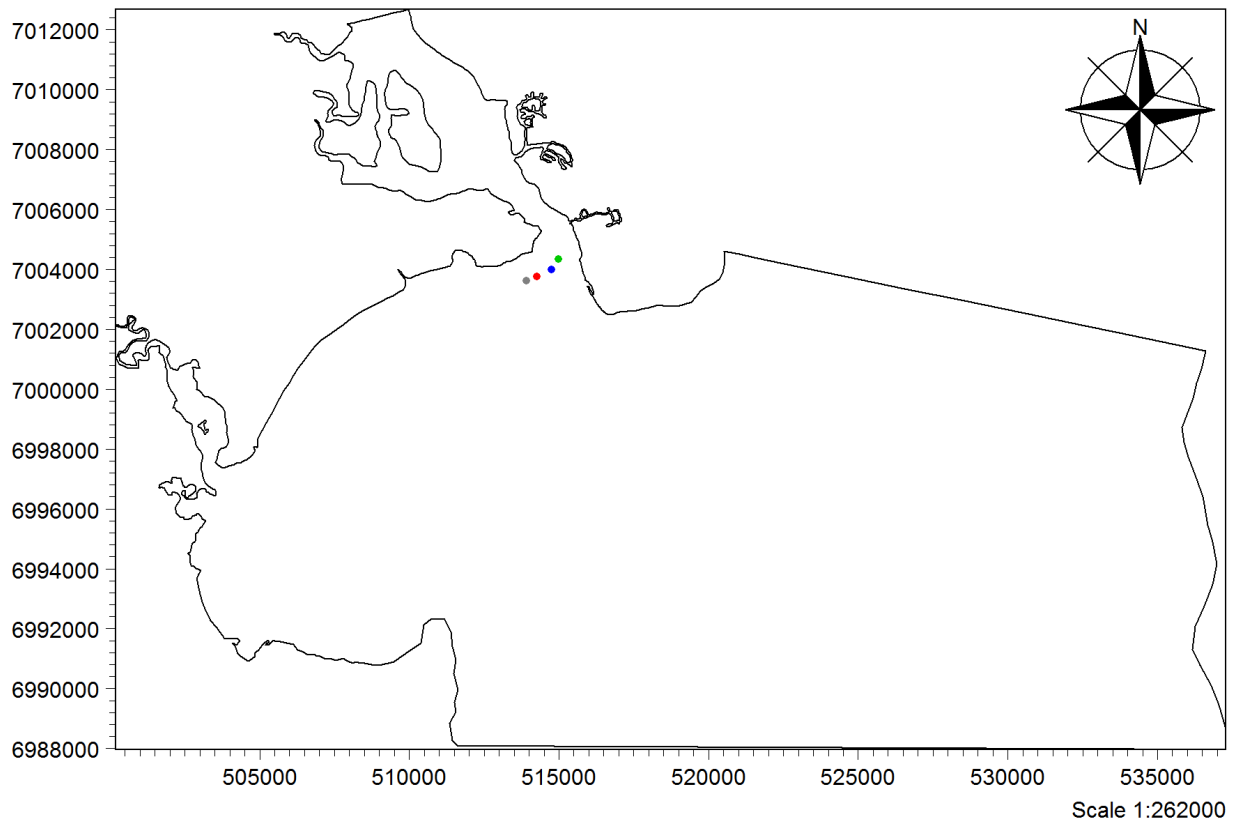


Figure 26 Starting sites for particle tracking at study site

The following particle tracking plots are shown for clay particles only. Particle tracking simulations were undertaken for sand and silt, however both of these particle sizes settled out quickly and were not transported outside of the study area over the simulation period of 30 days.

Comparisons of particle tracking simulations for April (Figure 27) and November 2006 (Figure 28) clearly show differences in clay particle movement between months. During April, clay particles tend to stay localised near their starting point and/or move northwards through Pumicestone Passage. Conversely, clay particle simulations for November show particle transport across the entire Deception Bay and to other parts of Moreton Bay. No particles were tracked through Pumicestone Passage during the November simulation period. These differences in particle tracking are likely to be due to differences in wind climates between the two months. The strong northerly winds that tend to dominate during November are the likely reason that clay particles are transported away from the study site, whereas in April, the results suggest that tidal currents play a stronger role in particles movement when lighter south-easterly winds persist.

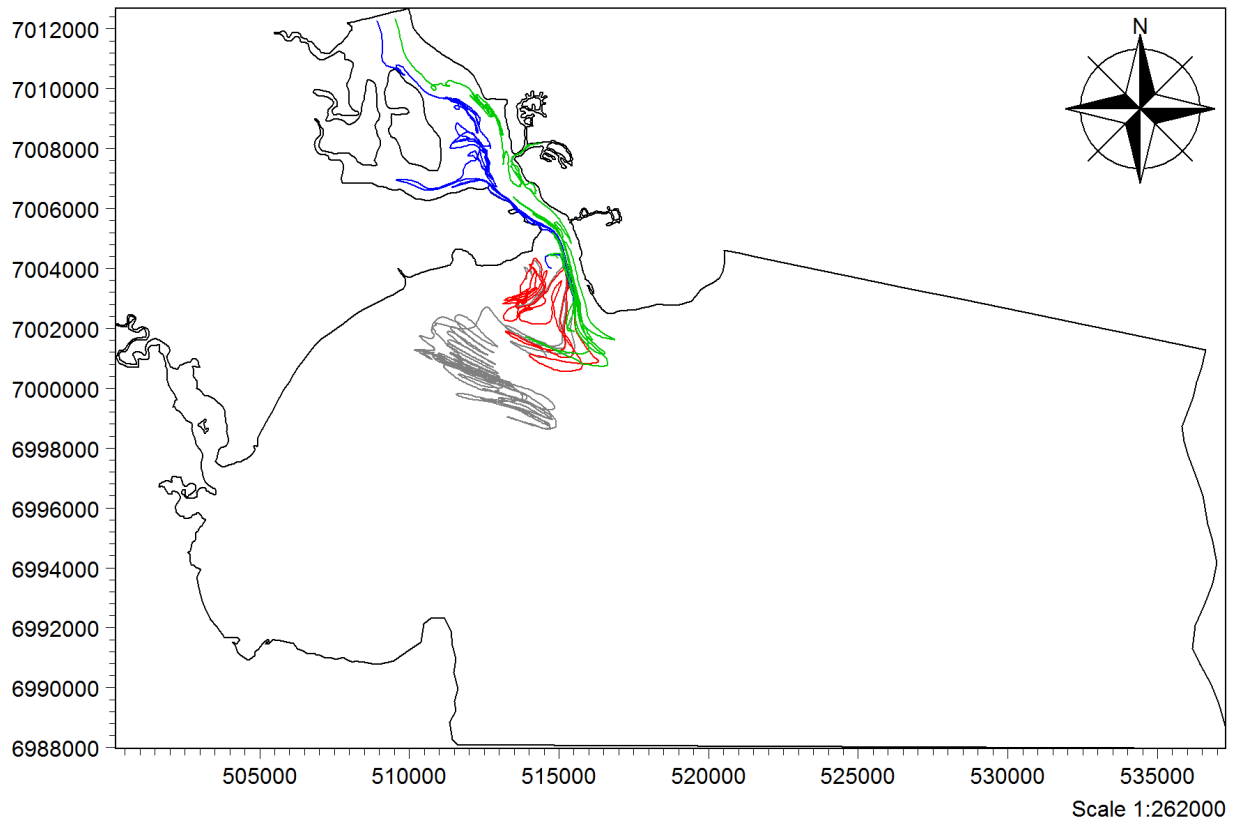


Figure 27 Clay particle tracking simulation for April 2006 starting at study site

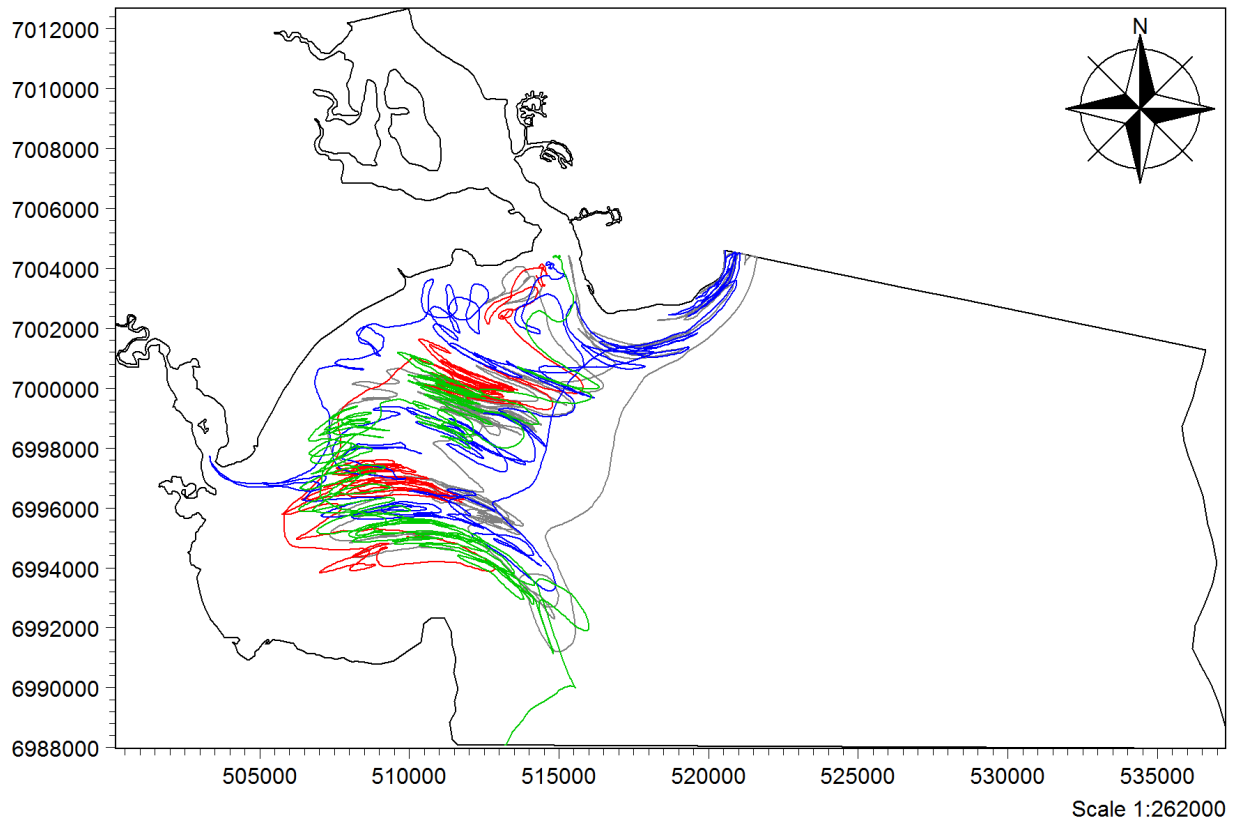


Figure 28 Clay particle tracking simulation for November 2006 starting at study site

An additional particle tracking simulation was undertaken to assess the potential of local sources for the supply of sediment to the study site. Particles were tracked from starting points at the Deception Bay entrance of Pumicestone Passage and at the mouth of the Caboulture River. Both these locations are shown in Figure 29. Particle tracking simulations were again undertaken for the same periods in April and November 2006. The results of source particle tracking are shown for April in Figure 30 and for November in Figure 31.

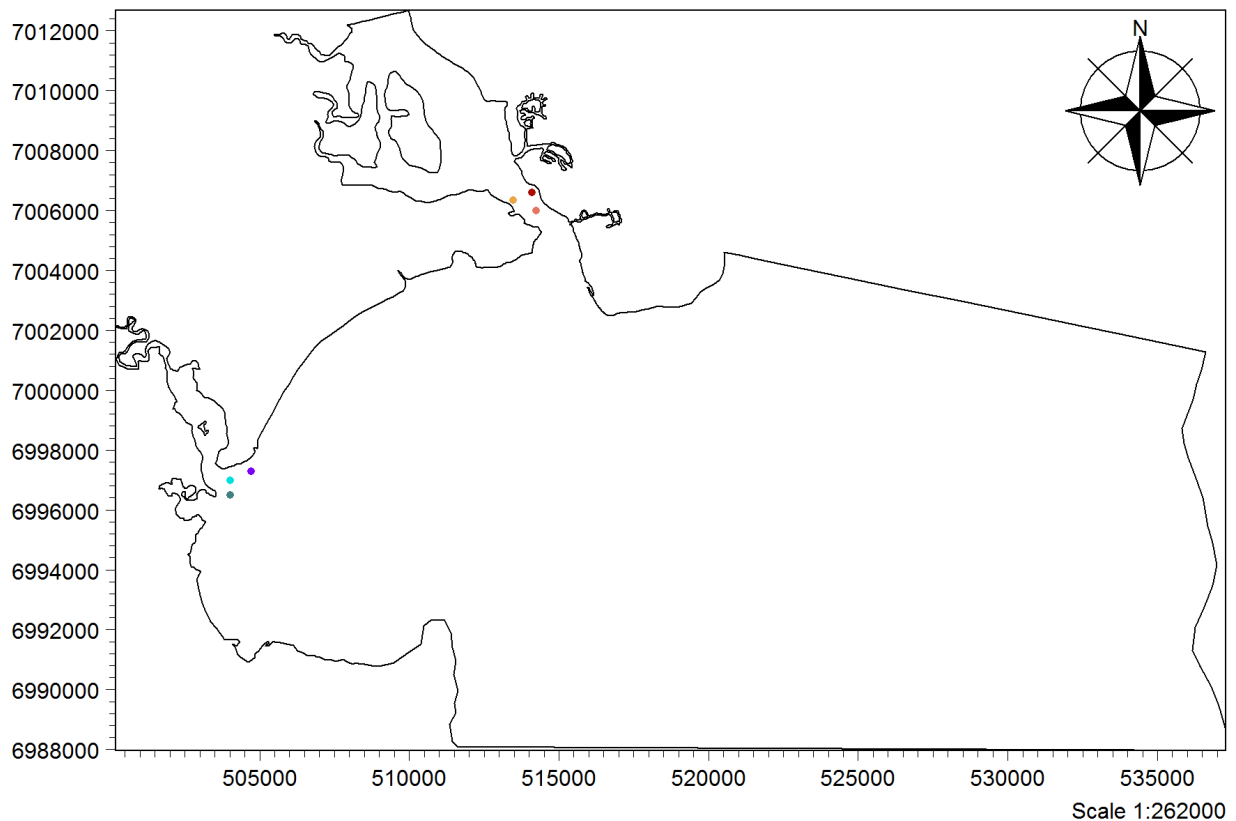


Figure 29 Starting sites for particle tracking at Pumicestone Passage and the mouth of the Caboulture River

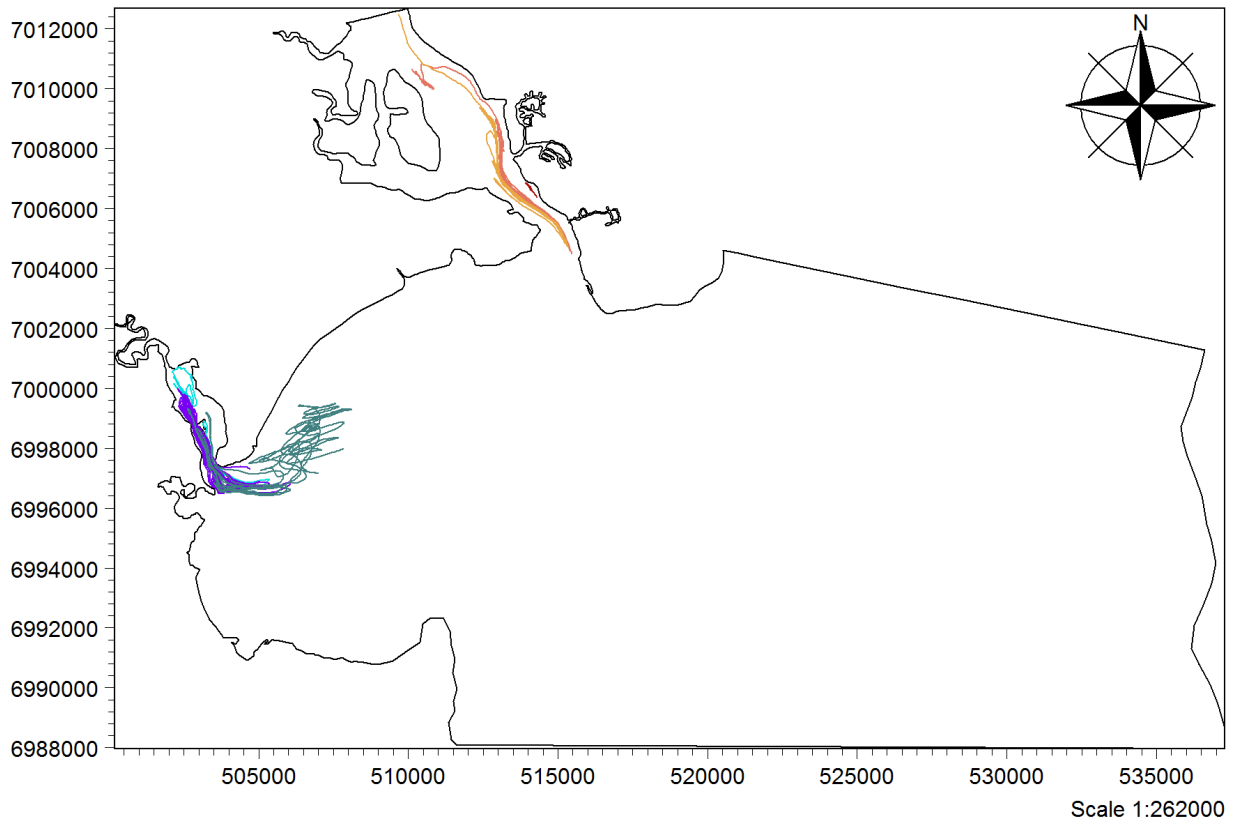


Figure 30 Clay particle tracking simulation for April 2006 starting at Pumicestone Passage and the mouth of the Caboolture River

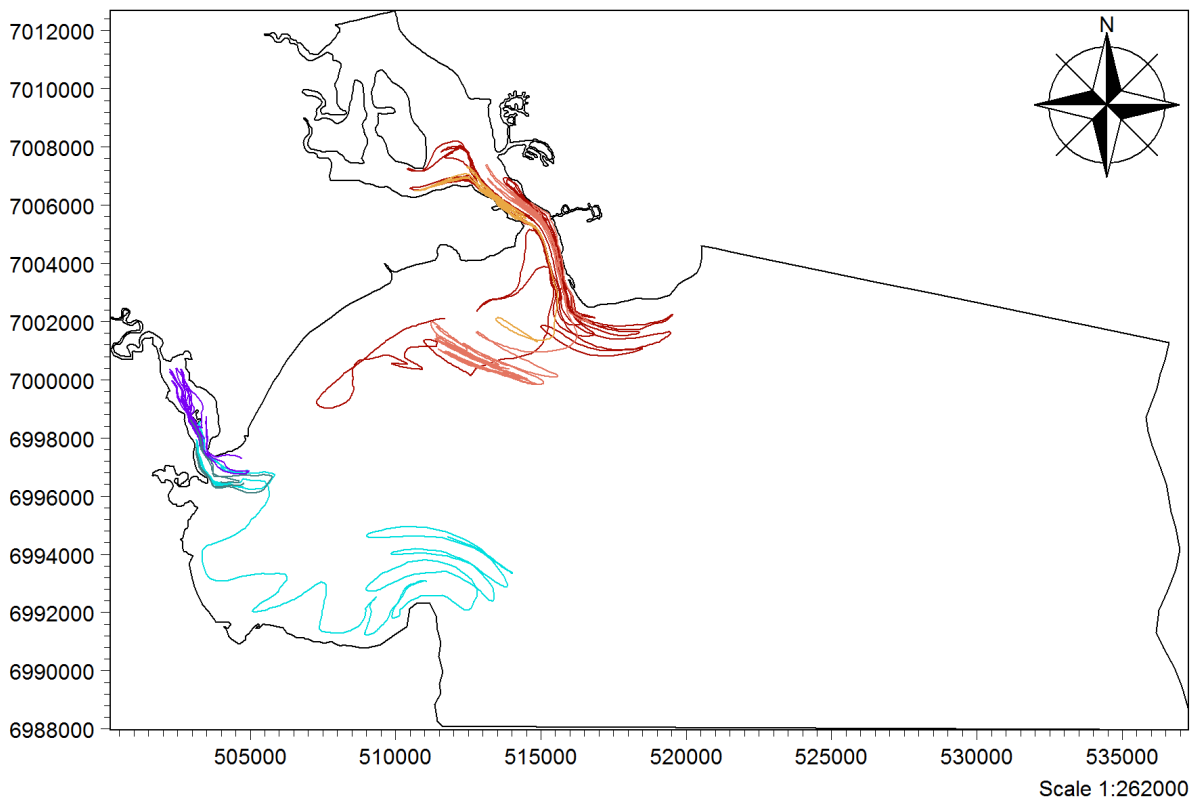


Figure 31 Clay particle tracking simulation for November 2006 starting at Pumicestone Passage and the mouth of the Caboolture River

The results of the source particle tracking simulations show similar results to that of previous particle tracking simulations where differences between April and November are evident. The results of the April simulation show that particle movement is relatively confined compared with that of November, where particles are tracked over a much wider spatial area. The results suggest that both Pumicestone Passage and the Caboulture River are potential sources of particles (sediment and other materials) to the study site. The relative contribution of each source on a given day however, is likely to vary due to the variability in local wind conditions interacting with tidal changes. The results of all particle tracking simulations clearly show that wind has a major influence on the movement of fine particles within the study area of Deception Bay.

5.5. Conclusions

Comparisons between modelled and measured water level, current speed and current direction show a satisfactory calibration of the model. Of these three parameters, current speed is not as well reproduced by the model compared to other parameters. Improvement in modelled current speeds could be gained by more accurate, finer-scale bathymetry and the collection of current measurements at finer spatial scales. Nevertheless, the model has been used successfully to show that both tide and wind are major drivers of water movement in Deception Bay.

The results of this modelling exercise demonstrate that sediment dynamics at the Deception Bay study site can not be simply described by short-term studies that are limited in temporal and spatial scale. The movement of sediment is a dynamic process that is influenced by factors that operate over varying spatial and temporal scales. The results of modelling simulations reported in this chapter show that both wind and tide influence the material transport across the study site. However, the scale of these influences is still not fully understood. Future sediment-based studies need to consider the dynamic nature of the area and the natural variability of the system.

The results of modelling show that the benthos of northern Deception Bay receives material from outside sources, but due to the dynamic nature of water movement in the area, material that is deposited at the benthos is readily resuspended and transported elsewhere. This highlights the importance of seagrass as a substrate for retaining sediments and its potential contribution to the sedimentary organic carbon pool.

Future work

As discussed, the model would benefit from further finer-scaled bathymetry and current measurements. Future model refinement could also include sediment resuspension and deposition processes, but this would require further detailed field data characterising the benthic substrate and sediment behaviour at the benthic / water column interface.

Chapter 6

Synthesis and conclusions

6.1. Summary and key findings

This thesis was initially driven by the need to better understand the linkages between benthic processes and the growth of the bloom-forming cyanobacterium *Lyngbya majuscula*. In particular, it aimed to investigate whether the benthos could supply sufficient quantities of iron and phosphorous in the forms required for *L. majuscula* growth, and the key mechanisms that drive these processes.

In January 2011, midway through this study, a major flood event occurred in the Brisbane River causing the widespread loss of seagrass and macroalgal communities from northern Deception Bay. There was also no formation of *L. majuscula* blooms over the 2010-2011 summer as had previously occurred in northern Deception Bay. However, the flood event provided an opportunity to investigate the maximum situation for sediment and material delivery to *L. majuscula* growth areas, as well as a chance to assess the broader ecological significance of such an event in an area already subject to degradation due to regular algal blooms. To capture the impacts of such an infrequent event, and to better understand the effects of benthic community change on key sediment biogeochemical processes, the study evolved to encompass the following aims:

1. To quantify the rates and pathways of carbon and nutrient flows within the flood impacted sediments of Deception Bay (Chapters 2, 4 & 5);
2. To determine the potential for these sediments to underpin key local phenomena such as *L. majuscula* blooms and biogeochemical cycling (Chapter 3);
3. To examine the implications of such community change for the cycling of nutrients at an ecosystem scale (Chapters 4 & 5).

Key findings of the study are discussed below.

Benthic carbon and nutrient pathways

Pre-flood sediments in northern Deception Bay were relatively low in organic carbon, phosphorus and iron and showed clear spatial distributions (Chapter 2). Post-flood sediments that were devoid of seagrass showed even lower carbon, phosphorus and iron levels compared with pre-flood sediments (Chapter 3). Although post-flood sampling was restricted spatially compared with that of pre-flood sampling, the results suggest that seven months after the flood, material had not accumulated at the benthos where seagrass had been lost. Some of the material would have been remineralised by benthic processes, however most of the material is likely to have been exported to other parts of Moreton Bay (Chapter 4). This notion is supported by hydrodynamic modelling (Chapter 5) which shows that sediment transport is influenced by wind and tidal currents, which are likely to resuspend material at the benthos and export it elsewhere. The loss of seagrass and macroalgal cover is likely to exacerbate this process as seagrass is known to trap sediment and reduce sediment resuspension (Chapter 4).

Hydrodynamic modelling (Chapter 5) shows that material can enter the northern Deception Bay study site from sources in the north, via Pumicestone Passage and from southern Moreton Bay. The 2011 Brisbane River flood plume showed a northerly flow of material from southern and central parts of Moreton Bay out through the northern passage adjacent to northern Deception Bay. This northerly flow of water within Moreton Bay has been documented in previous modelling (see Chapter 5) and is shown to be seasonally influenced by wind. High rates of sediment deposition were recorded across the study site during the flood (Chapter 4) which was a significant source of organic carbon and nutrients to the benthos.

As discussed in Chapter 4, the loss of the seagrass *S. isoetifolium* from Deception Bay has implications for benthic carbon and nutrient cycling and the growth of *L. majuscula* blooms (Chapter 3).

Implications of benthic community change on sediment biogeochemical processes

This study has shown that changes in community composition can have significant implications for system-wide functions. As a result of the 2011 floods, the loss of a dominant seagrass species (*S. isoetifolium*) from the Deception Bay seagrass meadow suggests a shift from a net heterotrophic seagrass dominated system to a net autotrophic bare-sediment / microphytobenthic and seagrass system (Chapter 4). The conceptual

diagram presented in Figure 32 depicts this change in community composition and shows the magnitude of change in DO fluxes and the overall shift in net ecosystem metabolism (NEM). Such a change has implications for key benthic processes and local phenomena such as the growth of *L. majuscula* blooms (Chapters 3 and 4).

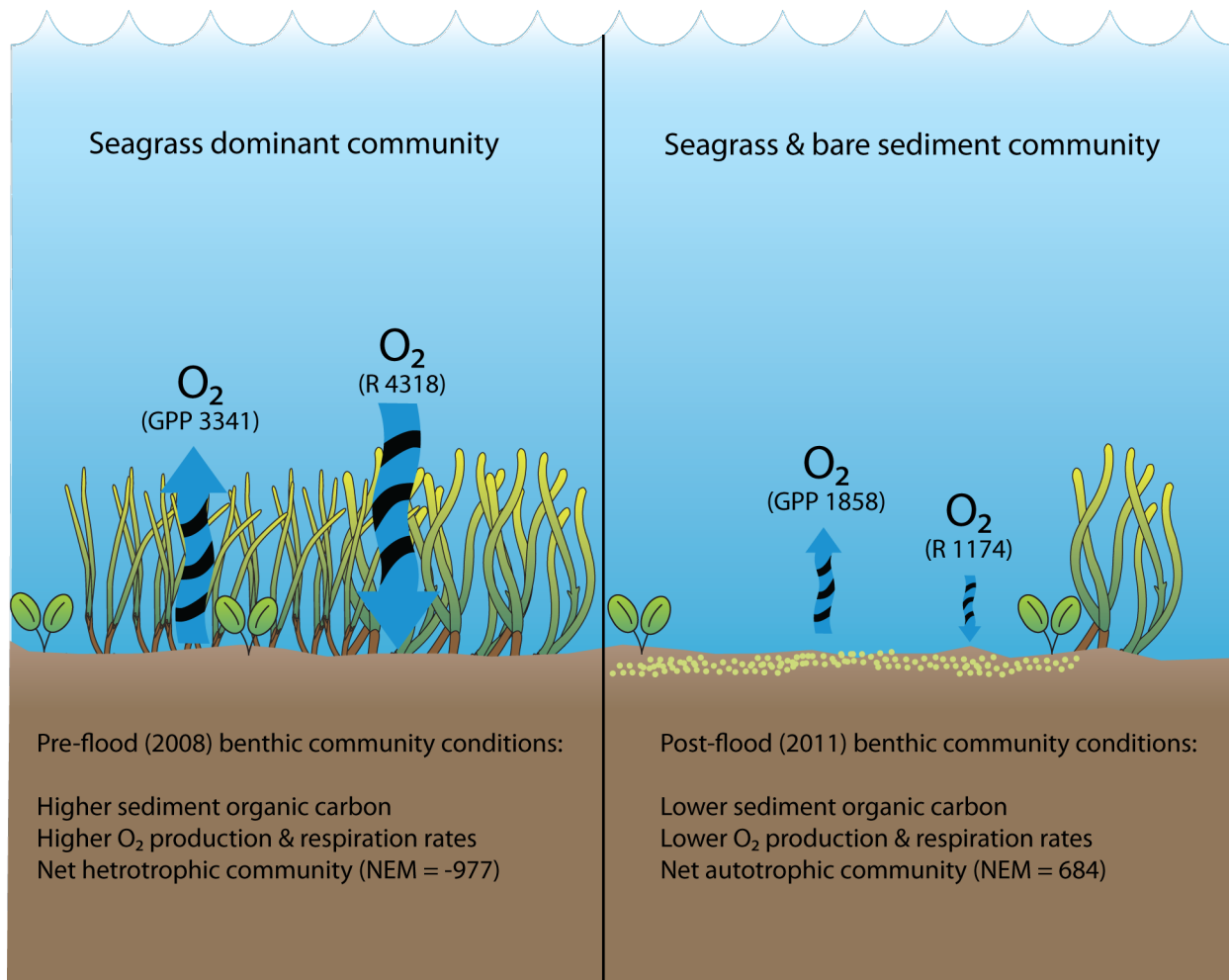


Figure 32 Conceptual diagram showing changes in net ecosystem metabolism as a result of flood related changes in benthic community composition. Rates are given in units of $t\ C\ yr^{-1}$ based on Chapter 4 benthic community areas. (GPP: gross primary production; R: respiration; NEM: net ecosystem metabolism.)

This study has highlighted that different seagrass species and their associated sediment communities can play very different functional roles within a seagrass ecosystem. Loss of seagrass and benthic community diversity therefore has implications for system-wide functions, such as benthic nutrient and carbon cycling. Therefore, managing and assessing the health of seagrass ecosystems requires a knowledge of key functions at species / community level.

The significance of benthic sediments for the growth of *L. majuscula* blooms

A central hypothesis of this study was that the initiation and growth of an *L. majuscula* bloom is linked to a benthic release of P and Fe, triggered by changes in sediment oxygen and redox conditions. This hypothesis was built from the knowledge that when sediment porewater dissolved oxygen (DO) becomes depleted, sediment respiration then proceeds through redox reactions involving alternative electron acceptors such as NO_3^- , Mn(IV), Fe(III), SO_4^{2-} and CO_2 (Testa and Kemp, 2012). The reduction of sedimentary Fe(III) through anaerobic respiration therefore mobilises Fe(II) into the sediment porewaters and then potentially into the overlying water column. The results presented here support this notion, as does numerous studies that describe the link between DO, sediment redox and the benthic cycling of P and Fe (Cook et al., 2010; Ingall and Jahnke, 1997; McManus et al., 1997; Sundby et al., 1992).

This study has quantified for the first time a benthic release of Fe(II) from sediments sampled from northern Deception Bay. To our knowledge, this study represents the first documented benthic release of Fe(II) from permeable sandy sediments of a shallow subtropical embayment. The results show that post-flood sediment communities are capable of supplying >1700 % of the daily Fe demands and up to 10.6 % of daily P requirements for the growth of *L. majuscula* blooms. This result suggests that the growth of *L. majuscula* blooms in Deception Bay is likely to be P limited.

These results are based on sediment incubation experiments that were undertaken on bare sediments dominated by a microphytobenthic community (Chapter 3). Although this study could not repeat these incubations on seagrass-sediment communities, the results provide an insight into the mechanism with which benthic Fe and P release occurs. As discussed above, seagrass dominated sediments are likely to receive higher inputs of organic matter compared with non-vegetated sediments and therefore result in higher levels of sedimentary organic carbon. Comparisons between pre and post-flood sediment carbon levels in Deception Bay support this notion (Chapter 4). Higher sedimentary carbon levels stimulate sediment microbial activity resulting in higher rates of benthic nutrient remineralisation (Hansen et al., 2000). Therefore, it is reasonable to expect that higher rates of benthic Fe and P release may occur in seagrass dominated sediments, however, further work is required to substantiate this notion.

In the case of Deception Bay, *L. majuscula* blooms have been observed to initiate and grow from seagrass-sediment communities. Once *L. majuscula* growth increases,

mats form on the benthos resulting in anaerobic sediment conditions beneath the *L. majuscula* matt. Once sediment oxygen levels are depleted, benthic respiration processes result in the reduction of Fe-bound P (Chapter 3). In the absence of an oxygenated sediment surface layer, Fe(II) and PO_4^{3-} efflux is uninhibited and likely to result in flux rates much higher than those measured by this study (Chapter 3).

6.2. Implications of the work

The key findings and implications of this study can be summarised as follows:

1. Sediment communities of northern Deception Bay are capable of supplying all Fe requirements for *L. majuscula* bloom development. In addition, growth of *L. majuscula* blooms in Deception Bay is likely to be P limited. Future management actions that are targeted towards reducing *L. majuscula* blooms in Moreton Bay need to include a strategy for reducing P loads to the Bay.
2. Sandy sediments that are relatively low in organic carbon are capable of supplying bioavailable Fe at levels significant for the growth of benthic organisms. The presence of seagrasses within these sediments are likely to play a significant role in the cycling of carbon and other nutrients that support benthic organisms.
3. This study documents the complete loss of the *Syringodium isoetifolium* dominated seagrass community in northern Deception Bay following the Brisbane River flood in January 2011. Other seagrass communities appeared to be relatively unaffected, most likely due to their higher tolerance to low salinity and low light levels. These findings demonstrate the differing ability of seagrass species to tolerate environmental change, and highlight the importance of monitoring to the dominant species/community level following such extreme events.
4. Changes in benthic community composition can have implications for system-wide functions. This study highlights the importance of different benthic community types and their relative contribution to whole-of-system function. Any assessments of the health and resilience of seagrass ecosystems need to consider the role and function of its components.

5. The shallow waters of the northern Deception Bay seagrass meadow are greatly influenced by wind and tidal currents. This creates a dynamic environment where deposition, resuspension and export of material readily occur. The magnitude of these processes are likely to vary across spatial and temporal scales. Future studies therefore need to consider such variability in their design.

6.3. Future research

Based on the outcomes of this study and the gaps in knowledge that this research has highlighted, the following recommendations for future research are given:

1. Further benthic Fe(II) and PO_4^{3-} flux measurements should be undertaken to assess the capacity of other benthic communities to support the growth of *L. majuscula* blooms. This should target benthic community types dominated by different seagrass and macroalgae species in northern Deception Bay.

In addition, a comparison study should be undertaken to measure benthic Fe(II) and PO_4^{3-} fluxes at the Eastern Banks seagrass meadow, on the eastern side of Moreton Bay, where *L. majuscula* blooms have also been known to occur.

2. Any additional measurements should also account for and investigate seasonal variability. This could be achieved by undertaking sampling in different seasons and across multiple years (to cover wet-dry years). Follow-up surveys of the northern Deception Bay seagrass meadow should be undertaken to document its recovery. The methods used should be sufficiently detailed to record dominant macroflora species. Maps should be generated using a combination of field observations/transects and spatial interpolation (as undertaken in this study) so that direct comparisons can be made. Community distribution maps could also be refined by combining the existing maps/methods with benthic cover mapping derived from aerial imagery.

As per above, future surveys should also account for and investigate seasonal variability in the benthic macroflora community distribution.

3. Further research is needed to investigate light and salinity tolerances of individual seagrass species and their combined effect on growth and survivorship.
4. The model presented in this study would benefit from further fine-scaled measurements in bathymetry and currents. Future model refinements should also include sediment resuspension and deposition processes, and account for seasonal variability.

References

- Abal, E.G., Dennison, W.C., 1996. Seagrass depth range and water quality in southern Moreton bay, Queensland, Australia. *Marine and Freshwater Research* 47, 763-771.
- Ahern, K.S., Ahern, C.R., Savige, G.M., Udy, J.W., 2007a. Mapping the distribution, biomass and tissue nutrient levels of a marine benthic cyanobacteria bloom (*Lyngbya majuscula*). *Marine and Freshwater Research* 58, 883-904.
- Ahern, K.S., Ahern, C.R., Udy, J.W., 2007b. Nutrient additions generate prolific growth of *Lyngbya majuscula* (cyanobacteria) in field and bioassay experiments. *Harmful Algae* 6, 134-151.
- Ahern, K.S., O'Neil, J.M., Udy, J.W., Albert, S., 2006. Effects of iron additions on filament growth and productivity of the cyanobacterium *Lyngbya majuscula*. *Marine and Freshwater Research* 57, 167-176.
- Albert, S., O'Neil, J.M., Udy, J.W., Ahern, K.S., O'Sullivan, C.M., Dennison, W.C., 2005. Blooms of the cyanobacterium *Lyngbya majuscula* in coastal Queensland, Australia: disparate sites, common factors. *Marine Pollution Bulletin* 51, 428-437.
- Alongi, D.M., 1998. Coastal ecosystem processes. CRC Press, New York.
- APHA, 2005. Standard Methods for the Examination of Water and Waste Water, 21st ed. American Public Health Association (APHA) & American Water Works Association (AWWA) & Water Environment Federation (WEF), Washington DC.
- Australian Bureau of Statistics, 2001. Census of Population and Housing: Population Growth and Distribution, Australia, 2001 Australian Bureau of Statistics, Canberra.
- Babister, M., Retallick, M., 2011. Brisbane river 2011 flood event - flood frequency analysis. WMAwater.
- Balzer, W., 1982. On the distribution of iron and manganese at the sediment water interface - thermodynamic versus kinetic control. *Geochimica Et Cosmochimica Acta* 46, 1153-1161.
- Barron, C., Marbà, N., Terrados, J., Kennedy, H., Duarte, C.M., 2004. Community metabolism and carbon budget along a gradient of seagrass (*Cymodocea nodosa*) colonization. *Limnology and Oceanography* 49, 1642-1651.
- Bell, P.R.F., Elmetri, I., 2007. Some chemical factors regulating the growth of *Lyngbya majuscula* in Moreton Bay, Australia: importance of sewage discharges. *Hydrobiologia* 592, 359-371.
- Berner, R.A., 1980. Early Diagenesis: A Theoretical Approach. Princeton University Press, Princeton (NJ).

-
- Berner, R.A., Rao, J.L., 1994. Phosphorus in sediments of the Amazon River and estuary: Implications for the global flux of phosphorus to the sea. *Geochimica Et Cosmochimica Acta* 58, 2333-2339.
- Blomqvist, S., Hakanson, L., 1981. A review on sediment traps in aquatic environments. *Archiv Fur Hydrobiologie* 91, 101-132.
- Bouillon, S., Boschker, H.T.S., 2006. Bacterial carbon sources in coastal sediments: a cross-system analysis based on stable isotope data of biomarkers. *Biogeosciences* 3, 175-185.
- Bouillon, S., Moens, T., Dehairs, F., 2004. Carbon sources supporting benthic mineralization in mangrove and adjacent seagrass sediments (Gazi Bay, Kenya). *Biogeosciences* 1, 71-78.
- Burdige, D.J., 2012. Estuarine and coastal sediments - coupled biogeochemical cycling, in: McLusky, D., Wolanski, E. (Eds.), *Treatise on Estuarine and Coastal Science*. Elsevier, pp. 279-316.
- Burfeind, D.D., Udy, J.W., 2009. The effects of light and nutrients on *Caulerpa taxifolia* and growth. *Aquatic Botany* 90, 105-109.
- Campbell, S.J., McKenzie, L.J., 2004. Flood related loss and recovery of intertidal seagrass meadows in southern Queensland, Australia. *Estuarine Coastal and Shelf Science* 60, 477-490.
- Cardoso, P.G., Pardal, M.A., Lillebo, A.I., Ferreira, S.M., Raffaelli, D., Marques, J.C., 2004. Dynamic changes in seagrass assemblages under eutrophication and implications for recovery. *Journal of Experimental Marine Biology and Ecology* 302, 233-248.
- Chiffings, A.W., 2007. Integration of the *Lyngbya* research and management program 2005-2007: Final synthesis report. South East Queensland Healthy Waterways Partnership, Brisbane.
- Cline, J.D., 1969. Spectrophotometric determination of hydrogen sulfide in natural waters. *Limnology and Oceanography* 14, 454-&.
- Cook, P.L.M., Holland, D.P., Longmore, A.R., 2010. Effect of a flood event on the dynamics of phytoplankton and biogeochemistry in a large temperate Australian lagoon. *Limnology and Oceanography* 55, 1123-1133.
- Corbett, D.R., 2010. Resuspension and estuarine nutrient cycling: insights from the Neuse River Estuary. *Biogeosciences* 7, 3289-3300.
- Cowan, J.L.W., Pennock, J.R., Boynton, W.R., 1996. Seasonal and interannual patterns of sediment-water nutrient and oxygen fluxes in Mobile Bay, Alabama (USA): Regulating factors and ecological significance. *Marine Ecology Progress Series* 141, 229-245.

-
- Cox, M., Labadz, M., Hodgkinson, J., 2007. Lyngbya Task 5.2 - Catchment Loads of Nutrients of Concern to Deception Bay: Groundwater. South East Queensland Healthy Waterways Partnership, Brisbane.
- D'Avanzo, C., Kremer, J.N., Wainright, S.C., 1996. Ecosystem production and respiration in response to eutrophication in shallow temperate estuaries. *Mar. Ecol.-Prog. Ser.* 141, 263-274.
- Davie, P., 2011. Wild guide to Moreton Bay and adjacent coasts, second edition ed. Queensland Museum, Brisbane.
- Davies, S., Mirfenderesk, H., Tomlinson, R., Szykarski, S., 2009. Hydrodynamic, Water Quality and Sediment Transport Modeling of Estuarine and Coastal Waters on the Gold Coast Australia. *Journal of Coastal Research*, 937-941.
- de Boer, W.F., 2007. Seagrass-sediment interactions, positive feedbacks and critical thresholds for occurrence: a review. *Hydrobiologia* 591, 5-24.
- de longh, H.H., Wenno, B.J., Meelis, E., 1995. Seagrass distribution and seasonal biomass changes in relation to dugong grazing in the Moluccas, East Indonesia. *Aquatic Botany* 50, 1-19.
- Dennison, W.C., Abal, E.G., 1999. Moreton Bay study: a scientific basis for the healthy waterways campaign. South East Queensland Regional Water Quality Management Strategy, Brisbane.
- Dennison, W.C., O'Neil, J.M., Duffy, E., Oliver, P., Shaw, G., 1999. Blooms of the cyanobacterium *Lyngbya majuscula* in coastal waters of Queensland, in: Charpy, L., Larkum, A.W.D. (Eds.), *Proceeding of the International Symposium on Marine Cyanobacteria*, November 1997. Institut Oceanographique, Paris.
- Dennison, W.C., Orth, R.J., Moore, K.A., Stevenson, J.C., Carter, V., Kollar, S., Bergstrom, P.W., Batiuk, R.A., 1993. Assessing water quality with submersed aquatic vegetation. *Bioscience* 43, 86-94.
- DERM, 2011. South East Queensland event monitoring summary (6th-16th January 2011): Preliminary suspended solids loads calculations, Healthy Waterways. Queensland Department of Environment and Resource Management, Brisbane.
- DHI, 2011. User Guide, MIKE 21 Flow Model FM, Hydrodynamic Module. DHI Water and Environment, Horsholm, Denmark, p. 108.
- Diaz, M.R., Corredor, J.E., Morell, J.M., 1990. Nitrogenase activity of microcoleus mat communities in a eutrophic, tropical marine environment. *Limnology and Oceanography* 35, 1788-1795.

-
- Douglass, J.G., France, K.E., Richardson, J.P., Duffy, J.E., 2010. Seasonal and interannual change in a Chesapeake Bay eelgrass community: Insights into biotic and abiotic control of community structure. *Limnology and Oceanography* 55, 1499-1520.
- Duarte, C.M., 1995. Submerged aquatic vegetation in relation to different nutrient regimes. *Ophelia* 41, 87-112.
- Duarte, C.M., 2000. Marine biodiversity and ecosystem services: an elusive link. *Journal of Experimental Marine Biology and Ecology* 250, 117-131.
- Duarte, C.M., 2002. The future of seagrass meadows. *Environ. Conserv.* 29, 192-206.
- Duarte, C.M., Chiscano, C.L., 1999. Seagrass biomass and production: a reassessment. *Aquatic Botany* 65, 159-174.
- Duarte, C.M., Middelburg, J.J., Caraco, N., 2005. Major role of marine vegetation on the oceanic carbon cycle. *Biogeosciences* 2, 1-8.
- Dunn, R.J.K., Welsh, D.T., Teasdale, P.R., Lee, S.Y., Lemckert, C.J., Meziane, T., 2008. Investigating the distribution and sources of organic matter in surface sediment of Coombabah Lake (Australia) using elemental, isotopic and fatty acid biomarkers. *Cont. Shelf Res.* 28, 2535-2549.
- EHMP, 2006. Ecosystem Health monitoring Program 2004-2005 Annual Technical Report. South East Queensland Healthy Waterways Partnership, Brisbane.
- Elmetri, I., Bell, P.R.F., 2004. Effects of phosphorus on the growth and nitrogen fixation rates of *Lyngbya majuscula*: implications for management in Moreton Bay, Queensland. *Mar. Ecol.-Prog. Ser.* 281, 27-35.
- Eyre, B., France, L., 1997. Importance of marine inputs to the sediment and nutrient load of coastal-plain estuaries: a case study of Pumicestone Passage, south-eastern Queensland, Australia. *Marine and Freshwater Research* 48, 277-286.
- Eyre, B.D., Ferguson, A.J.P., 2002. Comparison of carbon production and decomposition, benthic nutrient fluxes and denitrification in seagrass, phytoplankton, benthic microalgae- and macroalgae-dominated warm-temperate Australian lagoons. *Mar. Ecol.-Prog. Ser.* 229, 43-59.
- Eyre, B.D., Ferguson, A.J.P., Webb, A., Maher, D., Oakes, J.M., 2011a. Denitrification, N-fixation and nitrogen and phosphorus fluxes in different benthic habitats and their contribution to the nitrogen and phosphorus budgets of a shallow oligotrophic sub-tropical coastal system (southern Moreton Bay, Australia). *Biogeochemistry* 102, 111-133.

-
- Eyre, B.D., Ferguson, A.J.P., Webb, A., Maher, D., Oakes, J.M., 2011b. Metabolism of different benthic habitats and their contribution to the carbon budget of a shallow oligotrophic subtropical coastal system (southern Moreton Bay, Australia). *Biogeochemistry* 102, 87-110.
- Ferguson, A., Eyre, B., Gay, J., Emtage, N., Brooks, L., 2007. Benthic metabolism and nitrogen cycling in a sub-tropical coastal embayment: spatial and seasonal variation and controlling factors. *Aquatic Microbial Ecology* 48, 175-195.
- Ferguson, A.J.P., Eyre, B.D., 2010. Carbon and nitrogen cycling in a shallow productive subtropical coastal embayment (Western Moreton Bay, Australia): the importance of pelagic-benthic coupling. *Ecosystems* 13, 1127-1144.
- Gacia, E., Duarte, C.M., Middelburg, J.J., 2002. Carbon and nutrient deposition in a Mediterranean seagrass (*Posidonia oceanica*) meadow. *Limnology and Oceanography* 47, 23-32.
- Geider, R.J., La Roche, J., 2002. Redfield revisited: variability of C : N : P in marine microalgae and its biochemical basis. *European Journal of Phycology* 37, 1-17.
- Goni, M.A., Voulgaris, G., Kim, Y.H., 2009. Composition and fluxes of particulate organic matter in a temperate estuary (Winyah Bay, South Carolina, USA) under contrasting physical forcings. *Estuarine Coastal and Shelf Science* 85, 273-291.
- Goovaerts, P., 1997. *Geostatistics for natural resources evaluation*. Oxford University Press, New York.
- Guisan, A., Zimmermann, N.E., 2000. Predictive habitat distribution models in ecology. *Ecological Modelling* 135, 147-186.
- Hanington, P., Hunnam, K., Johnstone, R., 2015. Widespread loss of the seagrass *Syringodium isoetifolium* after a major flood event in Moreton Bay, Australia: Implications for benthic processes. *Aquatic Botany* 120, 244-250.
- Hansen, J.W., Udy, J.W., Perry, C.J., Dennison, W.C., Lomstein, B.A., 2000. Effect of the seagrass *Zostera capricorni* on sediment microbial processes. *Mar. Ecol.-Prog. Ser.* 199, 83-96.
- Hemminga, M.A., Duarte, C.M., 2000. *Seagrass Ecology*. Cambridge University Press, Cambridge.
- Herbert, R.A., 1999. Nitrogen cycling in coastal marine ecosystems. *Fems Microbiology Reviews* 23, 563-590.
- Hohnen, L., Wood, R., Newton, P., Jahan, N., Vieira, S., 2008. Fishery economic status report 2007, ABARE Report 08.10 prepared for the Fisheries Resources Research Fund. ABARE, Canberra.

-
- Holmer, M., Andersen, F.O., Nielsen, S.L., Boschker, H.T.S., 2001. The importance of mineralization based on sulfate reduction for nutrient regeneration in tropical seagrass sediments. *Aquatic Botany* 71, 1-17.
- Holmes, K.W., Van Niel, K.P., Kendrick, G.A., Radford, B., 2007. Probabilistic large-area mapping of seagrass species distributions. *Aquatic Conservation: Marine and Freshwater Ecosystems* 17, 385-407.
- Hopkinson, C.S., Giblin, A.E., Tucker, J., Garritt, R.H., 1999. Benthic metabolism and nutrient cycling along an estuarine salinity gradient. *Estuaries* 22, 863-881.
- Hunnam, K., 2008. The ecological significance of changes in seagrass communities in northern Deception Bay, South-East Queensland (Honours Thesis), School of Integrative Biology. University of Queensland.
- Hyland, S.J., Courtney, A.J., Butler, C.T., 1989. Distribution of seagrass in the Moreton region from Coolangatta to Noosa, Queensland Department of Primary Industries Information Series, p. 42.
- Ingall, E., Jahnke, R., 1997. Influence of water-column anoxia on the elemental fractionation of carbon and phosphorus during sediment diagenesis. *Marine Geology* 139, 219-229.
- Johnson, P., Johnstone, R., 1995. Productivity and nutrient dynamics of tropical sea-grass communities in Puttalam Lagoon, Sri Lanka. *Ambio* 24, 411-417.
- Johnstone, R.W., 2001. Sediment Interactions: Flux of Nutrients from Sediment in *Lyngbya majuscula* Bloom and Nearby Areas. Report for the SEQ Regional Water Quality Management Strategy Office, Brisbane City Council. Centre for Marine Studies, The University of Queensland.
- Johnstone, R.W., Pantos, O., Hanington, P.J., 2007. The role of benthic sediments in *Lyngbya majuscula* blooms in Deception Bay. Technical Report. South East Queensland Healthy Waterways Partnership, Brisbane.
- Kaldy, J.E., Eldridge, P.M., Cifuentes, L.A., Jones, W.B., 2006. Utilization of DOC from seagrass rhizomes by sediment bacteria: C-13-tracer experiments and modeling. *Marine Ecology Progress Series* 317, 41-55.
- Kendrick, G.A., Aylward, M.J., Hegge, B.J., Cambridge, M.L., Hillman, K., Wyllie, A., Lord, D.A., 2002. Changes in seagrass coverage in Cockburn Sound, Western Australia between 1967 and 1999. *Aquatic Botany* 73, 75-87.
- Kennedy, H., Gacia, E., Kennedy, D.P., Papadimitriou, S., Duarte, C.M., 2004. Organic carbon sources to SE Asian coastal sediments. *Estuarine Coastal and Shelf Science* 60, 59-68.

-
- Kerr, E.A., Strother, S., 1985. Effects of irradiance, temperature and salinity on photosynthesis of *Zostera muelleri*. *Aquatic Botany* 23, 177-183.
- Kirk, J.T.O., 2011. *Light and Photosynthesis in Aquatic Ecosystems*, 3rd ed. Cambridge University Press, Cambridge, GBR.
- Kirkman, H., 1978. Decline of seagrass in northern areas of Moreton Bay, Queensland. *Aquatic Botany* 5, 63-76.
- Koch, M.S., Benz, R.E., Rudnick, D.T., 2001. Solid-phase phosphorus pools in highly organic carbonate sediments of northeastern Florida Bay. *Estuarine Coastal and Shelf Science* 52, 279-291.
- Kristensen, E., Kostka, J.E., 2005. Macrofaunal burrows and irrigation in marine sediment: Microbiological and biogeochemical interactions, in: Kristensen, E., Kosta, J.E., Haese, R.H. (Eds.), *Interactions between macro- and microorganisms in marine sediments*. AGU, Washington, pp. 125-157.
- Krom, M.D., Berner, R.A., 1981. The diagenesis of phosphorus in a nearshore marine sediment. *Geochimica Et Cosmochimica Acta* 45, 207-216.
- Küster-Heins, K., de Lange, G.J., Zabel, M., 2010. Benthic phosphorus and iron budgets for three NW African slope sediments: a balance approach. *Biogeosciences* 7, 469-480.
- Larkum, A.W.D., West, R.J., 1990. Long-term changes of seagrass meadows in Botany Bay, Australia. *Aquatic Botany* 37, 55-70.
- Lirman, D., Cropper, W.P., 2003. The influence of salinity on seagrass growth, survivorship, and distribution within Biscayne Bay, Florida: Field, experimental, and modeling studies. *Estuaries* 26, 131-141.
- Liu, X.H., Huang, W.R., 2009. Modeling sediment resuspension and transport induced by storm wind in Apalachicola Bay, USA. *Environ. Modell. Softw.* 24, 1302-1313.
- Long, W.J.L., Mellors, J.E., Coles, R.G., 1993. Seagrasses between Cape York and Hervey Bay, Queensland, Australia. *Australian Journal of Marine and Freshwater Research* 44, 19-31.
- Longstaff, B.J., 2003. *Investigations into the light requirements of seagrasses in northeast Australia*, Department of Botany. The University of Queensland.
- Longstaff, B.J., Loneragan, N.R., O'Donohue, M.J., Dennison, W.C., 1999. Effects of light deprivation on the survival and recovery of the seagrass *Halophila ovalis* (RBr) Hook. *Journal of Experimental Marine Biology and Ecology* 234, 1-27.
- Loring, D.H., Rantala, R.T.T., 1992. Manual for the geochemical analyses of marine sediments and suspended particulate matter. *Earth-Sci. Rev.* 32, 235-283.

-
- Lotze, H.K., Lenihan, H.S., Bourque, B.J., Bradbury, R.H., Cooke, R.G., Kay, M.C., Kidwell, S.M., Kirby, M.X., Peterson, C.H., Jackson, J.B.C., 2006. Depletion, degradation, and recovery potential of estuaries and coastal seas. *Science* 312, 1806-1809.
- Lukawska-Matuszewska, K., Bolalek, J., 2008. Spatial distribution of phosphorus forms in sediments in the Gulf of Gdansk (southern Baltic Sea). *Cont. Shelf Res.* 28, 977-990.
- Lukkari, K., Leivuori, M., Vallius, H., Kotilainen, A., 2009. The chemical character and burial of phosphorus in shallow coastal sediments in the northeastern Baltic Sea. *Biogeochemistry* 94, 141-162.
- Marbà, N., Holmer, M., Gacia, E., Barrón, C., 2006. Seagrass beds and coastal biogeochemistry, in: Larkum, A.W.D., Orth, R.J., Duarte, C.M. (Eds.), *Seagrasses: Biology, Ecology and Conservation*. Springer, Dordrecht, pp. 135-157.
- Mateo, M., A., Cebrián, J., Dunton, K., Mutchler, T., 2006. Carbon flux in seagrass ecosystems, in: Larkum, A.W.D., Orth, R.J., Duarte, C.M. (Eds.), *Seagrasses: biology, ecology and conservation*. Springer, Dordrecht, pp. 159-192.
- Maxwell, P., Stevens, A., Udy, J., Savage, G., 2007. LYNGBYA TASK 9 - Monitoring of *Lyngbya majuscula* distribution and the environmental conditions in Moreton Bay. South East Queensland Healthy Waterways Partnership, Brisbane, Australia, p. 96.
- McAlister, A., 2007. LYNGBYA TASK 5 & 10 - Estimating Loads of Nutrients of Concern to Lyngbya Beds in Deception Bay: Catchment and Receiving Water Quality Modelling. South East Queensland Healthy Waterways Partnership, Brisbane, Australia, p. 86pp.
- McGlathery, K.J., Sundback, K., Anderson, I.C., 2007. Eutrophication in shallow coastal bays and lagoons: the role of plants in the coastal filter. *Mar. Ecol.-Prog. Ser.* 348, 1-18.
- McGlathery, K.J., Sundbäck, K., Anderson, I.C., 2004. The importance of primary producers for benthic nitrogen and phosphorus cycling, in: Nielsen, S., Banta, G., Pedersen, M. (Eds.), *Estuarine nutrient cycling: the influence of primary producers*. Kluwer Academic Publishers, The Netherlands, pp. 1-15.
- McManus, J., Berelson, W.M., Coale, K.H., Johnson, K.S., Kilgore, T.E., 1997. Phosphorus regeneration in continental margin sediments. *Geochimica Et Cosmochimica Acta* 61, 2891-2907.
- Meyers, P.A., 1994. Preservation of elemental and isotopic source identification of sedimentary organic-matter. *Chem. Geol.* 114, 289-302.
- Micheli, F., Bishop, M.J., Peterson, C.H., Rivera, J., 2008. Alteration of seagrass species composition and function over two decades. *Ecological Monographs* 78, 225-244.

-
- Moore, K.A., Short, F.T., 2006. *Zostera*: biology, ecology, and management, in: Larkum, A.W.D., Orth, R.J., Duarte, C.M. (Eds.), *Seagrasses: Biology, Ecology and Conservation*. Springer, Dordrecht, pp. 361-386.
- Morse, J.W., Thomson, H., Finneran, D.W., 2007. Factors controlling sulfide geochemistry in subtropical estuarine and bay sediments. *Aquat. Geochem.* 13, 143-156.
- Nagel, J.L., 2007. Plant-sediment interactions and biogeochemical cycling for seagrass communities in Chesapeake and Florida Bays, Centre for Environmental Science. University of Maryland.
- Nicholls, R.J., Wong, P.P., Burkett, V.R., Codignotto, J.O., Hay, J.E., McLean, R.F., Ragoonaden, S., Woodroffe, C.D., 2007. Coastal systems and low-lying areas, in: Parry, M.L., Canziani, O.F., Palutikof, J.P., van der Linden, P.J., Hanson, C.E. (Eds.), *Climate Change 2007: Impacts, Adaptation and Vulnerability. Contribution of Working Group II to the Fourth Assessment Report of the Intergovernmental Panel on Climate Change*. Cambridge University Press, Cambridge, UK, pp. 315-356.
- NLWRA, 2002. Australian Catchment, River and Estuary Assessment. National Land and Water Resources Audit, Canberra.
- O'Neil, J.M., Davis, T.W., Burford, M.A., Gobler, C.J., 2012. The rise of harmful cyanobacteria blooms: The potential roles of eutrophication and climate change. *Harmful Algae* 14, 313-334.
- Orth, R.J., Carruthers, T.J.B., Dennison, W.C., Duarte, C.M., Fourqurean, J.W., Heck, K.L., Hughes, A.R., Kendrick, G.A., Kenworthy, W.J., Olyarnik, S., Short, F.T., Waycott, M., Williams, S.L., 2006. A global crisis for seagrass ecosystems. *Bioscience* 56, 987-996.
- Osborne, N., Seawright, A., Shaw, G., 2008. Dermal toxicology of *Lyngbya majuscula*, from Moreton Bay, Queensland, Australia. *Harmful Algae* 7, 584-589.
- Osborne, N.J.T., Webb, P.M., Shaw, G.R., 2001. The toxins of *Lyngbya majuscula* and their human and ecological health effects. *Environment International* 27, 381-392.
- Paerl, H.W., 2006. Assessing and managing nutrient-enhanced eutrophication in estuarine and coastal waters: Interactive effects of human and climatic perturbations. *Ecological Engineering* 26, 40-54.
- Pakhornova, S.V., Hall, P.O.J., Kononets, M.Y., Rozanov, A.G., Tengberg, A., Vershinin, A.V., 2007. Fluxes of iron and manganese across the sediment-water interface under various redox conditions. *Mar. Chem.* 107, 319-331.
- Parsons, T.R., Maita, Y., Lalli, C.M., 1984. *A Manual of Chemical and Biological Methods for Seawater Analysis*, 1 ed. Pergamon Press, New York.

-
- Pedersen, M.F., Nielsen, S.L., Banta, G.T., 2004. Interactions between vegetation and nutrient dynamics in coastal marine ecosystems: an introduction, in: Nielsen, S., Banta, G., Pedersen, M. (Eds.), Estuarine nutrient cycling: the influence of primary producers. Kluwer Academic Publishers, The Netherlands, pp. 1-15.
- Phinn, S., Roelfsema, C., Dekker, A., Brando, V., Anstee, J., 2008. Mapping seagrass species, cover and biomass in shallow waters: An assessment of satellite multi-spectral and airborne hyper-spectral imaging systems in Moreton Bay (Australia). *Remote Sens. Environ.* 112, 3413-3425.
- Pittman, S.J., Pittman, K.M., 2005. Short-term consequences of a benthic cyanobacterial bloom (*Lyngbya majuscula* Gomont) for fish and penaeid prawns in Moreton Bay (Queensland, Australia). *Estuarine Coastal and Shelf Science* 63, 619-632.
- Preen, A., 1995. Impacts of dugong foraging on seagrass habitats - observational and experimental evidence for cultivation grazing. *Marine Ecology Progress Series* 124, 201-213.
- Preen, A.R., Long, W.J.L., Coles, R.G., 1995. Flood and cyclone related loss, and partial recovery, of more than 1000 km(2) of seagrass in Hervey Bay, Queensland, Australia. *Aquatic Botany* 52, 3-17.
- R Development Core Team, 2011. R: A Language and Environment for Statistical Computing.
- Ralph, P.J., Durako, M.J., Enriquez, S., Collier, C.J., Doblin, M.A., 2007. Impact of light limitation on seagrasses. *Journal of Experimental Marine Biology and Ecology* 350, 176-193.
- Rapport, D.J., Costanza, R., McMichael, A.J., 1998. Assessing ecosystem health. *Trends in Ecology & Evolution* 13, 397-402.
- Rayment, G.E., Higginson, F.R., 1992. Australian Laboratory Handbook of Soil and Water Chemical Methods. Inkata Press, Melbourne.
- Ridler, M.S., Dent, R.C., Arrington, D.A., 2006. Effects of two hurricanes on *Syringodium filiforme*, manatee grass, within the Loxahatchee River Estuary, southeast Florida. *Estuaries and Coasts* 29, 1019-1025.
- Roelfsema, C., Kovacs, E.M., Saunders, M.I., Phinn, S., Lyons, M., Maxwell, P., 2013. Challenges of remote sensing for quantifying changes in large complex seagrass environments. *Estuarine Coastal and Shelf Science* 133, 161-171.
- Roelfsema, C.M., Phinn, S.R., Udy, N., Maxwell, P., 2009. An integrated field and remote sensing approach for mapping seagrass cover, Moreton Bay, Australia. *Journal of Spatial Science* 54, 45-62.

-
- Rose, A.L., Salmon, T.P., Lukondeh, T., Neilan, B.A., Waite, T.D., 2005. Use of superoxide as an electron shuttle for iron acquisition by the marine cyanobacterium *Lyngbya majuscula*. *Environmental Science & Technology* 39, 3708-3715.
- Rose, A.L., Waite, T.D., 2001. Chemiluminescence of luminol in the presence of iron(II) and oxygen: Oxidation mechanism and implications for its analytical use. *Analytical Chemistry* 73, 5909-5920.
- Rose, A.L., Waite, T.D., 2005. Reduction of organically complexed ferric iron by superoxide in a simulated natural water. *Environmental Science & Technology* 39, 2645-2650.
- Rozan, T.F., Taillefert, M., Trouwborst, R.E., Glazer, B.T., Ma, S.F., Herszage, J., Valdes, L.M., Price, K.S., Luther, G.W., 2002. Iron-sulfur-phosphorus cycling in the sediments of a shallow coastal bay: Implications for sediment nutrient release and benthic macroalgal blooms. *Limnology and Oceanography* 47, 1346-1354.
- Ruesink, J.L., Feist, B.E., Harvey, C.J., Hong, J.S., Trimble, A.C., Wisehart, L.M., 2006. Changes in productivity associated with four introduced species: ecosystem transformation of a 'pristine' estuary. *Marine Ecology Progress Series* 311, 203-215.
- Santos, R., Silva, J., Alexandre, A., Navarro, N., Barron, C., Duarte, C.M., 2004. Ecosystem metabolism and carbon fluxes of a tidally-dominated coastal lagoon. *Estuaries* 27, 977-985.
- Short, F.T., Wyllie-Echeverria, S., 1996. Natural and human-induced disturbance of seagrasses. *Environ. Conserv.* 23, 17-27.
- Silbergeld, E.K., Grattan, L., Oldach, D., Morris, J.G., 2000. *Pfiesteria*: Harmful algal blooms as indicators of human: Ecosystem interactions. *Environmental Research* 82, 97-105.
- Slomp, C.P., Malschaert, J.F.P., Van Raaphorst, W., 1998. The role of adsorption in sediment-water exchange of phosphate in North Sea continental margin sediments. *Limnology and Oceanography* 43, 832-846.
- South East Queensland Healthy Waterways Partnership, 2007. LYNGBYA TASK 1 - Lyngbya Management Strategy DRAFT 29th June 2007. South East Queensland Healthy Waterways Partnership, Brisbane, Australia, p. 86.
- Sundback, K., McGlathery, K.J., 2005. Interactions between benthic macroalgal and microalgal mats, in: Kristensen, E., Kosta, J.E., Haese, R.H. (Eds.), *Interactions between macro- and microorganisms in marine sediments*. AGU, Washington, pp. 7-29.
- Sundback, K., Miles, A., Hulth, S., Pihl, L., Engstrom, P., Selander, E., Svenson, A., 2003. Importance of benthic nutrient regeneration during initiation of macroalgal blooms in shallow bays. *Mar. Ecol.-Prog. Ser.* 246, 115-126.

-
- Sundby, B., Gobeil, C., Silverberg, N., Mucci, A., 1992. The phosphorus cycle in coastal marine sediments. *Limnology and Oceanography* 37, 1129-1145.
- Terrados, J., Duarte, C.M., Fortes, M.D., Borum, J., Agawin, N.S.R., Bach, S., Thampanya, U., Kamp-Nielsen, L., Kenworthy, W.J., Geertz-Hansen, O., Vermaat, J., 1998. Changes in community structure and biomass of seagrass communities along gradients of siltation in SE Asia. *Estuarine Coastal and Shelf Science* 46, 757-768.
- Terrados, J., Duarte, C.M., Kamp-Nielsen, L., Agawin, N.S.R., Gacia, E., Lacap, D., Fortes, M.D., Borum, J., Lubanski, M., Greve, T., 1999. Are seagrass growth and survival constrained by the reducing conditions of the sediment? *Aquatic Botany* 65, 175-197.
- Testa, J.M., Kemp, W.M., 2012. Oxygen - dynamics and biological consequences, in: McLusky, D., Wolanski, E. (Eds.), *Treatise on Estuarine and Coastal Science*. Elsevier, pp. 163-199.
- Theil, M., Westphalen, G., Collings, G., Cheshire, A., 2007. *Caulerpa taxifolia* responses to hyposalinity stress. *Aquatic Botany* 87, 221-228.
- Thomas, J., 2003. *Caulerpa taxifolia* in Moreton Bay - distribution and seagrass interactions, Department of Botany. The University of Queensland.
- Tyler, A.C., McGlathery, K.J., Anderson, I.C., 2001. Macroalgae mediation of dissolved organic nitrogen fluxes in a temperate coastal lagoon. *Estuarine Coastal and Shelf Science* 53, 155-168.
- UNEP, 2006. Marine and coastal ecosystems and human wellbeing: A synthesis report based on the findings of the Millennium Ecosystem Assessment. United Nations Environment Programme, p. 76.
- Valiela, I., McClelland, J., Hauxwell, J., Behr, P.J., Hersh, D., Foreman, K., 1997. Macroalgal blooms in shallow estuaries: Controls and ecophysiological and ecosystem consequences. *Limnology and Oceanography* 42, 1105-1118.
- van den Honert, R.C., McAneney, J., 2011. The 2011 Brisbane floods: causes, impacts and implications. *Water* 3, 1149-1173.
- Vink, S., Chambers, R.M., Smith, S.V., 1997. Distribution of phosphorus in sediments from Tomales bay, California. *Marine Geology* 139, 157-179.
- Viollier, E., Inglett, P.W., Hunter, K., Roychoudhury, A.N., Van Cappellen, P., 2000. The ferrozine method revisited: Fe(II)/Fe(III) determination in natural waters. *Appl. Geochem.* 15, 785-790.
- Vitousek, P.M., Mooney, H.A., Lubchenco, J., Melillo, J.M., 1997. Human domination of Earth's ecosystems. *Science* 277, 494-499.

-
- Voice, M., Harvey, N., Walsh, K., 2006. (Editors) Vulnerability to Climate Change of Australia's Coastal Zone: Analysis of gaps in methods, data and system thresholds. Report to the Australian Greenhouse Office, Canberra, Australia.
- Ward, T.J., Butler, A., 2006. Coasts and oceans, theme commentary prepared for the 2006 Australia State of the Environment Committee. Department of Environment and Heritage, Canberra.
- Watkinson, A.J., O'Neil, J.M., Dennison, W.C., 2005. Ecophysiology of the marine cyanobacterium, *Lyngbya majuscula* (Oscillatoriaceae) in Moreton Bay, Australia. *Harmful Algae* 4, 697-715.
- Waycott, M., Duarte, C.M., Carruthers, T.J.B., Orth, R.J., Dennison, W.C., Olyarnik, S., Calladine, A., Fourqurean, J.W., Heck, K.L., Hughes, A.R., Kendrick, G.A., Kenworthy, W.J., Short, F.T., Williams, S.L., 2009. Accelerating loss of seagrasses across the globe threatens coastal ecosystems. *Proc. Natl. Acad. Sci. U. S. A.* 106, 12377-12381.
- Waycott, M., McMahon, K., Mellors, J.E., Calladine, A., Kleine, D., 2004. A guide to tropical seagrasses of the Indo-West Pacific. James Cook University, Townsville.
- Webster, R., Oliver, M.A., 2001. Geostatistics for environmental scientists. John Wiley & Sons, Ltd., Chichester.
- Wood, S.N., 2006. Generalized Additive Models: An Introduction with R. Chapman and Hall / CRC, Boca Raton.
- Wulff, F., Eyre, B.D., Johnstone, R., 2011. Nitrogen versus phosphorus limitation in a subtropical coastal embayment (Moreton Bay; Australia): Implications for management. *Ecological Modelling* 222, 120-130.
- Young, P.C., Kirkman, H., 1975. The seagrass communities of Moreton Bay, Queensland. *Aquatic Botany* 1, 191-202.
- Zhang, J.Z., Fischer, C.J., Ortner, P.B., 2004. Potential availability of sedimentary phosphorus to sediment resuspension in Florida Bay. *Glob. Biogeochem. Cycle* 18.
- Zharikov, Y., Skilleter, G.A., Loneragan, N.R., Taranto, T., Cameron, B.E., 2005. Mapping and characterising subtropical estuarine landscapes using aerial photography and GIS for potential application in wildlife conservation and management. *Biological Conservation* 125, 87-100.